

ABSTRACT

HAN, DONG. Development of Fabric Image Models and Invariance Property of Variance-Area Curve Within Fabric. (Under the direction of Dr. Warren J. Jasper and Dr. Moon W. Suh.)

This thesis is concerned with the development of two prediction models for fabric quality, 2-D and 3-D images for visualization of fabric qualities, and the application of variance-area curves in fabric quality rating. Two types of variance-area curves, CV(A) curve and CB(A) curve, are introduced. They together provide a new way to judge the fabric quality quantitatively in its dependence on the measured area. An invariance property of the variance-area curves within a fabric was also investigated by using fabric prediction models and measured yarn data.

Based on two different ways in which weft yarns are mapped onto a fabric, two models are developed by simulating the fabric using measured yarn data and, subsequently, 2-D macro and 3-D micro fabric imaging methods were developed. Application of variance-area curves to woven fabrics and its invariance property were also studied. These are done by using MATLAB[®] programs.

The actual yarn data were captured by an advanced yarn measurement system incorporated by a CTT (Constant Tension Transport) unit, a 12 bit CCD line scan camera, and a program written in C, called "camera1", running on a Linux Operating System platform.

Development of Fabric Image Models and Invariance Property of Variance-Area Curve Within Fabric

by

DONG HAN

A thesis submitted to the Graduate Faculty of
North Carolina State University
in partial fulfillment of the
requirements for the Degree of
Master of Science

TEXTILE ENGINEERING AND SCIENCE

Raleigh

2002

APPROVED BY

Dr. Larry Norris

Dr. Warren Jasper
(Co-Chair of Advisory Committee)

Dr. Moon Suh
(Co-Chair of Advisory Committee)

BIOGRAPHY

Dong Han, the son of Xuezheng Han and Huilan Wang, was born on October 11, 1976 in Lanzhou, P. R. China. He received his elementary and high school education in the same city in China. He received his Bachelor of Science degree in Textile Engineering from China Textile University in Shanghai in July, 1998. After graduation, he worked in Beijing Qinghe Worsted Mill as an assistant engineer.

In August, 2000, the author started his graduate studies in Textile Engineering at the College of Textiles, North Carolina State University in United States. Since then he has been working towards his Master of Science degree.

He married Miss Yi Gong in December, 2001.

ACKNOWLEDGEMENTS

I would like to express my sincere appreciation to Dr. Warren Jasper and Dr. Moon Suh, Co-Chairmen of my Advisory Committee, for their guidance and all the support that I needed over the course of this study. I would also like to extend a big thank to Dr. Larry Norris for his precious time and special interest.

Thanks are also due to the faculty, staff and my graduate student colleagues for providing me with an excellent studying environment. The financial support from National Textile Center for this study is also greatly appreciated.

My parents, I would like to give the most important thanks to them for always being with me and supporting me in my entire life. To my brother, Bo: “Thank you for your help in any way...”.

Finally, and most especially, I am most grateful to my beloved wife, Yi Gong, for her encouragement, patient sacrifice and deep love.

Table of Contents

List of Tables.....	vi
List of Figures.....	vii
Chapter 1. Introduction.....	1
Chapter 2. Review of Literature	3
2.1 Uniformity of Spun Yarns	3
2.1.1 Variation of Yarn Mass.....	4
2.1.2 Variation of Yarn Diameter	7
2.1.3 Effects of Yarn Irregularity on Fabric Properties	10
2.2 Methods for Measuring Uniformity of Spun Yarns.....	12
2.2.1 Subjective Methods.....	12
2.2.2 Mechanical Methods.....	13
2.2.3 Capacitive Methods	17
2.2.4 Optical Methods.....	20
2.3 Methods for Expressing Irregularities of Spun Yarns	22
2.3.1 Coefficient of Variation	22
2.3.2 Variance-Length Curves	23
Chapter 3. Development of Models for 2-D and 3-D Image Representation ...	27
3.1 Data Points in a Yarn.....	28
3.2 Geometry of Yarn Layout within a Woven Fabric.....	28
3.3 2-D And 3-D Representations of Fabric Quality	31

Chapter 4. Variance-Area Curves for Fabric Uniformity	32
4.1 Earlier Work on Variance-Area Relation	32
4.2 Application of Variance-Area Curves to Woven Fabrics.....	33
Chapter 5. Yarn Measurement.....	37
5.1 Calibration of CDD Camera	37
5.2 Calibration of CTT.....	45
5.3 Control Program Modification.....	47
5.4 Yarn Sample Tests	51
Chapter 6. Results and Conclusions	53
6.1 2-D Image Representation	54
6.2 3-D Image Representation	57
6.3 Simulated Images from CYROS® System.....	61
6.4 Variance-Area Curves.....	65
6.5 A Specialty Yarn Sample and The 3-D image Representation for The Overall Quality and Local Quality	70
6.6 Major Conclusions.....	74
6.7 Major Accomplishments.....	75
Chapter 7. References.....	77
Appendix I 2-D Gray Scale Images for 10 Samples from 2 Models	83
Appendix II Simulated Images from CYROS® System.....	94
Appendix III Variance-Area Curves of 10 Samples	104
Appendix IV Matlab Program Samples	116

List of Tables

Table 5.1	Abnormal Pixels and Correction Factors	42
Table 5.2	Results of Metal Wire Tests	45
Table 5.3	Structure of Yarn Data File Header	49
Table 5.3	Structure of Yarn Data File Header (Continued)	50
Table 5.4	Tested Yarn Samples.....	52
Table 6.1	Yarn Densities Used in CYROS [®] Simulation.....	61
Table 6.2	The CV(A) And CB(A) Results of Ten Samples for Model I	67
Table 6.3	The CV(A) And CB(A) Results of Ten Samples for Model II...	68

List of Figures

Figure 2.1	Samples of Yarn Board for Subjective Estimation	13
Figure 2.2	Diagrammatic View of Cut Hank Device	15
Figure 2.3	Compression Method I	16
Figure 2.4	Compression Method II	17
Figure 2.5	Working Principle for Zweigle [®] G585	21
Figure 2.6	General Shapes of V(L) and B(L)	25
Figure 3.1	Measured Yarn Data Within a Yarn	28
Figure 3.2(a)	Plain Weave Pattern	29
Figure 3.2(b)	Side View of Plain Weave Fabric	29
Figure 3.3	Weft Yarn Arrangement on Shuttleless Loom Fabric	31
Figure 4.1	Difference Between The Two CV(A) Computation Methods	35
Figure 5.1	Light Intensity Values of Pixels With Block of Light Source	38
Figure 5.2	Shape of Resulting Curve without a Light Blockage	39
Figure 5.3	Nine Curves in a Same Coordinate	40
Figure 5.4	Upper Limit of Proper Working Light Intensity	41
Figure 5.5	Light Intensity Values After Calibration	43
Figure 5.6	Typical Output of Line Scan Camera	44
Figure 5.7	Constant Tension Transport	46
Figure 6.1	2-D Image for Data #2 Processed by Model I	54

Figure 6.2	2-D Image for Data #10 Processed by Model I.....	55
Figure 6.3	2-D Image for Data #2 Processed by Model II.....	56
Figure 6.4	3-D Image with 160,000 Data Points.....	57
Figure 6.5	3-D Image with 10,000 Points	58
Figure 6.6	3-D Image with 10,000 Points	59
Figure 6.7	2-D Image with Two Specified Squares	60
Figure 6.8	CYROS [®] IV Software Interface.....	62
Figure 6.9	Simulated Fabric Image for Sample #2.....	63
Figure 6.10	Simulated Fabric Image for Sample #10.....	64
Figure 6.11	The CB(A) Curves for Sample #2 and #10 (Model I)	65
Figure 6.12	The CV(A) Curves for Sample #2 and #10 (Model I).....	66
Figure 6.13	The CV(A) And CB(A) Curves of Sample #1 from Model I	69
Figure 6.14	CV(A) And CB(A) Curves of Sample #1 from Model II	70
Figure 6.15	Smoothed Local 3-D Image of an Extended Area	72
Figure 6.16	Unsmoothed Local 3-D Micro Image	73

Chapter 1. Introduction

During the last few years, the textile industry throughout the world has been under extreme pressure to produce higher quality yarns and fabrics due to increased awareness of consumers on product qualities and severe global competition. Emphases on ring-spun yarns and high-quality casual wear now demand the highest possible yarn and fabric qualities.

To achieve a better quality, a method for predicting fabric qualities directly from the measured yarn properties, while extremely difficult, is highly desirable. One approach is to construct a control system for electronically imaging the quality attributes (basis weight, appearance uniformity, physical properties, etc.) of the fabric directly from an on-line yarn diameter or mass measurement system without having to weave or knit a fabric. Inherently, all yarns are subject to periodic and random irregularities. However, their effects on the final product (woven or knitted fabric) are difficult to assess. Current assessment of such irregularities involves the capacitive testing of yarn evenness (determination of mass). In order to form an idea as to how good or bad the tested yarn is, the yarn data are often compared against the standard values, or the so-called standard yarn boards. In addition to traditional yarn boards, fabric samples are produced on sample looms or sample knitting machines although they are quite expensive. Hence, it is most ideal to obtain the information on yarn properties, process the

data on-line or off-line and predict the aesthetic and appearance qualities of the resulting fabrics without having to weave or knit.

There are several systems that predict the resulting fabric qualities through fabric images created directly from the yarn profiles captured from certain yarn measurement systems, such as CYROS[®], USTER[®] EXPERT and OASYS[®] systems. However, these systems are not completely satisfactory because of the way yarn data are converted to fabric images and also due to the fact that the images have to be visually judged in the absence of a quantitative measure.

This thesis will focus on creation of models for representing the qualities of fabric. The representation will be done numerically by use of a new measure called “variance-area” curve in conjunction with an advanced yarn measurement system (CTT machine mounted with a 12 bit CDD line scan camera controlled by programs set up on a Linux OS platform) and CYROS[®] system.

Chapter 2. Review of Literature

This chapter reviews some of the widely studied topics on factors of yarns that affect the fabric appearance, yarn measurement methods and variance-length curves.

2.1 Uniformity of Spun Yarns

In yarns, the variation in fineness is usually understood as “yarn evenness” or “yarn irregularity”. It is widely accepted that yarn quality has a significant impact on the visual quality of the resulting fabric. Both random and periodic variations of mass and diameter along a yarn occur frequently. Irregularity of yarn diameter has been considered as a primary cause of a number of fabric defects. These yarn irregularities are in a form of neps, cloudiness, streakiness or barre in resulting fabric.

Kim [1] stated that the effects of yarn evenness on visual appearance of fabrics are categorized into the following five types:

- the effect on visual appearance of the fabric itself,
- the effect on the dyeability or color uniformity of the fabric,
- the effect on fabric weight uniformity,
- the effect on fabric structure, and
- the effect on take-up and let-off motions.

2.1.1 Variation of Yarn Mass

Length analyses of tops have shown that the fibers are very evenly distributed in this stage, but this evenness will be destroyed after tops are reduced in thickness by drafting operations. In his book, Balls[2] has suggested that this non-random re-distribution of fibers is due to the method of roller drafting in ring spinning. He depicted the fiber movement in drafting procedure in detail. During the drafting procedure, many floating fibers move prematurely at the speed of the front rollers either by cohering with fibers that are positively gripped by the front rollers or by direct entanglement with them. This process is cumulative because the greater the number of fibers moving forward with the speed of the front rollers, the more floating fibers are likely to be drawn forward prematurely by inter-fiber cohesion. A considerably large number of floating fibers will be drawn forward at one time to give a thick place in the issuing sliver and this will be followed by a corresponding thin place due to the premature movement of floating fibers. This cycle will repeat periodically and will give rise to a succession of thick and thin places along the length of the sliver or yarn which has been termed as drafting wave by Balls. Drafting waves are caused by the mechanical methods of drafting so they are independent of the properties of the materials being processed. The work was done on cotton originally. According to Goodings[3] and Martindale[4]'s work, this drafting wave property also applies to wool and they described the factors influencing the length and amplitude of these waves.

Martindale[5] stated that draft waves are only partly responsible for the irregularity of worsted yarn. Even the most perfect drafting equipment with full control of short fibers would not give a uniform sliver or yarn, but only one in which the fibers were arranged at random. Such a random arrangement would produce an irregular product. Martindale also computed the irregularity of a yarn caused by a random distribution of the fibers in a yarn. He assumed that the probability of a fiber crossing a given section in a yarn is proportional to the length of the fiber. The distribution of number of fibers between the various cross-section of the yarn is described by Poisson distribution. Hence, this distribution determines the irregularity of a yarn made up of a random arrangement of fibers of equal lengths. According to the characteristics of a Poisson distribution, if the average number of fibers in a cross-section is n , the standard deviation of the number in a cross-section

$$\sigma_n = \sqrt{n}$$

and the coefficient of variation

$$CV = \frac{100}{\sqrt{n}}$$

This shows that the irregularity arising from this kind of fiber arrangement is dependent only on the mean number of fibers per cross-section and the variability of the fiber thickness, and is independent of any other fiber properties including length or variability of length.

Foster[6] pointed out that the drafting wave is the result of the dragging forward of the floating fibers by those gripped by the fast rollers. Therefore, it is

characteristic of the drafting of cotton by means of the ordinary roller system. Amplitude and length of drafting wave should depend only upon the draft, roller setting, the properties of the cotton and the condition in which the cotton is presented to the rollers. They should be independent of the frame upon which the drafting is performed.

Abeele[7] considered the variation of the number of fibers in a yarn cross section as the most important factor for predicting the variations of thickness in a yarn, roving or sliver.

Grosberg[8] found that there is a very marked correlation between mean fiber length and yarn irregularity. From this correlation, one can calculate the yarn irregularity from the mean fiber length, diameter and the count of the yarn. This relationship also shows that for a given fiber diameter, increases in mean fiber length would produce decreases in yarn mass variation.

Foster[9] assumed a form of fiber movement in which all fibers move at the back roller velocity until their mid-points reach a certain boundary between the back and front rollers. When the fibers cross this boundary, they will move faster at the velocity of the front roller. This velocity will remain until these fibers leave the drafting zone. This concept of a “change point” was also used by Cox and Ingham[10].

Rao[11] had developed a mathematical model for the ideal sliver based on Martindale’s ideas on sliver structure. A definition of an ideal sliver was also given out. With minimum number of subsidiary assumptions, it was shown that

drafting waves are generally a consequence of the correlations between the transition times of fibers in the drafting zone.

Cavaney and Forster[12] studied the laws governing the increased irregularity when slivers are reduced in thickness to yarns. It was shown that the amount of irregularity added by a number of successive drafts is independent of the number and magnitudes of these drafts and depends only upon the total draft. When this draft is high, the irregularity is also unaffected by the doubling.

Suh[13] developed a most general model for obtaining the irregularity CV(%) at any arbitrary unit length of a spun yarn as a function of the fiber fineness and fiber length. He also showed that the results are equivalent to that obtained by Breny[14] and Martindale[5] under certain limiting conditions.

2.1.2 Variation of Yarn Diameter

The variation in mass per unit length along the yarn is a basic and important measure of yarn irregularity since it can influence so many other properties of the yarn and of fabric made from it. Yarn diameter variation along its length has been used as an alternative measure of yarn evenness or yarn irregularity and this measure tends to correlate better with fabric appearance. Smaller diameter in a yarn will give thin places in a fabric. One can observe the visual differences in yarn diameter in a fabric better than that of yarn mass or twist.

According to Burnashiv's work[15], yarn thickness is given by:

$$\text{Thickness} = \frac{Q}{V_n} \text{ kg/m}$$

Where Q is the feeding rate of the back roller in kg/sec.

V_n is the delivery speed of the front roller in m/sec.

From definition of yarn tex,

Tex = weight in g of a 1000 m length

$$\begin{aligned} T &= \frac{kg}{m} \cdot 10^6 \text{ tex} \\ &= \frac{Q}{V_n} \cdot 10^6 \text{ tex} \end{aligned}$$

yarn diameter D_n is given by:

$$D_n = \alpha \sqrt{\frac{T}{1000}}$$

where T = yarn linear density in tex,

α = empirical factor.

Then,

$$D_n = \alpha \sqrt{\frac{1000}{V_n} \cdot Q}$$

However, not only the delivery speed and feeding rate but also yarn twist has influence on yarn diameter. Barella[16] cited that yarn-mass irregularity and yarn-diameter irregularity can not be directly compared. These two types of irregularity come from different sources. Only the comparison made among the same type of irregularity gives a meaningful result. However, for a same yarn, yarn-mass irregularity and yarn-diameter irregularity have the relationship:

$$CV_m = 2CV_d \left(1 - \frac{3}{4} CV_d^2 + \dots\right)$$

CV_m : coefficient of variation of yarn mass.

CV_d : coefficient of variation of yarn diameter.

The expression above is actually the Taylor series expansion of the function

$$CV_m = \frac{CV_d \sqrt{4 + 2 \cdot CV_d^2}}{CV_d^2 + 1},$$

which was derived by Kim, Jasper, Suh and Woo[17].

This relationship can be simplified in the form:

$$CV_m = 2CV_d$$

According to the paper[17], the theoretical relationship between CV_m and CV_d agrees quite well with the experimental data. They also stated that different sizes for the measurement length generate different CV% values due to the variance-length effects.

In an earlier paper by Barella[18], it was found from experiments previously made that the observed CV_d values were almost twice the values of those theoretically predicted by the above relation. As we know, the twists are not uniformly distributed over a length of the yarn. The twists are concentrated in the thinnest parts in a yarn. These thin places will be compressed by the high twist, thus exaggerating variations in the apparent diameter. In order to study the influence of twist on irregularity, Barella had carried out some experiments. It follows after Barella's work that the more compact the yarn is, that is to say, the higher its twist and the more regularly this twist is distributed, the closer do the experimental values approach the theoretical ones.

In general, if there are large irregularities in the yarn, the variation of fineness can be easily detected in the resulting fabric. The problem will be more serious when a fault appears in a regular periodicity along the length of the yarn. In such cases, due to the characteristic of fabric construction, these yarn faults could be located in a pattern that can be easily seen. Twist tends to be higher at thin places in a yarn. Thus, penetration of a dye or finish is likely to be lower in such places than with lower twists.

2.1.3 Effects of Yarn Irregularity on Fabric Properties

It has been recognized that yarn irregularity is the fundamental cause of a number of defects in fabric. These defects are of great concern because they can make an otherwise perfectly satisfactory fabric totally unacceptable. Previous study reflect this topic either by giving a general review of the situation or by dealing with specific aspects.

Unwin and Reast[19] studied the effect of yarn irregularities on fine gauge. They classified faults and irregularities into the following categories:

- Irregularities in yarn and winding which are visible on the cone before it is put on to the knitting machine.
- Irregularities in yarn and winding which are not visible before the cone is put on to the knitting machine.
- Faults in hosiery which are readily seen during knitting or before dyeing.
- Faults in hosiery which are not readily visible until after the dyeing and finishing processes.

All of these faults and irregularities are due in part to unevenness in yarns. However, the review is very general and there was little allocation of specific causes to any one fault.

McFarlane's[20] work was focused on the effect of yarn irregularities on viscose fabrics. It was pointed out that different types of irregularity could cause similar faults in the finished fabric. Generally, those caused during fiber manufacture are normally insignificant compared with those caused during yarn or fabric production. He also classified the irregularity effects in terms of yarn, fabric and color defects. Specific sources were suggested for each fault category.

Walker and Sleath[21] discussed defects occurring in knitted structures as a result of yarn irregularities. They stated that yarn defects and irregularities are particularly noticeable in knitted structures because knitted structures don't have "ground" and "cover", which can help weavers to hide defects.

By examining cloths produced from a range of yarns blended in a variety of ways, Snowden and Sidi[22] found out that short-term yarn irregularity gives short weft streaks in the cloth. These streaks, unlike those variations in warp yarns, can't be concealed by weft-mixing. Mixing of weft yarns is limited to a small number of packages, usually no more than eight. Therefore, the problem of mixing weft yarn is much greater than that of warp yarn.

Bleakley[23] pointed out that cloth with serious yarn unevenness incorporated in it is very likely to suffer from disastrous defects. He also identified one of the

causes of this fault as extreme irregularity of diameter, causing pockets of close or open texture in the finished fabric.

Mahajan[24] investigated three cases of weft bars in cloth. In each of these three cases, causes of periodic count variation responsible for weft bars were studied. The relationship between weft bars and count variation was noticed. Garde, Bandyopadhyay and Subramanian[25] focused their work on influence of yarn unevenness on fabric appearance. They found moderate agreement between yarn unevenness values and the subjective rating of the appearance of fabric woven from the yarns.

2.2 Methods for Measuring Uniformity of Spun Yarns

Evaluation of yarn irregularity has been a main focus in textile industry for a long time. This is because of the importance of this topic with reference to the effects on the resulting fabrics produced from the yarn. Some commonly used methods and systems are introduced in the following few sections.

2.2.1 Subjective Methods

Subjective estimates were commonly made by winding yarns on a black card and looking for visible faults. There are three such yarn boards shown in Fig. 2.1.

Those faults in the yarn could be either random ones or periodic ones. Yarn boards are graded against a set of ASTM Standard panel photos within an enclosed viewing box equipped with a constant light source. Grades assigned to each sample board may range from A+ to D- [26]. Louis[27] once tried to compare

three methods of visual estimation by using results obtained by Uster technique to test the accuracy of each one. This work was based on the subjective method.

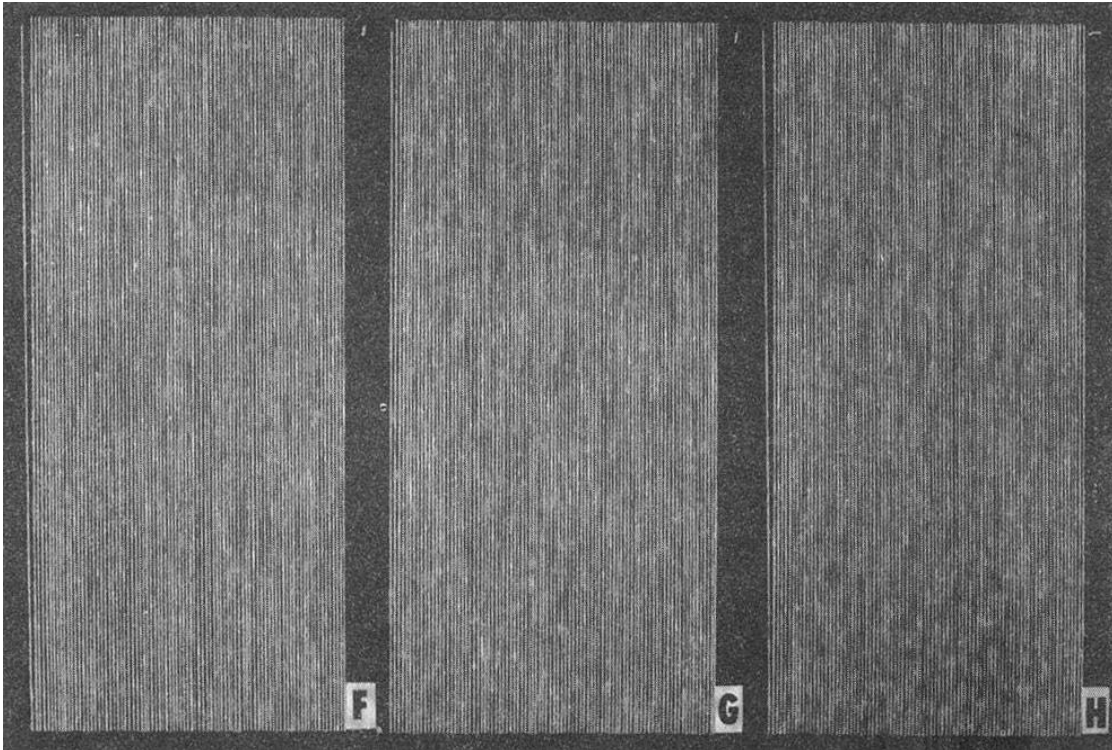


Figure 2.1 Samples of Yarn Board for Subjective Estimation

2.2.2 Mechanical Methods

Chronologically, the first method of quantitative measurement is the technique of cutting and weighing. Successive short lengths of material are cut and weighed. However, the precise cutting of a fixed small length is complicated by the fact that yarns are subject to stretching and requires some care in the exact placement of the

cutting device. Martindale[5] devised a cutting and weighing method, which may be called Cut Hank Method, so that these disadvantages could be avoided.

- Cut Hank Method

A diagrammatic view of Cut Hank device is shown in Fig. 2.2. A test is carried out by reeling 16 yards of yarn on the reel. The hank is tied near C. There will be 16 threads lying side by side on the face of B. The clamp A is then fastened up to grip them and a razor blade is run along both edges of A. this process gives sixteen 1-inch lengths and sixteen 35-inch lengths of the thread. These two portions of the hank are weighed separately. Generally, the weight of the 1-inch sample group will be different from the average weight per unit length of the 35-inch sample group and the greater the irregularity of the yarn the greater this difference will be.[5]

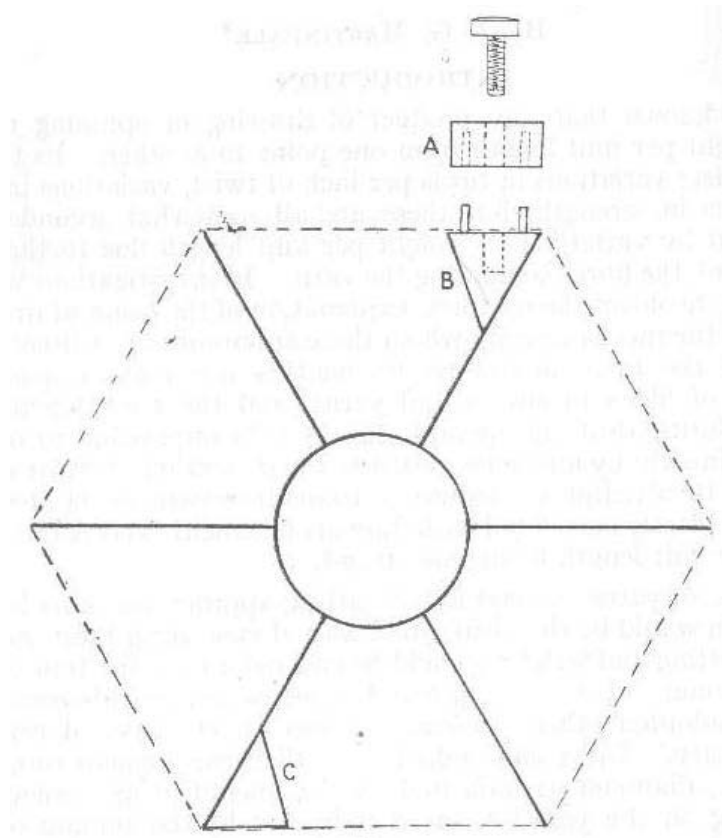


Figure 2.2 Diagrammatic View of Cut Hank Device

Barker[28] mentioned another mechanical method which is more suitable for cotton yarns.

- Compression Method

Devices based on this method respond to changes in yarn thickness, usually by means of mechanical sensors that move in response to such changes. The movement is subsequently magnified by suitable means to give a visible trace, which is proportional to the instantaneous yarn diameter. Fig. 2.3 is a diagrammatic view of a device.

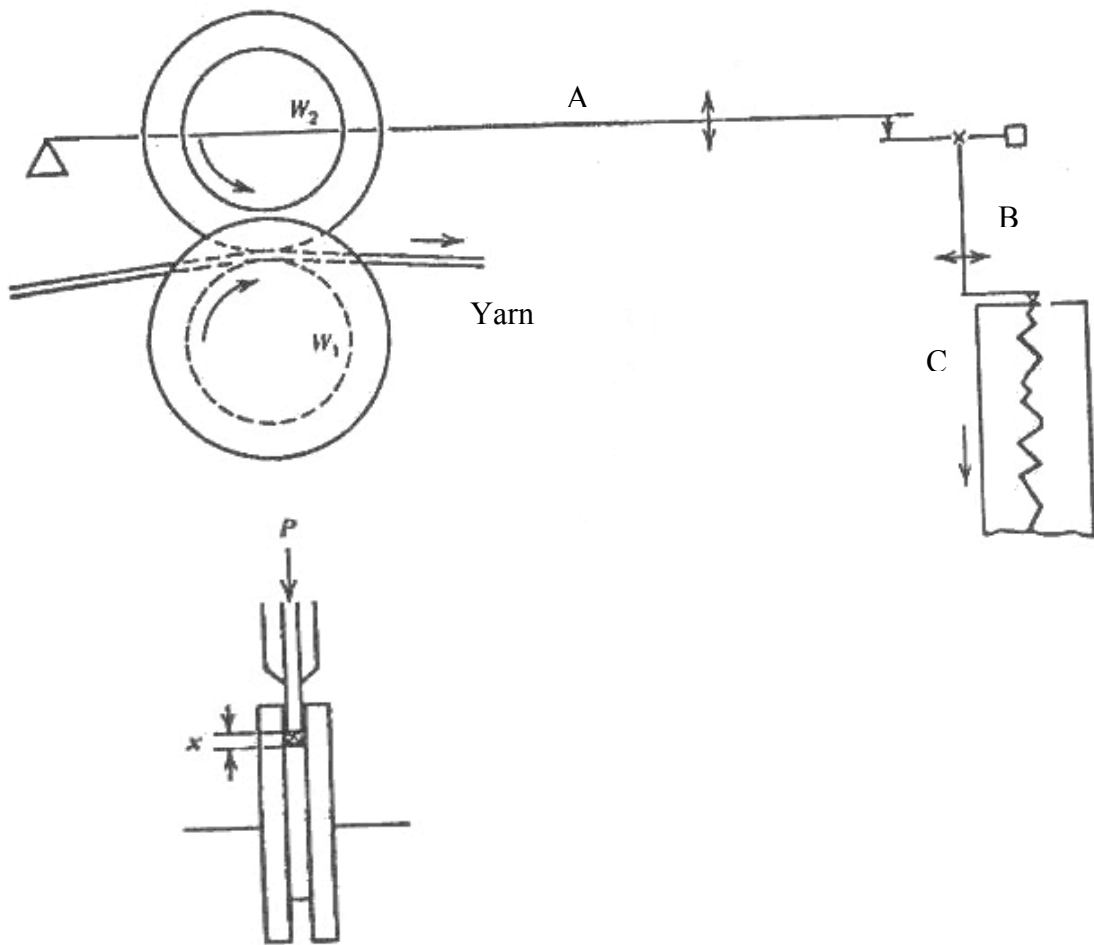


Figure 2.3 Compression Method I

The yarn was drawn between two wheels, W_1 and W_2 . The variations of diameter are magnified by a set of levers, A and B , and recorded on paper C .

Fig. 2.4 is a view of an other type of devices, which uses a mirror and light to magnify the yarn diameter variations. Light is concentrated by an adjustable lens, 9, and is reflected by a mirror, 8, on to a projection screen, 10.

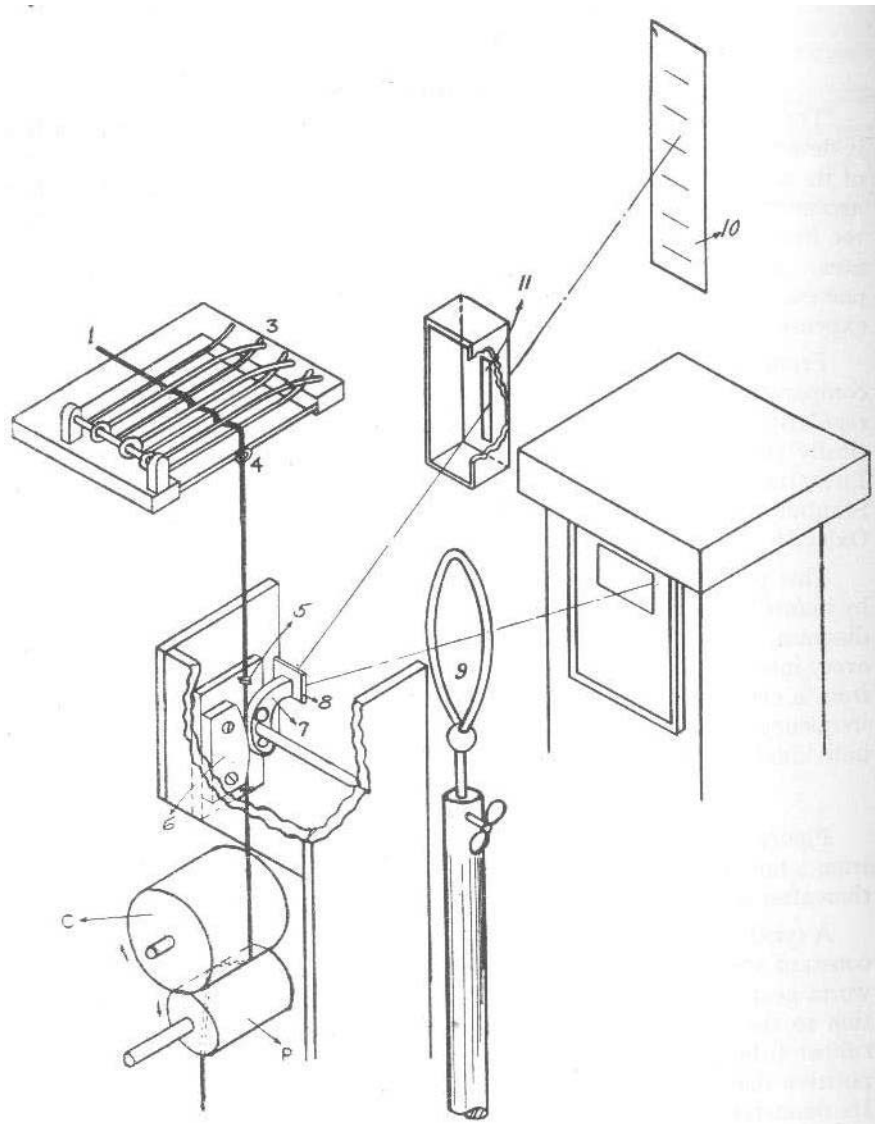


Figure 2.4 Compression Method II

2.2.3 Capacitive Methods

Capacitive methods of determining yarn irregularity are the most popular and widely used. This method simply provides accurate and reliable results when used

under proper conditions. Mack[29] provided a detailed investigation of principle of capacitive methods.

A change in the mass of the dielectric between two plates of an electronic capacitance sensor will change the capacity of the sensor. The capacitance of a capacitor is proportional to the quantity of charge that can be stored in it for each Volt difference in potential between its plates. Mathematically this relationship is written as:

$$C = \frac{Q}{V}$$

Where, C : capacitance in farads

Q : quantity of stored electrical charge in coulombs

V : difference in potential in Volts

The capacitance of a capacitor is also affected by three factors: the area of the plates, the distance between the plates and the dielectric constant of the material between the plates. Thus, capacitance C could also be determined by:

$$C = \epsilon \frac{A}{D}$$

Where, C : capacitance in farads

ϵ : dielectric constant in farads/meter

A : area of the plates in m²

D : distance between the plates in meters

ϵ is also defined as the permittivity of a material in terms of the capacitance of a capacitor. As an uneven yarn goes through the space between two plates, the

permittivity changes, and, consequently, the capacitance of the capacitor changes as well.

The key element in measuring yarn evenness is the detecting electrode. This consists of a pair of metal plates, acting as an air-spaced capacitor, between which the yarn is constrained to pass. The two plates need to be carefully placed in an accurately parallel position to ensure the accuracy of measurement. In Pelton and Slater's[30] work, the importance of an extra plate placed beside the effective plates, called guard electrode, was also addressed.

Boyd[31] stated that the capacity of a capacitor will change dependent upon the dielectric constant of the material, the amount introduced and its shape or form. In the case of relatively loose fibrous compositions, such as yarns and slivers, a capacitor can be chosen such that the change in capacity could be considered to be linearly proportional to the weight of material between the plates without introducing any serious error. However, Walker[32] pointed out that the relationship between yarn mass and capacity change becomes non-linear when the yarn/air ratio increases beyond acceptable limits and electrode becomes overloaded. Thus, indicated by him, the fiber assembly should not exceed 40% of the air gap between two plates. Some conclusions on changes in capacitance due to the insertion of a yarn were given by Mack[29]. They are:

- The yarn passing through the capacitor should be as cylindrical as possible.
- The yarn should not be asymmetric in texture.

- The radius of the yarn should be small compared with the dimensions of the capacitor.
- Position of the yarn between the plates is not important provided it is not near either plate and not near the edges of the plate.
- If the yarn can't keep same distance from two plates when passing through the testing zone, it is better for the yarn to be in constant contact with one of two plates.

2.2.4 Optical Methods

The fundamental principle of this method is the silhouette effect. A light source is directed onto a yarn, and the shadow cast, which should be proportional to the yarn thickness, is projected on a sensing device. This method measures yarn thickness which is better related to fabric appearance than yarn mass. But this method does have its own shortcomings. The major one concerns the cross-sectional profile of the specimen. As we know, the shape of yarn cross-section is not exactly circular. The position of light source and sensing device is fixed, but those asymmetrical yarns tend to go through testing interval in a preferential direction of alignment because of the guide rollers. This makes the measuring results inconsistent with the true ones. Hairiness of the yarn may also affect the results.

A photoelectric device was developed to overcome the problem of yarn alignment by using two incident beams of light, perpendicular to each other, to derive a signal. This device has better correlation with fabric irregularity[33].

Another more popular example of such apparatus is G585 Yarn Structure Tester from Zweigle[34]. Fig. 2.5 shows working principle of this tester.

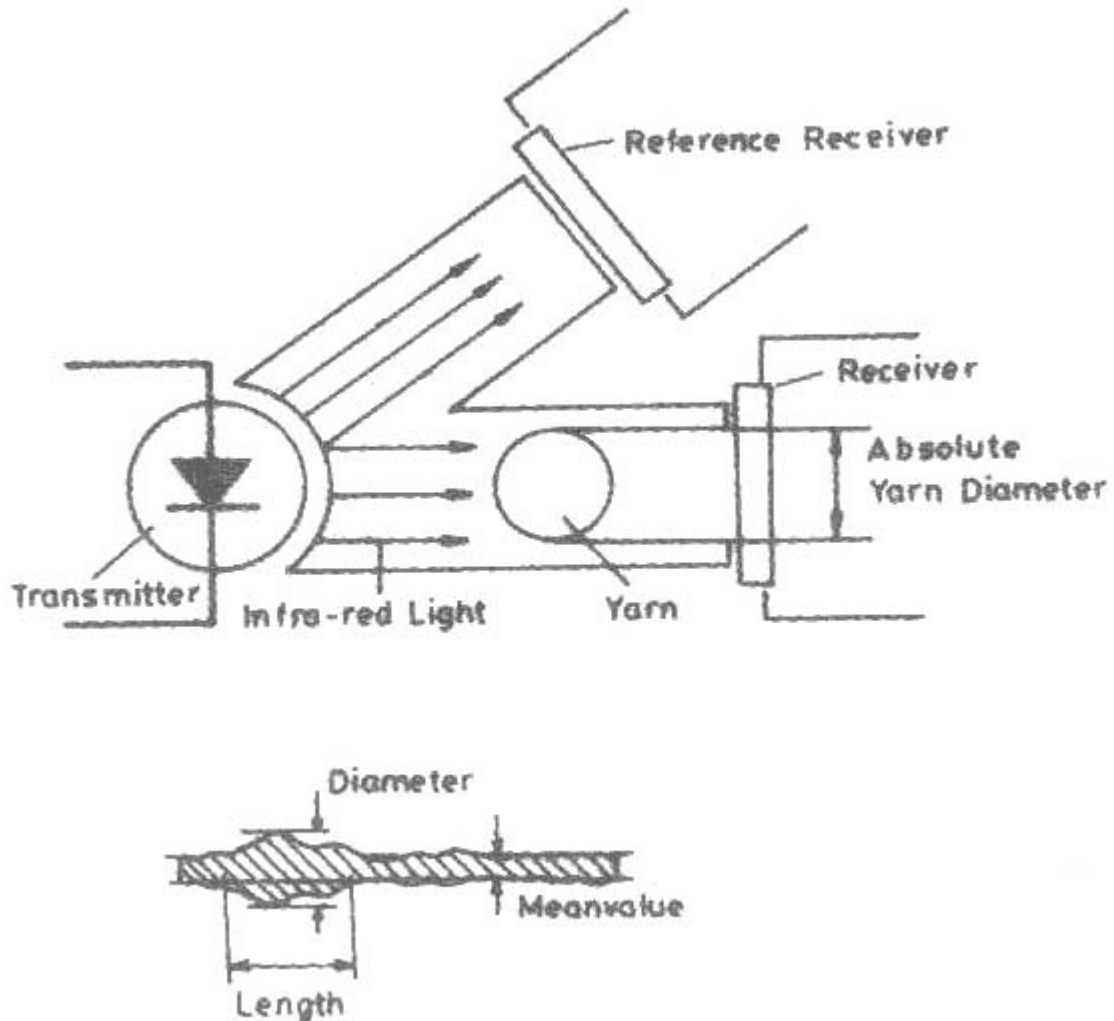


Figure 2.5 Working Principle for Zweigle® G585

Yarn passes between an infrared light source and a photo-receiver. Scanning of the yarn as it passes through the sensor is done every 2mm and the measured value of yarn diameter is compared with the constant reference mean to obtain

deviations in yarn diameters every 2mm of yarn length with reference to the length passing through the sensor. This apparatus is widely used in fabric simulation systems, such as CYROS[®], OASYS[®] etc., as yarn evenness testing device[35].

2.3 Methods for Expressing Irregularities of Spun Yarns

2.3.1 Coefficient of Variation

In order to handle large quantities of measured data statistically, the Coefficient of Variation (CV%) is commonly used to define variability. It is defined by the square root of the quadratic deviation of mass per unit length from the mean mass per unit length expressed as percentage of the mean mass per unit length. The precise mathematical definition is given as:

$$CV \% = \frac{100}{\bar{x}} \cdot \sqrt{\frac{1}{t} \int_0^t (x_i - \bar{x})^2 \cdot dt}$$

where, \bar{x} : mean value of measured estimates of the material mass per unit length

t : evaluation time

x_i : instantaneous value of the mass

Usually, the property is evaluated by the expression:

$$CV \% = 100 \cdot \frac{\sigma}{\bar{x}}$$

where, σ is the standard deviation of measured estimates.

An other description of irregularity is U%, which is defined as the percentage deviation of mass per unit length from the mean mass per unit length. The mathematical expression of the definition is:

$$U \% = \frac{100}{\bar{x} \cdot t} \int_0^t |x_i - \bar{x}| dt$$

Larger deviations from the mean value are much more intensively taken into consideration in CV% because of the term $(x_i - \bar{x})^2$ in the definition. Moreover, the larger deviations from the mean value have greater effect on appearance of yarns, processing behavior of yarns and, subsequently, the fabric properties. Thus, CV% is considered to be a better descriptor for yarn irregularity.

2.3.2 Variance-Length Curves

There are two types of variation-length curves; B(L) which measures the variation of masses between the unit lengths, and V(L) which measures the variation of masses within the unit lengths. Historically, the variance-length curves were determined by means of cutting and weighing equal lengths of a yarn, roving or sliver[36]. The pioneering work on this area was carried out by Townsend and Cox[37]. They mentioned and summarized earlier authors' work on some different aspects of the relation between variance and the length of yarn measured. Their original treatment was based on the relation between a measurement unit length L of yarn and the mean standardized variance, V(L), within random samples length L. The “mean standardized variance” is simply the

square of the CV. Then they defined $B(L)$ as the standardized variance between the means of lengths L of yarn and derived the relation:

$$V(L) + B(L) = V(\infty)$$

where, $V(\infty)$ is the overall variance.

The $B(L)$ and $V(L)$ can be calculated from mean fiber length and mean number of fibers in yarn cross section. When the unit length is greater than mean fiber length, the following relations hold:

$$B(L) = B(0) \cdot \frac{\bar{l}}{L}$$

and

$$B(0) = \left(\frac{100}{\sqrt{\bar{n}}}\right)^2$$

L : unit length

\bar{l} : mean fiber length

\bar{n} : mean number of fibers in yarn cross section

When the unit length is less than the fiber length:

$$B(L) = B(0) \cdot \left(1 - \frac{L}{3 \cdot \bar{l}}\right)$$

The $V(L)$ can also be calculated:

$$V(L) = V(\infty) - B(L) = B(0) - B(L)$$

In Cox and Ingham's work[10], they addressed that $V(\infty)$ is also equal to $B(0)$. Both $V(\infty)$ and $B(0)$ represent the overall variance. Also, $B(L)$ and $V(L)$ can be defined for thickness (number of fibers per cross-section), fiber end density and turns of twist per unit length, etc.

The general shapes of the $V(L)$ and $B(L)$ curves are given in Fig. 2.6.

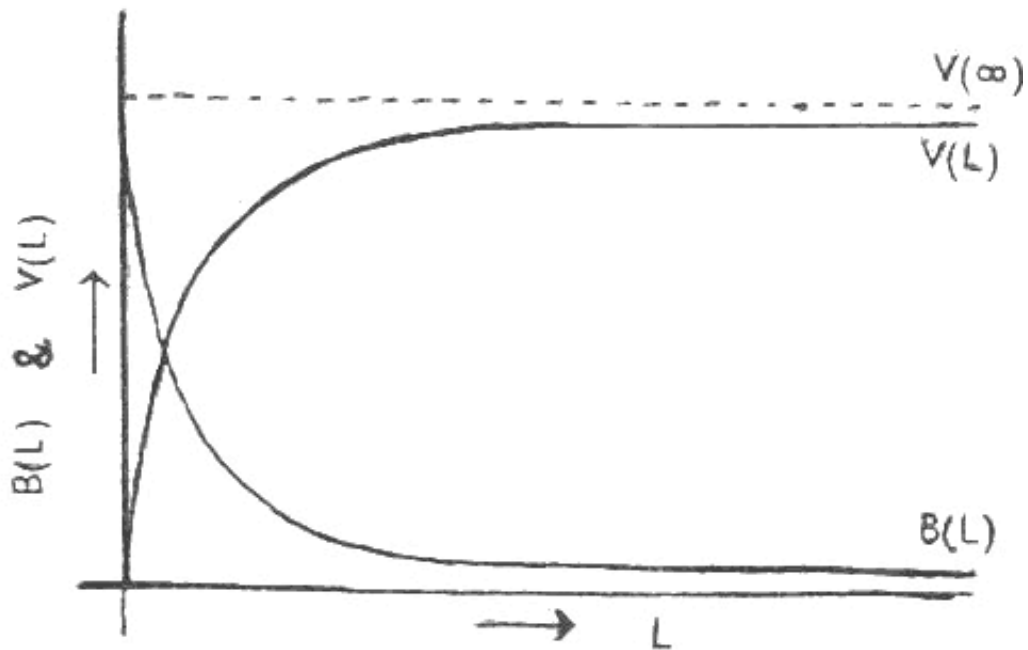


Figure 2.6 General Shapes of $V(L)$ and $B(L)$

As we can see from the figure above, the $V(L)$ value will increase as the yarn test length increase. This is simply because additional length involves more opportunity for variation to arise. However, when the cut-lengths increase to a sufficiently large value, almost all determinations of variation in a yarn will be in

one such length. Thus, the $V(L)$ curve will rise to an asymptotic value, $V(\infty)$. Since there is no variance within a yarn of zero length, the $V(L)$ curve should begin at the origin. Townsend and Cox[37] discussed the meaning of rapidity of approach to $V(\infty)$, the gradient at the origin and scatter of individual variance.

When the cut-lengths get longer, the differences between the lengths becomes less. This makes $B(L)$ a falling curve. $B(L)$ curve has an initial value of $B(0)$, which is also the overall variance, and then falls, rapidly at first and more slowly subsequently, to an asymptotic value of zero at very long lengths. It was quickly realized that the $B(L)$ curve is more useful than $V(L)$ curve. It is a more sensitive measure over the region where variation is most likely to exist and is easier to establish by the basic method of cutting and weighing pieces of yarn[33].

Evenness testers generally provide $B(L)$ values of many cut-lengths like 0.1m, 1m, 3m, 10m, 50m and 100m, which correspond to separate points along the $B(L)$ curve. The $B(L)$ curve is suitable particularly for the interpretation and indication of non-periodic mass variations.

Chapter 3. Development of Models for 2-D and 3-D

Image Representation

The main focus of the model development is on the yarn data captured from yarn measurement system and the woven fabric geometry. We try to use an image representation method to show the fabric appearance without actually weaving the fabric. These images should come from on-line yarn data directly. To achieve the goal, we need to build a model which takes the yarn data as the input and generate the fabric quality images as output. This method includes two parts. One is the simulation of yarn arrangement in the fabric; the other is the image representation method. In order to investigate properties of variance-area curves, two models are considered. One is the location-specific mapping with the weft yarn and the other is with the random arrangement of the weft yarns. In these two models, warp yarns are always considered to be arranged randomly. Shuttle and shuttleless looms have different mechanisms with respect to weft yarn insertion. In shuttle looms, the weft yarns are inserted in two directions, whereas in shuttleless looms, weft yarns travel in only one direction. We take the case of shuttleless loom for the model with weft yarn location-specific mapping. We consider fabric as a 2-D matrix. Every entry comes from entire yarn data set. The plain weave was chosen as the foundation of this model. Plain weave produces the simplest form of interlacing. The repeat

consists of 2 warp yarns and 2 weft yarns, each interlacing in alternate order over or under a pick.

3.1 Data Points in a Yarn

Yarn data captured is measured spatially, every 1mm, along a single yarn, we captured one data point for each 1mm segment. The measurement data is projected yarn cross section in mm. Fig. 3.1 shows the data within a yarn. Captured yarn diameter data from CTT machine is saved as .txt file, which is to be used as the input file of MATLAB programs.

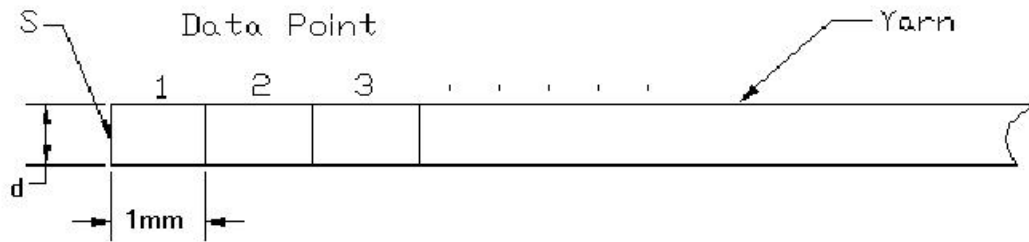


Figure 3.1 Measured Yarn Data Within a Yarn

3.2 Geometry of Yarn Layout within a Woven Fabric

Assign these data into two models (2-D matrix) according to plain weave fabric geometry. In these models, we are simulating a fabric with a total of 1412 weft yarns and 1412 warp yarns. The design is shown in Fig. 3.2(a). Interlacing points could be seen clearly in this diagram. Fig. 3.2(b) is a side view of plain weave fabric. The following assumptions are made for this model:

- For our 2-D matrix, we only chose those interlacing points as matrix entries.
- Weft density = warp density = 4 yarns/mm.
- There is no yarn waste in selvage part.

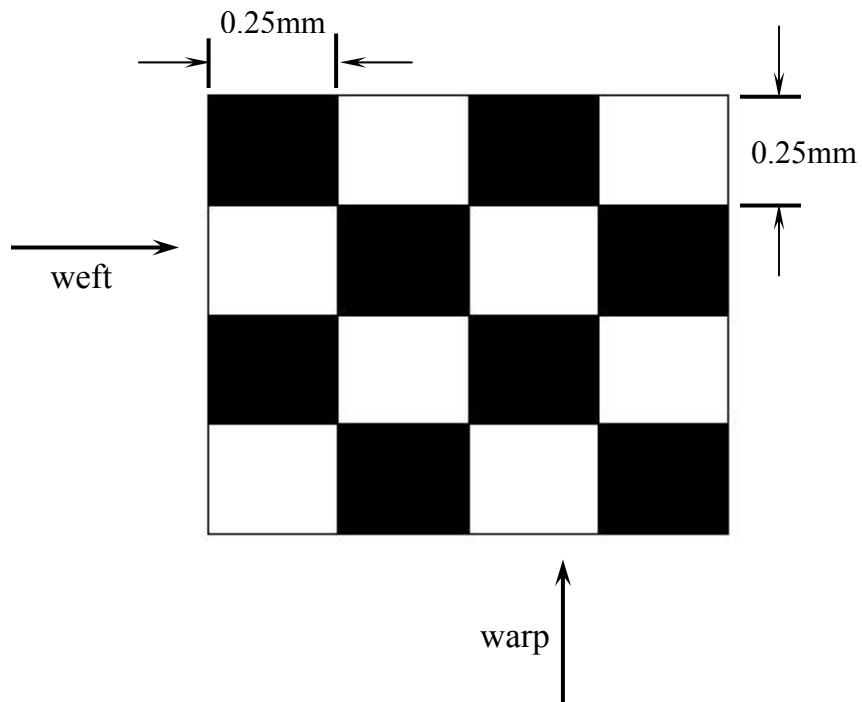


Figure 3.2(a) Plain Weave Pattern

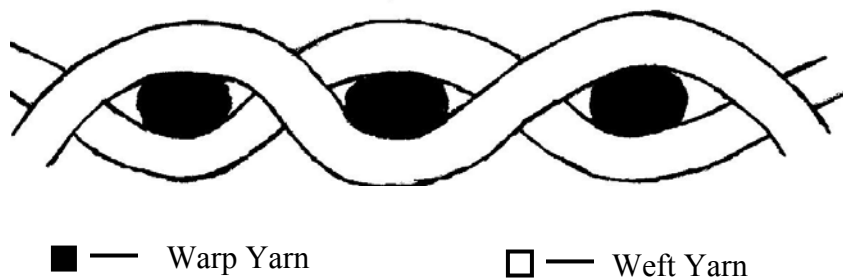


Figure 3.2(b) Side View of Plain Weave Fabric

Each entry in the model is the summation of weft yarn diameter data and warp yarn diameter data at that interlacing point. This 2-D matrix has total $1412 \times 1412 = 1,993,744$ entries (yarn interlacing points). As shown in Fig. 3.2(a), there are 4 interlace points in 1mm segment on one weft yarn or one warp yarn. Since we have 1412 warp yarns in the model, each weft yarn will have a length of $1412 \div 4 = 353$ mm. The total number of weft yarns is 1412. Thus, for the model with weft yarn location-specific mapping, $1412 \times 353 = 498,436$ yarn data points are needed. Warp yarn data will be randomly chosen from the same data set.

In our experiment, 500,000 yarn data is actually captured for each yarn sample. The data file is loaded as a column matrix and reassigned into a 2-D matrix by the MATLAB program.

On shuttleless loom fabric, all of weft yarns go in one direction. Fig. 3.3 shows the weft yarn arrangement on a shuttleless loom fabric. Point “S” in Fig. 3.3 is the same point also denoted by “S” in Fig. 3.1. Because we assumed that there is no selvage yarn waste, point “B” is the neighbor point of “A” in a yarn.

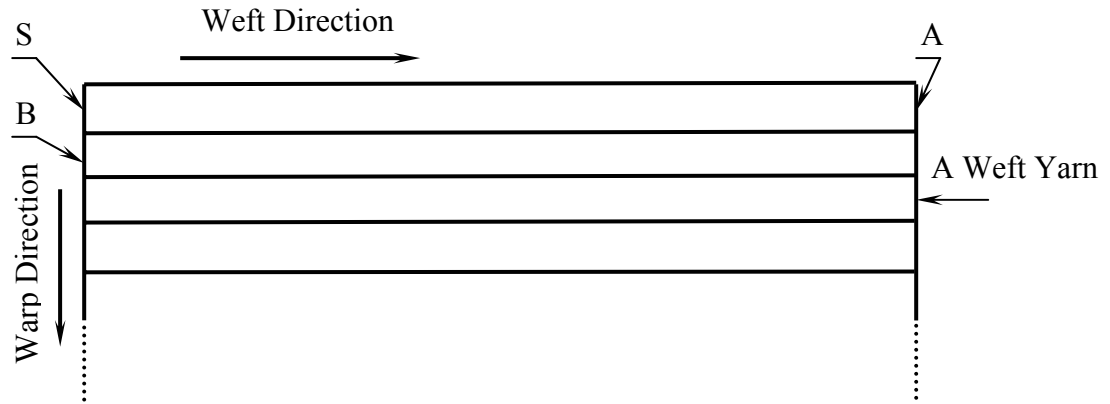


Figure 3.3 Weft Yarn Arrangement on Shuttleless Loom Fabric

For the model with random weft yarn arrangement, both of weft yarns and warp yarns are chosen from yarn data set randomly. In this case, the two points “A” and “B” in Fig. 3.3 are not necessarily the neighboring points in the yarn data set.

3.3 2-D And 3-D Representations of Fabric Quality

2-D and 3-D visualization of this 2-D matrix is done by MATLAB graphics package. 2-D gray scale image is used in representing thickness variation of a large area of fabric and 3-D image is for a small area of fabric.

In MATLAB program, any area on the 1412 weft yarns by 1412 warp yarns fabric can be represented in either 2-D or 3-D form.

Chapter 4. Variance-Area Curves for Fabric Uniformity

4.1 Earlier Work on Variance-Area Relation

Corresponding to the Variance-Length relation along a yarn, there is also a Variance-Area relation for textile fabrics. This relation stresses the variation of a property in its dependence on the measured area. Wegener[38] and his co-workers call this relation a Surface-Variation Function. By analogy with the ‘within’ and ‘between’ variance-length relations, Wegener also talked of ‘internal’ and ‘external’ surface-variation functions. Many different properties could be related to the functions, such as surface mass (g/cm²), fabric thickness and adsorption etc. Based on measured mass of many square fabric samples, the surface coefficient of variation, denoted by CB(F), is determined by:

$$CB(F) = \frac{100}{\bar{G}} \sqrt{\frac{1}{N-1} \cdot \sum_{i=1}^N (G_i - \bar{G})^2} (\%)$$

where, F : area of fabric samples (cm²)

\bar{G} : average mass of square samples of area F

G_i : mass of a square sample of fabric of surface area F

N : number of fabric samples

Wegener's paper focused on this external surface-variation function CB(F) of woven and knitted fabrics. Comparison between variance-length relation and variance-area relation for both woven and knitted fabrics was made.

4.2 Application of Variance-Area Curves to Woven Fabrics

The basic concept of variance-area relation was developed by Wegener, but it hasn't been used for evaluating the fabric qualities. Based on the two models depicted in chapter 3, we apply the concept of variance-area relation to the woven fabric. Seven different unit areas are chosen for plotting Variance-Area Curves of each yarn sample in both of the two models. For each unit area, CV(A) and CB(A) are calculated based on formula (1) and (2)

$$CV (A) = \frac{\sum_{i=1}^{N1} CV_i}{N1} \quad (1)$$

Where, CV_i : the CV% value of yarn data in i^{th} unit area;

$N1$: total number of unit areas within the fabric.

$$CB (A) = \frac{\sqrt{\sigma_B^2}}{\bar{\bar{x}}} \quad (2)$$

Where, $\bar{\bar{x}}$: total mean of all data points on the fabric, calculated by (3);

σ_B : standard deviation of mean values of all unit areas, calculated by

(4).

$$\bar{\bar{x}} = \frac{\sum_{i=1}^{N1} \bar{x}_i}{N1} \quad (3)$$

where, \bar{x}_i - mean value of all data points in i^{th} unit area.

$$\sigma_B^2 = \frac{\sum_{i=1}^{N1} (\bar{x}_i - \bar{\bar{x}})^2}{N1-1} \quad (4)$$

Another way to calculate the CV(A) is:

$$CV(A) = \frac{\sqrt{\frac{\sum_{i=1}^{N1} \sigma_{wi}^2}{N1}}}{\bar{\bar{x}}} \quad (5)$$

Where, σ_{wi} is the standard deviation within the i^{th} unit area, calculated by formula (6).

$$\sigma_{wi}^2 = \frac{\sum_{j=1}^N (x_{ij} - \bar{x}_i)^2}{N-1} \quad (6)$$

x_{ij} : value of the j^{th} interlacing point (data point) in the i^{th} unit area

N : total number of data points in a unit area

The value calculated by equation (5) is a little greater than the one calculated by (1). In the Fig. 4.1, the results are computed from the same yarn data set using

the same weft yarn mapping method. The dotted line (data1) represents computation results from equation (1), whereas the solid line (data2) represents computation results from equation (5).

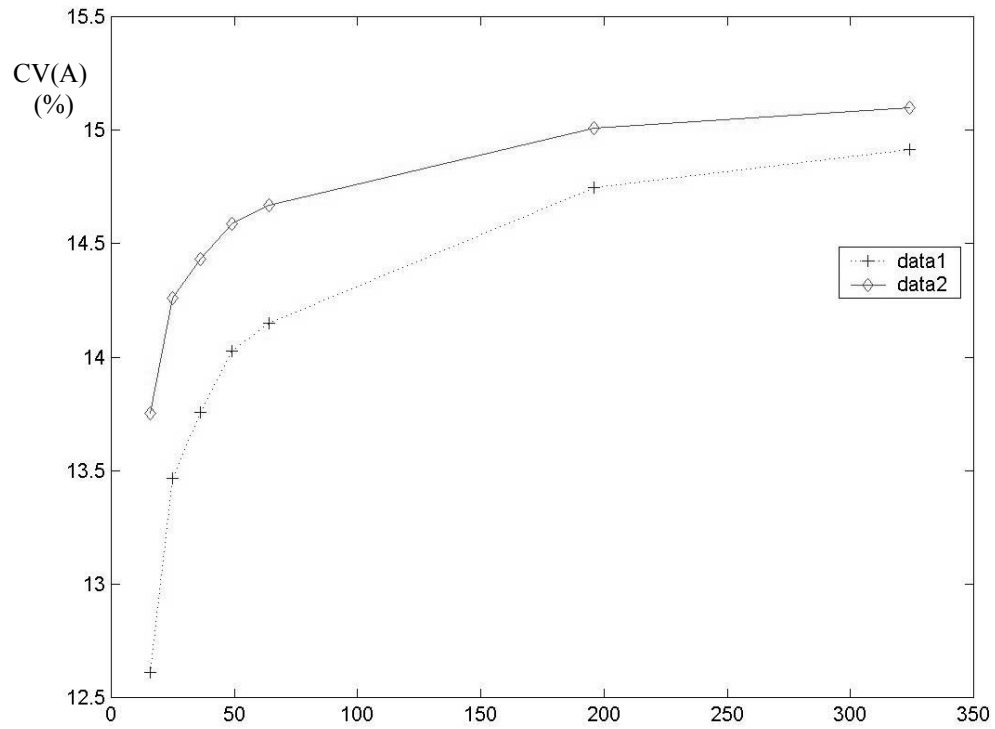


Figure 4.1 Difference Between The Two CV(A) Computation Methods

In this research work, the $CV(A)$ will be evaluated by equation (1). This method simplifies the computation process and parallels current practice of yarn uniformity test device.

All of these individual values of $CV(A)$ and $CB(A)$ are recorded and plotted in a coordinate. These curves are related to fabric appearance quality which will be shown in detail in later chapters.

Chapter 5. Yarn Measurement

A Lawson-Hemphill's CTT mounted with a Thompson 12-bit CCD line scan camera is the primary device for yarn measurement in this research. A program written in C, called "camera1", controls the camera and acquires the data. This program is running on a Linux Operating System platform. The line scan camera, a Thomson-CSF CCD TH78CA14, is a digital output camera with 1024 active pixel resolution. The number of pixels that are used in yarn diameter measurement is 1020.

Calibration of the measurement system and modification of the control program had to be finished before the yarn samples can be tested in order to obtain a set of accurate and useful yarn diameter data.

5.1 Calibration of CDD Camera

To make sure that the CCD line scan camera is working properly, we accomplished the following experiments:

1. Run the test procedure with light source blocked. This is to see if the camera will give out the similar light intensity value for every pixel used in tests. Fig. 5.1 shows the test results plotted in X coordinate as pixel number and Y axis as the light intensity. We can see that the light intensity of every pixel is about 30 without much variation.

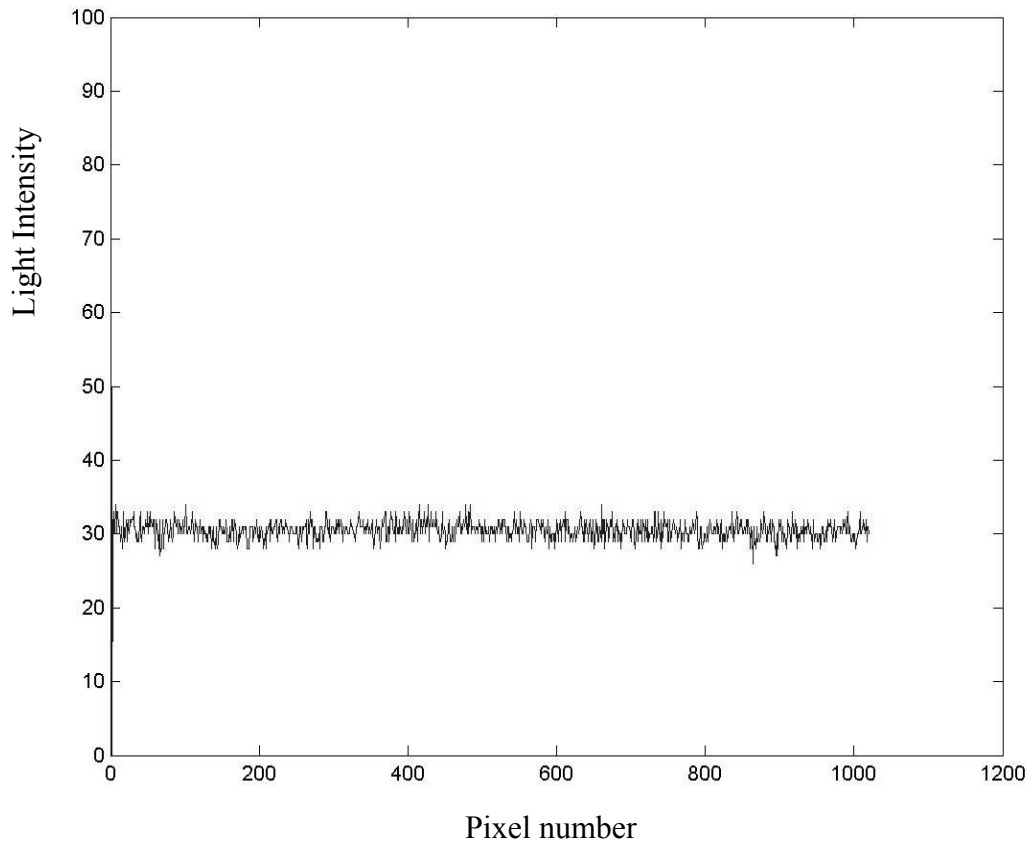


Figure 5.1 Light Intensity Values of Pixels With Block of Light Source

2. Run the test procedure without any block of light source. This was done using 10 different levels of light intensity. Shapes of plotted curves from results of these 10 levels of light intensity are very similar except for 10th curve. Fig. 5.2 shows the shape of the resulting curves. This curve is obviously different from the

curve in Fig. 5.1. Theoretically, the light intensity values of every pixel should be very close to each other when the light source is not blocked at all.

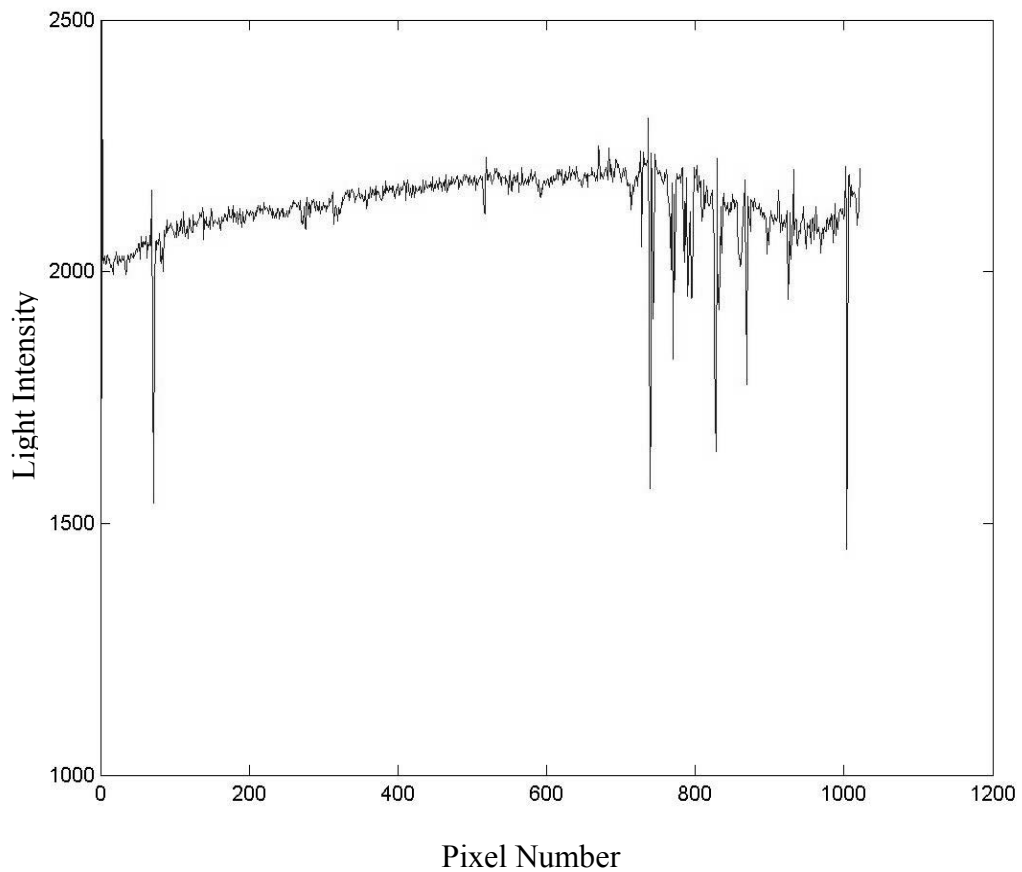


Figure 5.2 Shape of Resulting Curve without a Light Blockage

After we plot these 9 curves in a same coordinate, we found that those pixels that are far from mean light intensity value are always same ones. These 9 curves have same shape in different light intensity levels. This result is shown in Fig. 5.3.

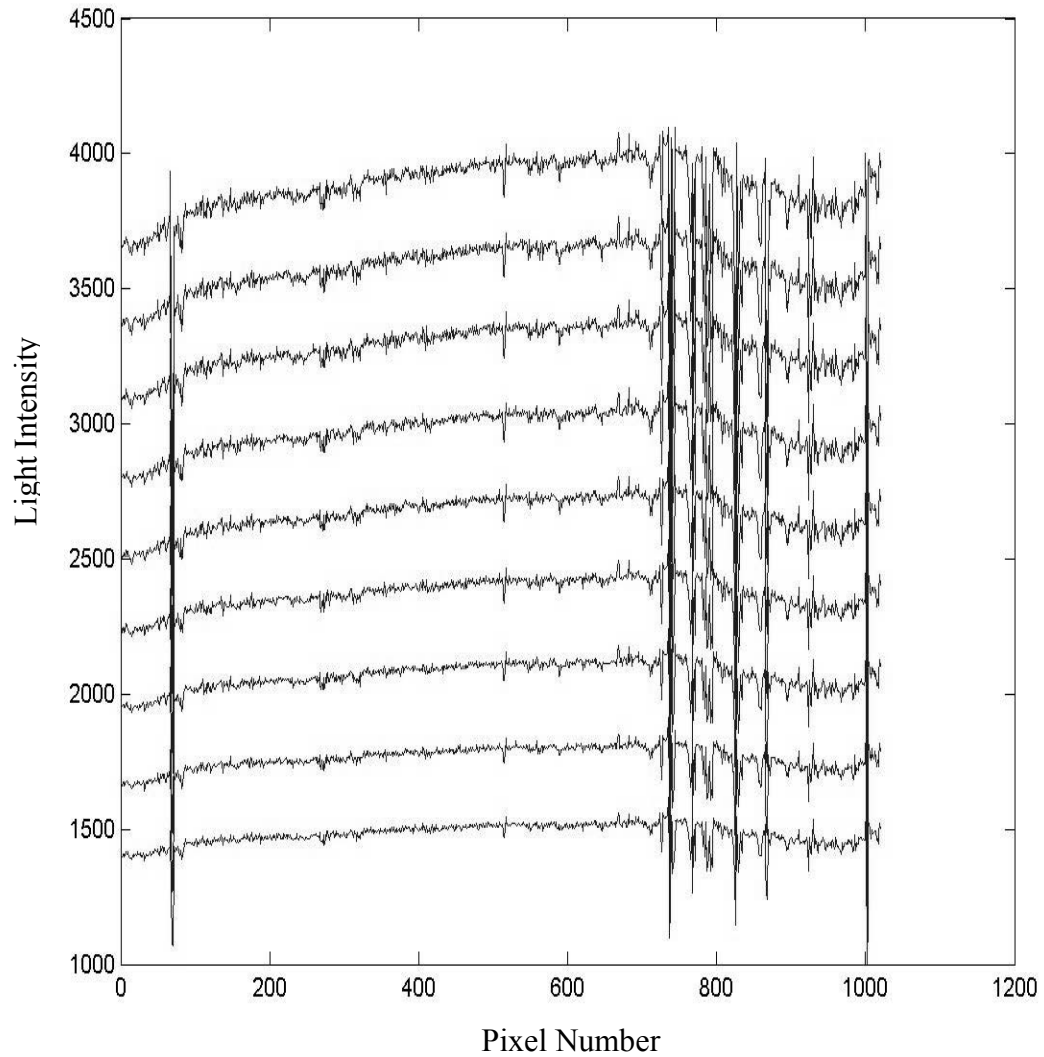


Figure 5.3 Nine Curves in a Same Coordinate

The last test done with the highest light intensity gave us an idea about the upper limit of light intensity, under which the CCD line scan camera can be used properly. This limit is shown in Fig. 5.4.

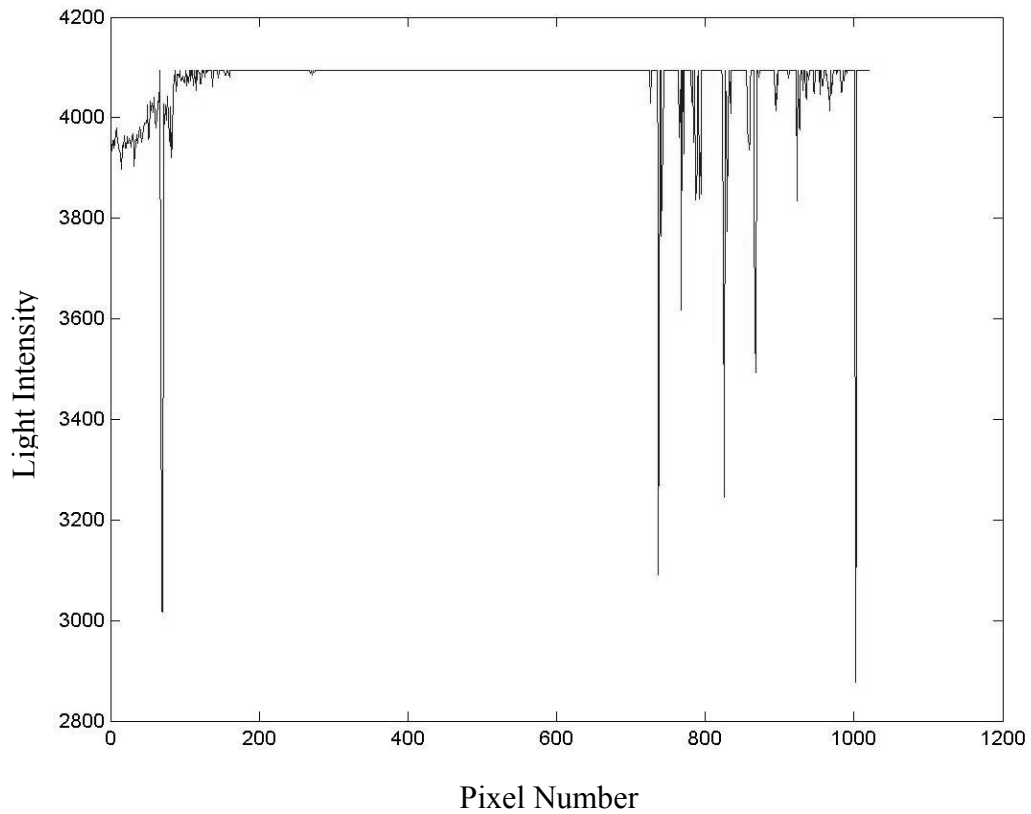


Figure 5.4 Upper Limit of Proper Working Light Intensity

3. Calibration of those abnormal pixels: In this step, the mean value of every pixel was calculated for the ten different light intensity levels and an error range was set between 6% less and 6% greater than the mean value. If an individual pixel value exceeds this range, this pixel is considered as an abnormal pixel. We found that each of these abnormal pixels always has the same ratio with the mean value, no matter what light intensity level we choose. In order to bring these abnormal pixels back into a normal range, each of these abnormal pixel values was multiplied by a certain factor.

Pixel number and correction factor are shown in table 5.1.

Pixel #	Factor						
68	1.143	69	1.348	70	1.351	71	1.052
735	0.946	736	1.117	737	1.387	738	1.256
741	1.139	742	1.110	768	1.153	787	1.071
788	1.066	792	1.072	794	1.072	824	1.124
825	1.227	826	1.277	829	1.071	830	1.092
866	1.106	867	1.181	868	1.200	923	1.071
1002	1.499	1003	1.294				

Table 5.1 Abnormal Pixels and Correction Factors

After this result was embedded in our camera control program, we tested CCD line scan camera again without any block of light source. The test result is shown in Fig. 5.5.

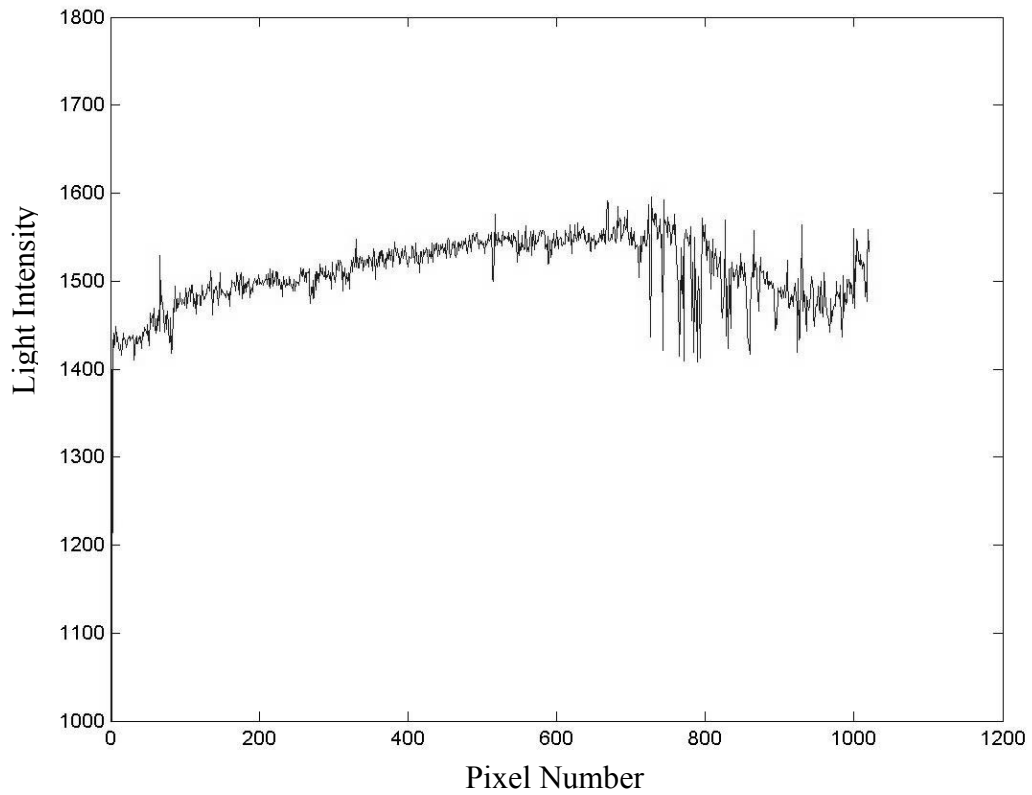


Figure 5.5 Light Intensity Values After Calibration

4. Relationship between camera output and real diameter: A typical output of line scan camera is the number of pixels which have lower light intensity value due to the block of light source. This is shown in Fig. 5.6.

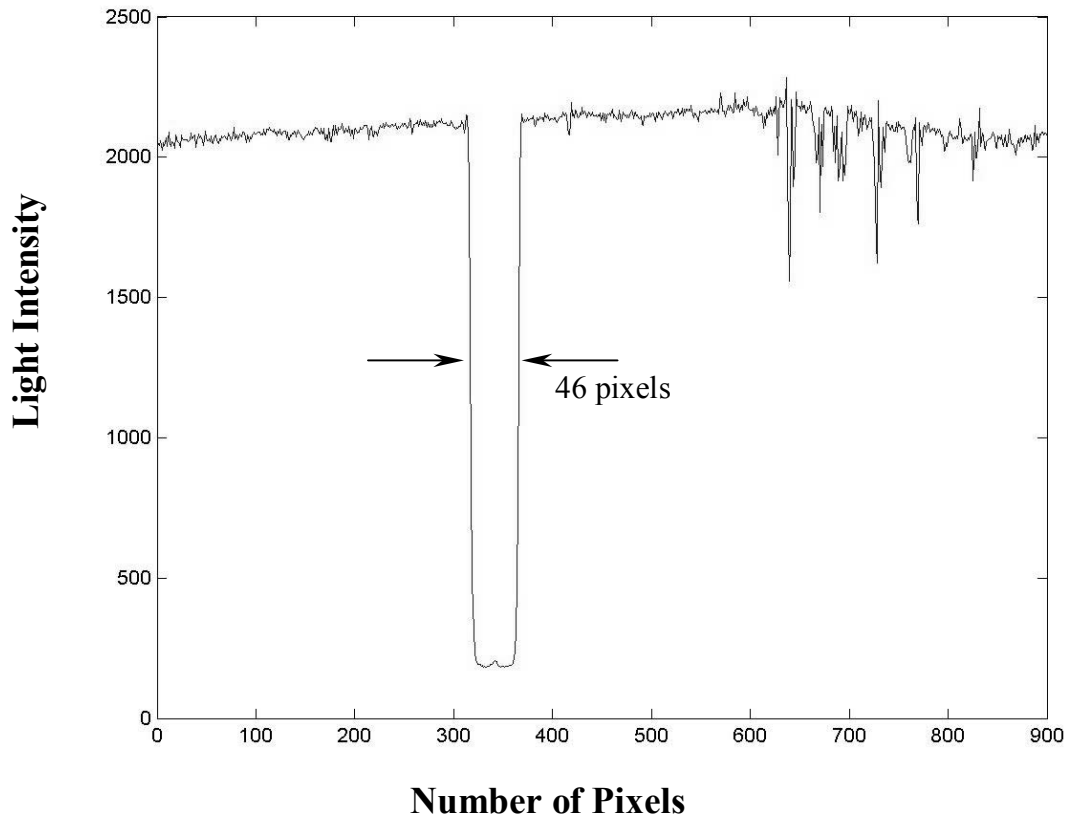


Figure 5.6 Typical Output of Line Scan Camera

However, what we need is not the number of pixels, but real diameters. In order to find out the relation between number of pixels and real diameter, 8 metal wire samples with different diameters were tested. The diameter (in mm) was found to be proportional to the pixel width by a factor of 0.0046 mm/pixels. Test results are shown in Table 5.2.

Sample #	Number of Pixels	Diameter (mm)	Factor
1	46	0.21	0.00457
2	79	0.36	0.00456
3	89	0.41	0.00461
4	109	0.50	0.00459
5	133	0.61	0.00459
6	158	0.73	0.00462
7	213	0.98	0.00460
8	233	1.10	0.00472

Table 5.2 Results of Metal Wire Tests

From these results, we concluded that:

$$\text{Diameter} = \text{camera output (number of pixels)} \times 0.0046 \text{ mm/pixels}$$

5.2 Calibration of CTT

CTT machine is to provide a constant tension and velocity to the yarn, which is being tested. Output rollers are running at a constant speed once the yarn transport speed is set. A mechanical system is responsible to adjust the speed of input rollers. In this way, tension on a tested yarn can be changed. After make sure that every roller and pulley is working properly with good lubrication, the only thing

that needs calibration is the tension arm. This tension arm and the mechanical system together is the device providing a constant tension. CTT machine and yarn path are shown in Fig. 5.7.

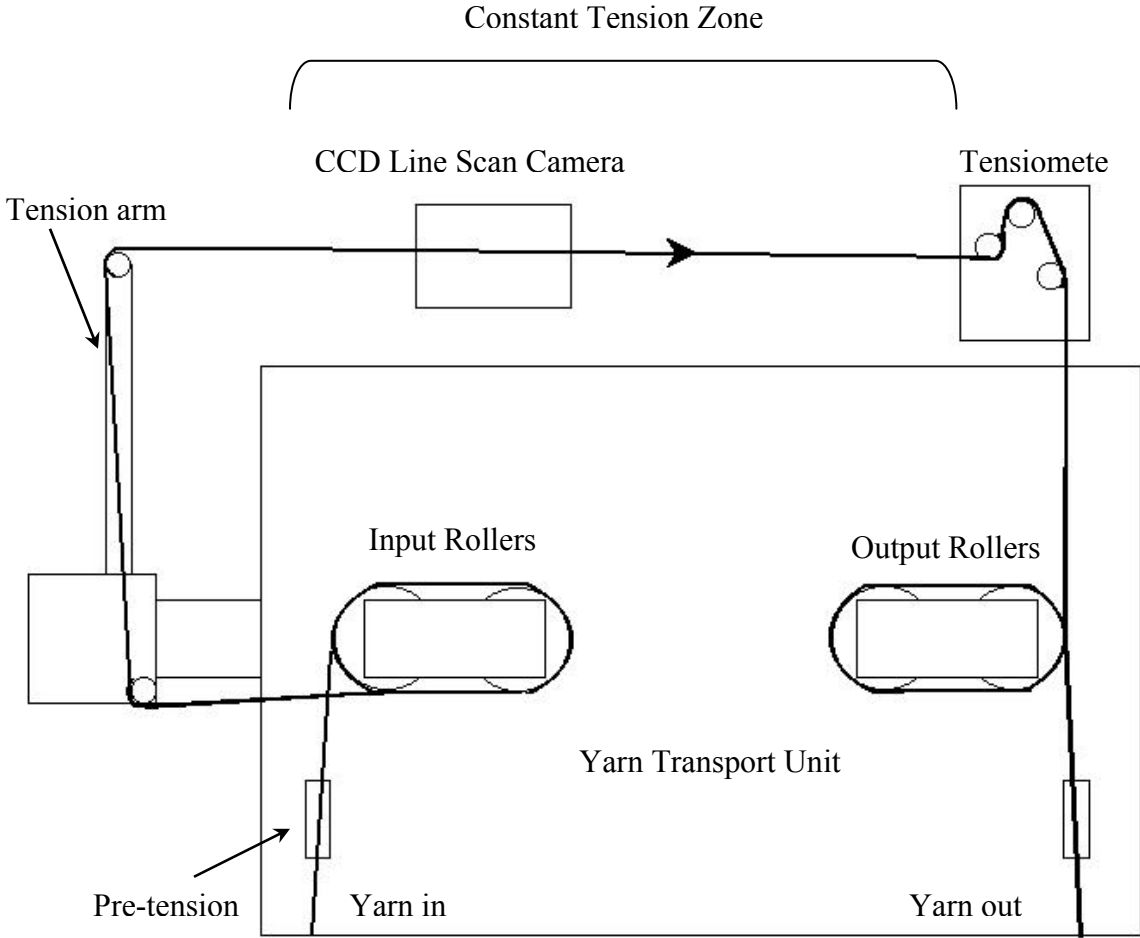


Figure 5.7 Constant Tension Transport

On the bottom of tension arm, there is a spring and a scale. Tightness of the spring can be adjusted by a screw so that a read number on the scale is actually the

tension, in Gram Force, applied on a tested yarn. Three different balance weights, 20g, 50g and 100g, were used for spring calibration.

After the camera calibration and the tension calibration were accomplished, another problem we encountered was to write an output data file for the CYROS[®] fabric simulation system.

5.3 Control Program Modification

CYROS[®] yarn data files have the extension ".dat" by default. They contain binary data and consist of 2 sections:

- A header containing information such as measure-speed, minimum diameter etc.
- The measured data

The header is a C-structure of type RD_HDR as defined below:

```

typedef struct {
    int    count;
    float  increment;
    float  mean_value;
    float  min_value;
    float  max_value;
    char   customer[STRINGLENGTH];
    char   user[STRINGLENGTH];
    char   material_name[STRINGLENGTH];
    char   yarn_number[STRINGLENGTH];
    char   rawmaterial1[STRINGLENGTH];
    float  percentage1;
    char   rawmaterial2[STRINGLENGTH];
    float  percentage2;
    char   rawmaterial3[STRINGLENGTH];
    float  percentage3;
    int    yarn_count;
    int    sample_count;
    float  measure_length;
    int    measure_speed;
} RD_HDR;

```

where, STRINGLENGTH = 128. Total size of the header is 944 bytes.

The following table, Table 5.3, gives detailed information for each entry in yarn data file header:

Entry #	Entry Name	Description	Length (bytes)
1 st	count	Most important entry: The number of measured data after the header	4
2 nd	increment	The distance between 2 samples on the thread in mm.	4
3 rd	mena_value	The mean-diameter of the yarn in mm	4
4 th	min_value	The minimum-diameter of the yarn in mm	4
5 th	max_value	The maximum-diameter of the yarn in mm	4
6 th	costumer	String to save various information	128
7 th	user	String to save information about the user	128
8 th	material_name		128
9 th	yarn_number	e.g. in NeC	128
10 th	rawmaterial1	Name of rawmaterial e.g. Cotton	128
11 th	percentage1	e.g. 50.0	4
12 th	rawmaterial2	e.g. Polyester	128
13 th	percentage2	e.g. 50.0 the sums of the percentages should give 100 obviously	4

Table 5.3 Structure of Yarn Data File Header

Entry #	Entry Name	Description	Length (bytes)
14 th	rawmaterial3		128
15 th	percentage3		4
16 th	yarn_count	CYROS can do measure several cones one after the other (yarn_count) and do several samples for each cone (sample_count)	4
17 th	sample_count		4
18 th	measure_length	Length of the measurement in m. Obviously one should have measure_length = 0.001 * increment * count	4
19 th	measure_speed	In meter per minute.	4

Table 5.3 Structure of Yarn Data File Header (Continued)

The yarn data is following this file header and has properties below:

- Each data is stored as one byte.
- Divide this byte by 100 to obtain yarn diameter in mm.
- Each yarn data has a valid range from 0.01 mm (binary 0) to 2.55mm (binary 255).

From this it follows that the size of a yarn data file in byte is $\text{sizeof}(\text{RD_HDR}) + \text{header.count}$, which is $944 +$ the number of measured yarn data. In the original control program, a function called “SaveYarndata” was embedded. This function is specifically for writing a CYROS[®] yarn data file.

5.4 Yarn Sample Tests

An external or internal source can be selected for generating a trigger to the camera. For internal source our camera is generating pulses in free mode, while the external source is generated from encoder pulses. These pulses are trigger signal to the frame grab control. When the camera works in free mode, it basically captures pictures and sends pixel values to control program as fast as it can. When external pulses are generated every 1mm from external encoder, corresponding to 1mm of yarn, it takes a picture.

In our yarn sample test procedure, external signal were used in order to capture one data every 1mm. We found that if we increase the yarn transport speed higher than 24 m/min on CTT, some data points were missed. This problem is related to the speed of CPU and PCI bandwidth. To make sure that we capture one data for every 1mm yarn segment, we decreased our yarn transport speed to 20m/min.

Ten yarn samples were chosen for our experiment. Material of these samples is 100% cotton. For each sample, 500m yarn was tested, or 500,000 data points. Some detailed information of these samples is shown in table 5.4.

Yarn sample #	Cotton Count	Twist (per inch)	Min (mm)	Max (mm)	Mean (mm)	CV%
1	18.4	16	0.13	1.6	0.25	18.7
2	28.7	21	0.09	1.27	0.21	24.38
3	40.5	23	0.09	0.81	0.17	19.07
4	5.6	10.5	0.26	1.64	0.5	18.82
5	10.1	12	0.17	1.84	0.37	21.81
6	19.6	16	0.13	1.99	0.27	21.99
7	12.4	11.5	0.17	1.20	0.38	19.19
8	24.4	17.5	0.12	1.24	0.23	18.85
9	34.4	5.5	0.10	1.32	0.20	23.03
10	18.8	17.5	0.14	1.07	0.25	16.33

Table 5.4 Tested Yarn Samples

Chapter 6. Results and Conclusions

For each of the 10 yarn samples, measured yarn diameter data was inputted in the Matlab[®] models and CYROS[®] system. 2-D gray scale images and 3-D fabric quality images are given by Matlab[®] models. Simulated fabric images are given by CYROS[®] system. These three different types of images have their own characteristics:

- 2-D Gray Scale Image:

Bigger valued data points in our models correspond to the darker points in images, analogous to the would-be appearance of the fabric specimen viewed with an evenly dispersed lighting behind – the more fabric mass to block the light transmission, the darker will be the appearance.

- 3-D Image:

Based on a plane, bigger measurement values in our models correspond to the higher peaks in 3-D images.

- Simulated Fabric Image:

This type of images will simulate actual fabric appearance with fabric structure.

Besides the image representations of predicted resulting fabrics, Variance-Area Curves for each sample are also given through calculations by Matlab[®] programs.

6.1 2-D Image Representation

As explained in section 3.2, there are total 500,000 data points measured for each yarn sample. That gives a fabric with 1412 warp yarns by 1412 weft yarns. Undoubtedly, a rectangle can be decided by two endpoints on the diagonal line. Thus, any rectangular area at any location within this 1412X1412 fabric can be conveniently picked out for 2-D image representation by choosing different sets of two points in the fabric. In this paper, the whole fabric (1412 yarns by 1412 yarns) is chosen for 2-D representation so that the overall appearance qualities of the predicted fabrics could be compared. For example, 2-D image for sample #2 is shown in Fig. 6.1.

2-D Image For Yarn Sample #2 (I)

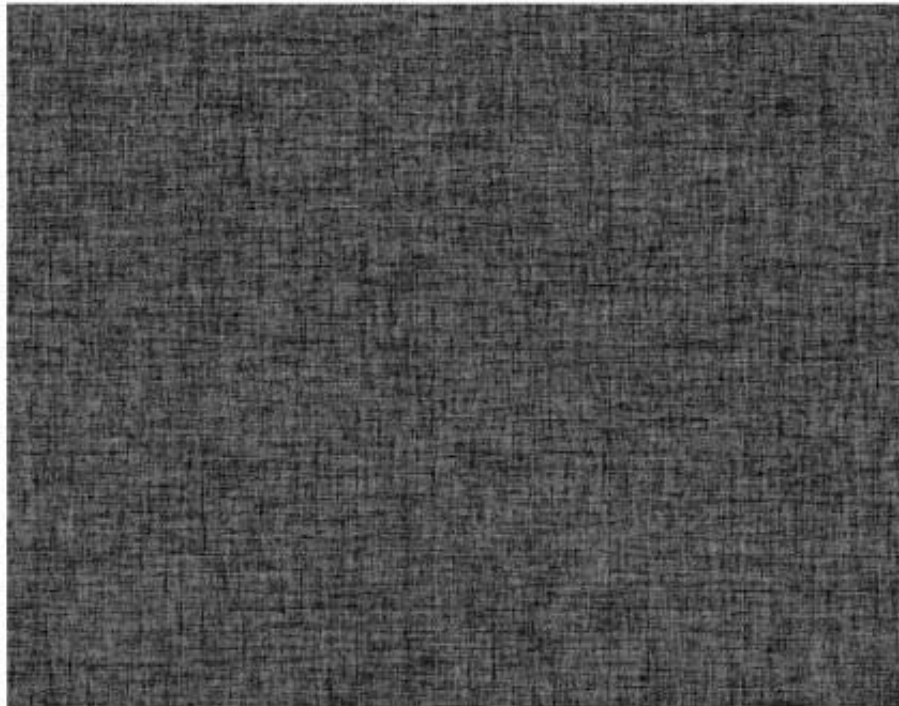


Figure 6.1 2-D Image for Data #2 Processed by Model I
- 1412X1412 Interlacing Points

This image is for yarn data sample #2 processed by model I, which is the model with weft yarn location-specific. It has relatively obvious appearance variations when we compare it with the image shown in Fig. 6.2, which is for sample #10. Cloudiness and neppiness effects could be more obviously seen in Fig. 6.1 and Fig. 6.3. The V-A curves of these two samples will be compared later in this chapter.

2-D Image For Yarn Sample #10 (I)

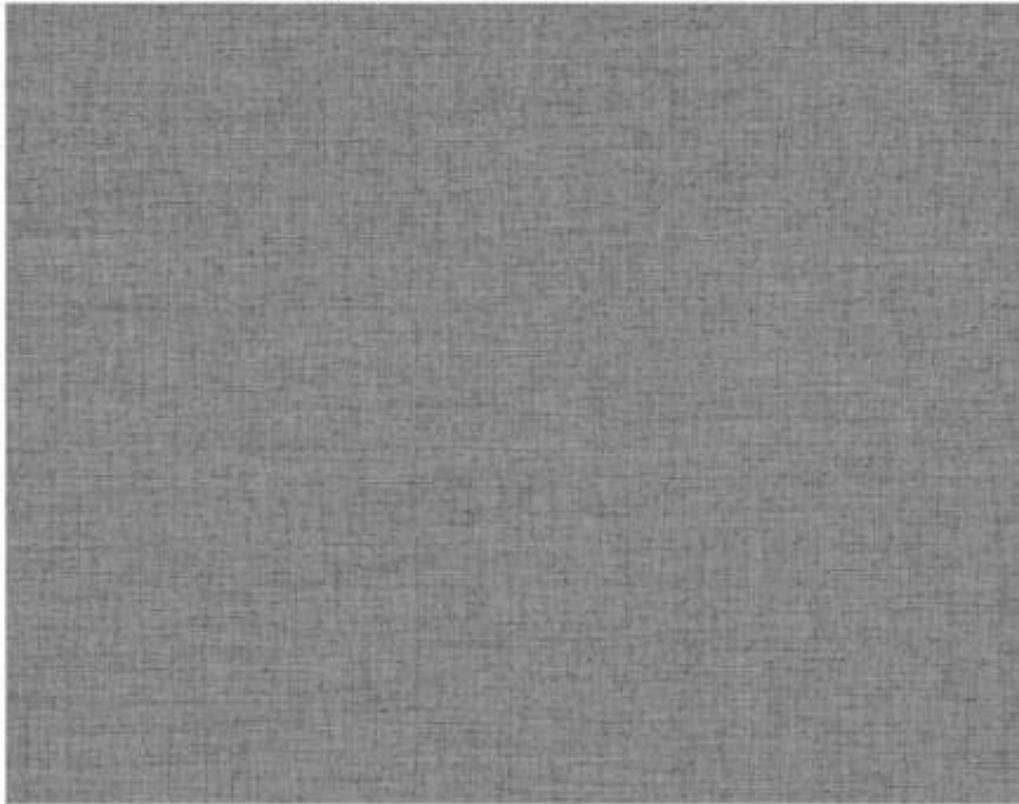


Figure 6.2 2-D Image for Data #10 Processed by Model I
- 1412X1412 Interlacing Points

When the difference between the results from model I and model II is studied, we can also see from images that for a same yarn data set, model I and model II doesn't make much difference. Fig. 6.3 shows a 2-D image for yarn data #2. But this time, the image is made by model II, which is without weft yarn location-specific.

2-D Image For Yarn Sample #2 (II)

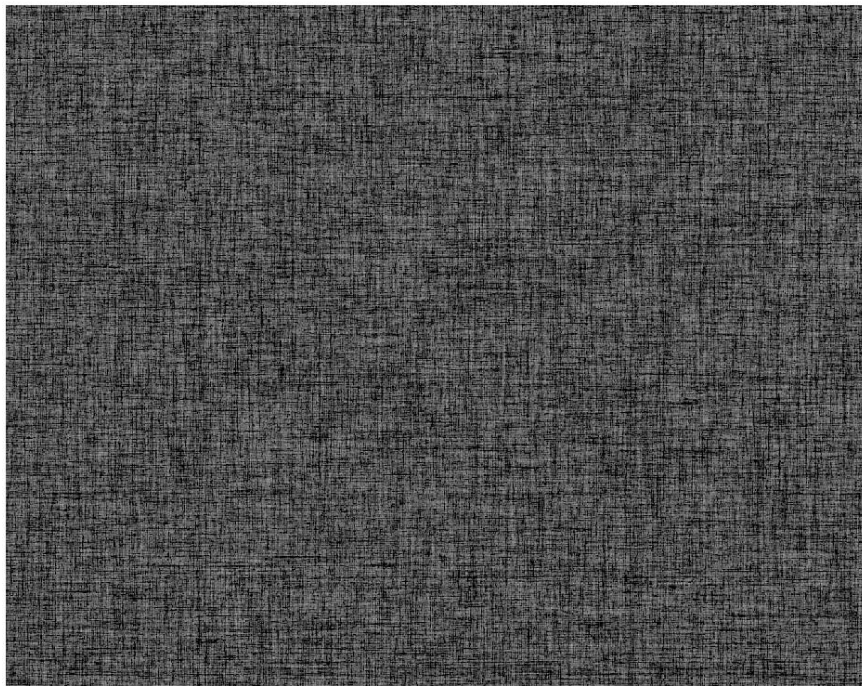


Figure 6.3 2-D Image for Data #2 Processed by Model II
- 1412X1412 Interlacing Points

Other 2-D images for each data sample will be presented in appendices following this paper.

6.2 3-D Image Representation

In our model, all of the points within the predicted fabric will be sampled. Each one of these corresponds a point in a 3-D image. Thus, a too large area on the fabric will cause too many points in one image, which makes it very hard to recognize the appearance quality. Fig. 6.4 shows an example of this situation. This image is from data set #11 and model II. The number of total points in this image is $400 \times 400 = 160,000$, which is even less than one twelfth of the amount in a 2-D image we processed. The 3-D effect is not clearly seen in this image.

3-D Fabric Quality Image for Sample #10 (II) (400 X 400 Points)

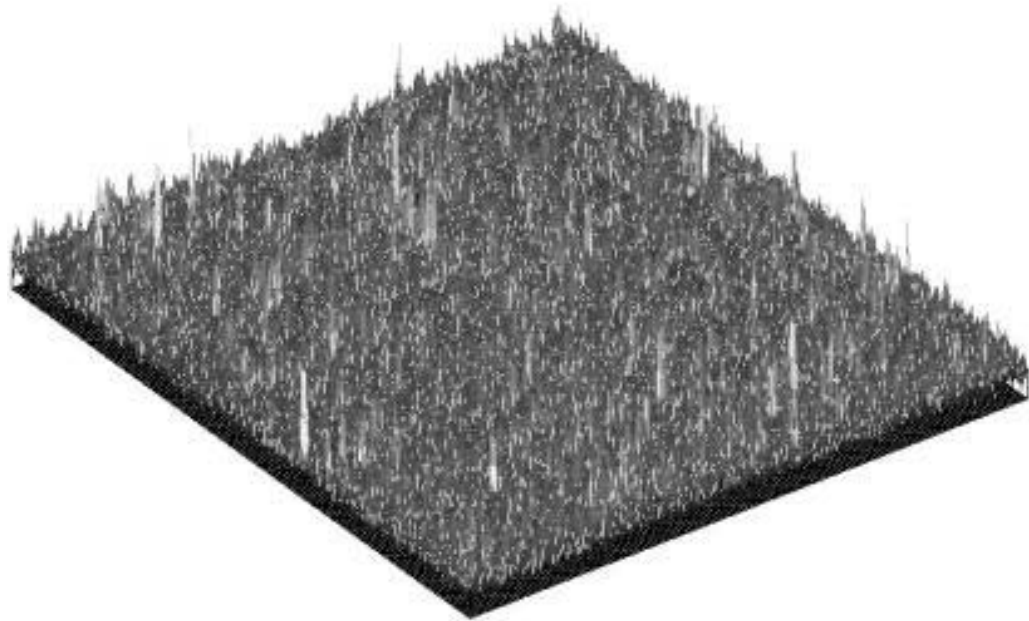


Figure 6.4 3-D Image with 160,000 Data Points
- 400X400 Interlacing Points

As explained in section 6.1, only two points on the fabric are needed to select a subset of the image data for quality comparison. Fig. 6.5 and Fig. 6.6 show two 3-D images, which are representative of two different local areas on a same predicted fabric. The size and location of these two 3-D images are shown in Fig. 6.7 with two squares. Fig. 6.5 corresponds to the left one and Fig. 6.6 corresponds to the other.

3-D Fabric Quality Image for Sample #10 (II) (100 X 100 Points)

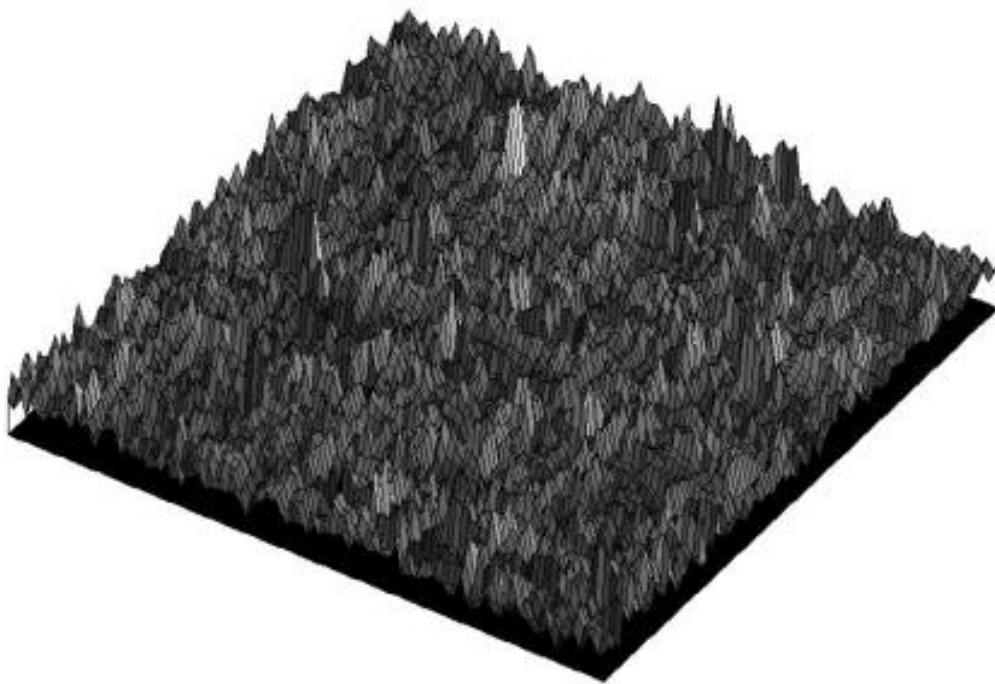


Figure 6.5 3-D Image with 10,000 Points
- Corresponding to Section A in Fig. 6.7

It could be clearly seen that there is larger appearance variation in the right square (Fig. 6.6) than that in the left square (Fig. 6.5) on the fabric.

3-D Fabric Quality Image for Sample #10 (II) (100 X 100 Points)

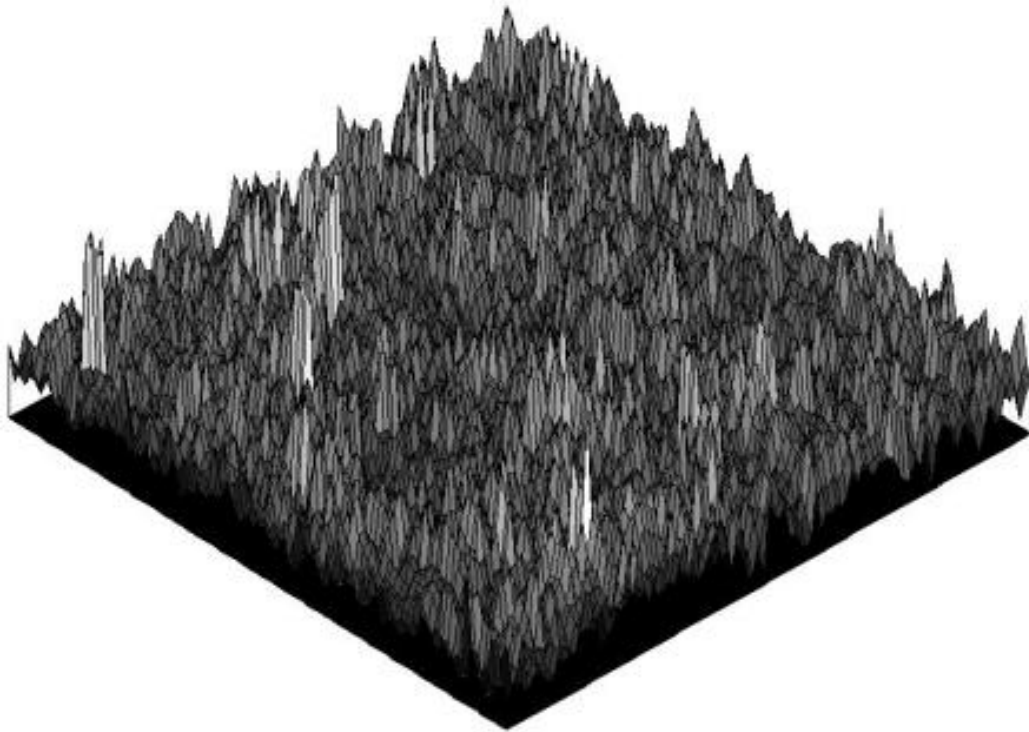


Figure 6.6 3-D Image with 10,000 Points
- Corresponding to Section B in Fig. 6.7

2-D Image For Yarn Sample #10 (II)

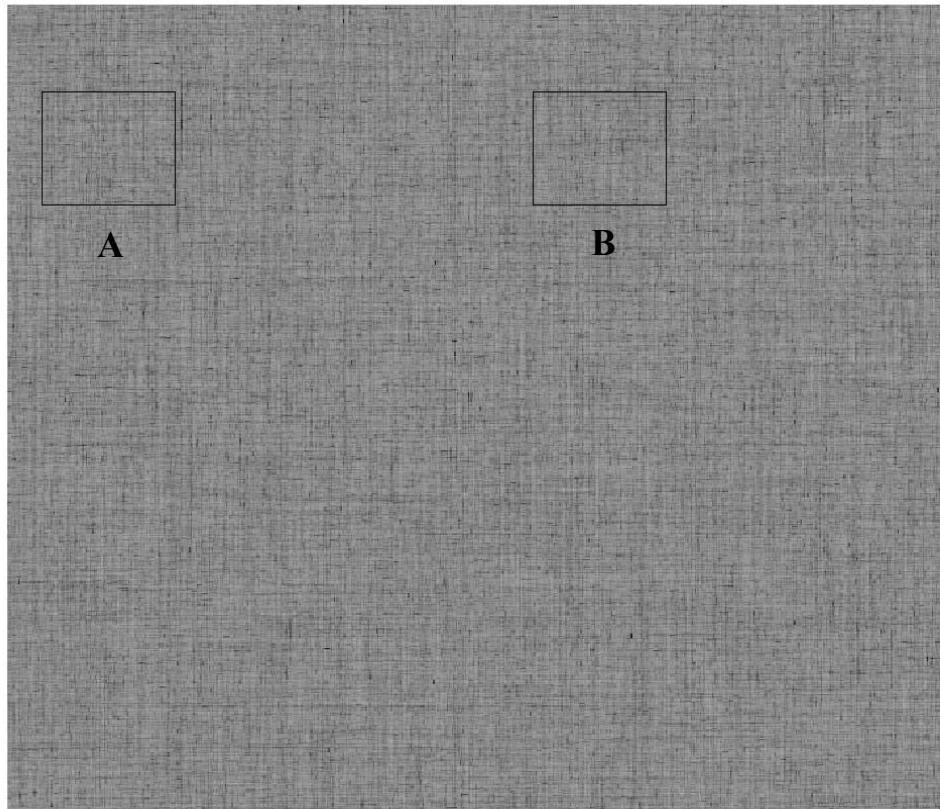


Figure 6.7 2-D Image with Two Specified Squares
- A & B for Micro Images Shown in
Fig. 6.5 & Fig. 6.6

6.3 Simulated Images from CYROS[®] System

CYROS[®] (Cotton Yarn Rating through On-line Simulation) system was developed by CIS graphics in collaboration with Cotton Inc. and College of Textiles, at North Carolina State University. This system is composed of a yarn evenness tester called PREMIER[®] Evenness Converter, a PC system, a high-resolution color printer and the CYROS[®] software. In this research, yarn diameter data is gained by using the yarn measuring system described in chapter 5 instead of PREMIER[®] tester. Different samples have different diameters. Hence, a simulated fabric image is produced for each sample with different yarn densities shown in Table.1. All other parameters used for all samples are same. Fig. 6.8 shows these parameters and the software interface.

Sample#	1	2	3	4	5	6	7	8	9	10
Yarn density (1/mm)	3.5	4.2	5.1	1.7	2.4	3.2	2.3	3.8	4.4	3.5

Table 6.1 Yarn Densities Used in CYROS[®] Simulation

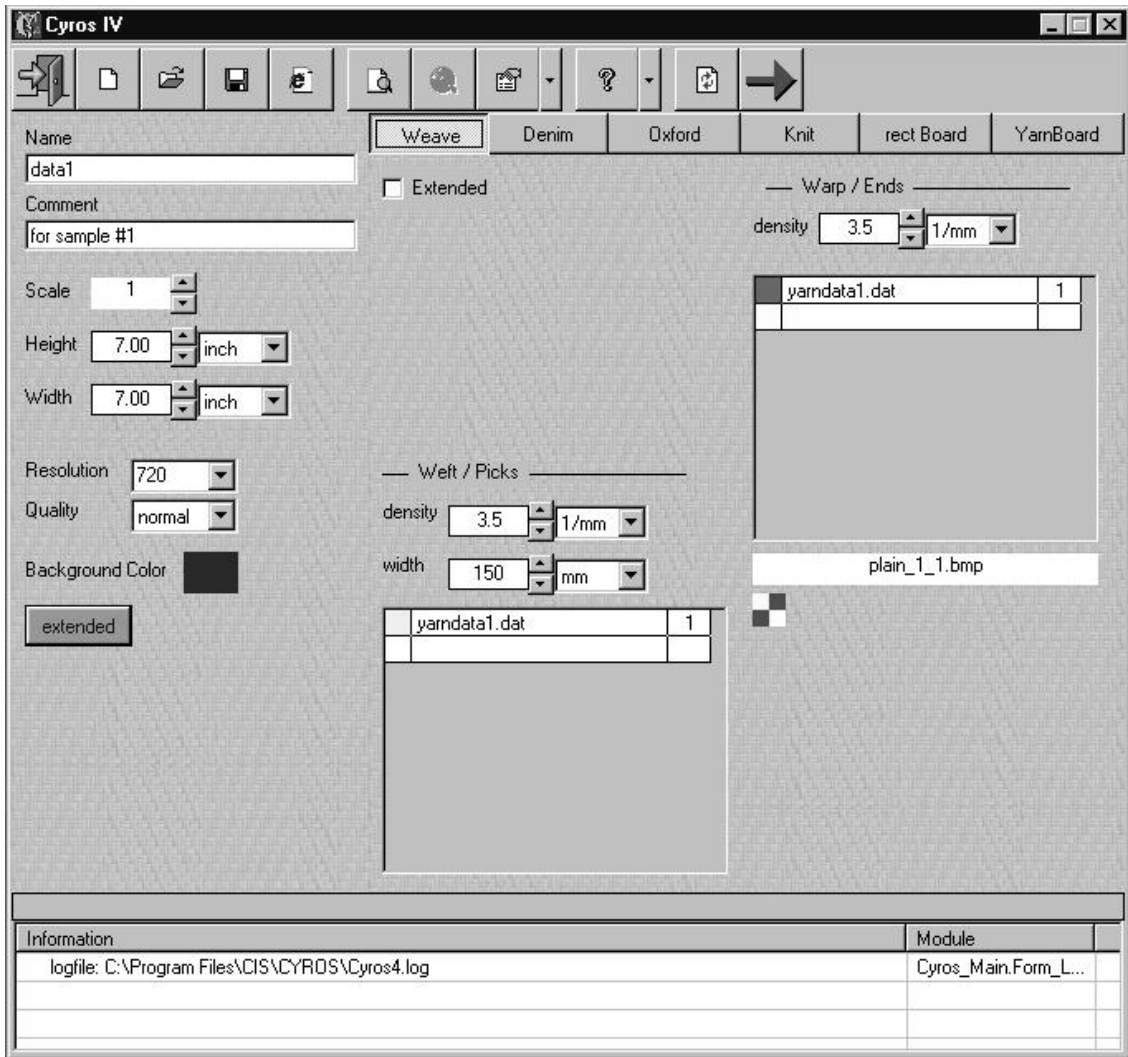


Figure 6.8 CYROS® IV Software Interface

All of ten simulated images will be given in the appendices. For comparison purpose, images for sample #2 and sample #10 are given here. Fig. 6.9 and Fig. 6.10 show the simulated fabric images for sample #2 and sample #10 respectively.

Obviously, the appearance variation in Fig. 6.10 is much smaller. The barre and streakiness effects can be clearly seen in Fig. 6.9 but not in Fig. 6.10. This difference can be related with CB(A) curves that will be discussed in next section.

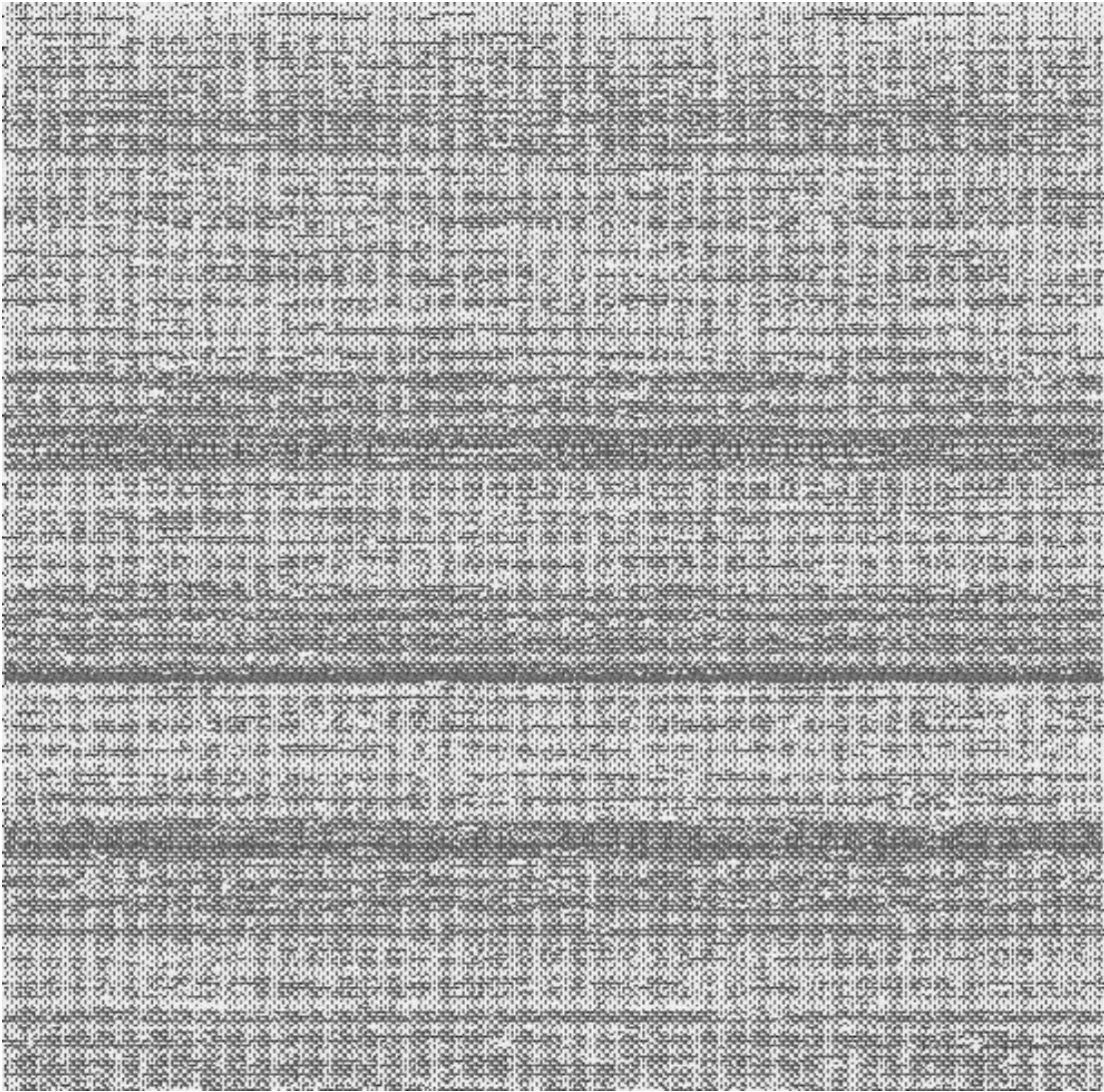


Figure 6.9 Simulated Fabric Image for Sample #2

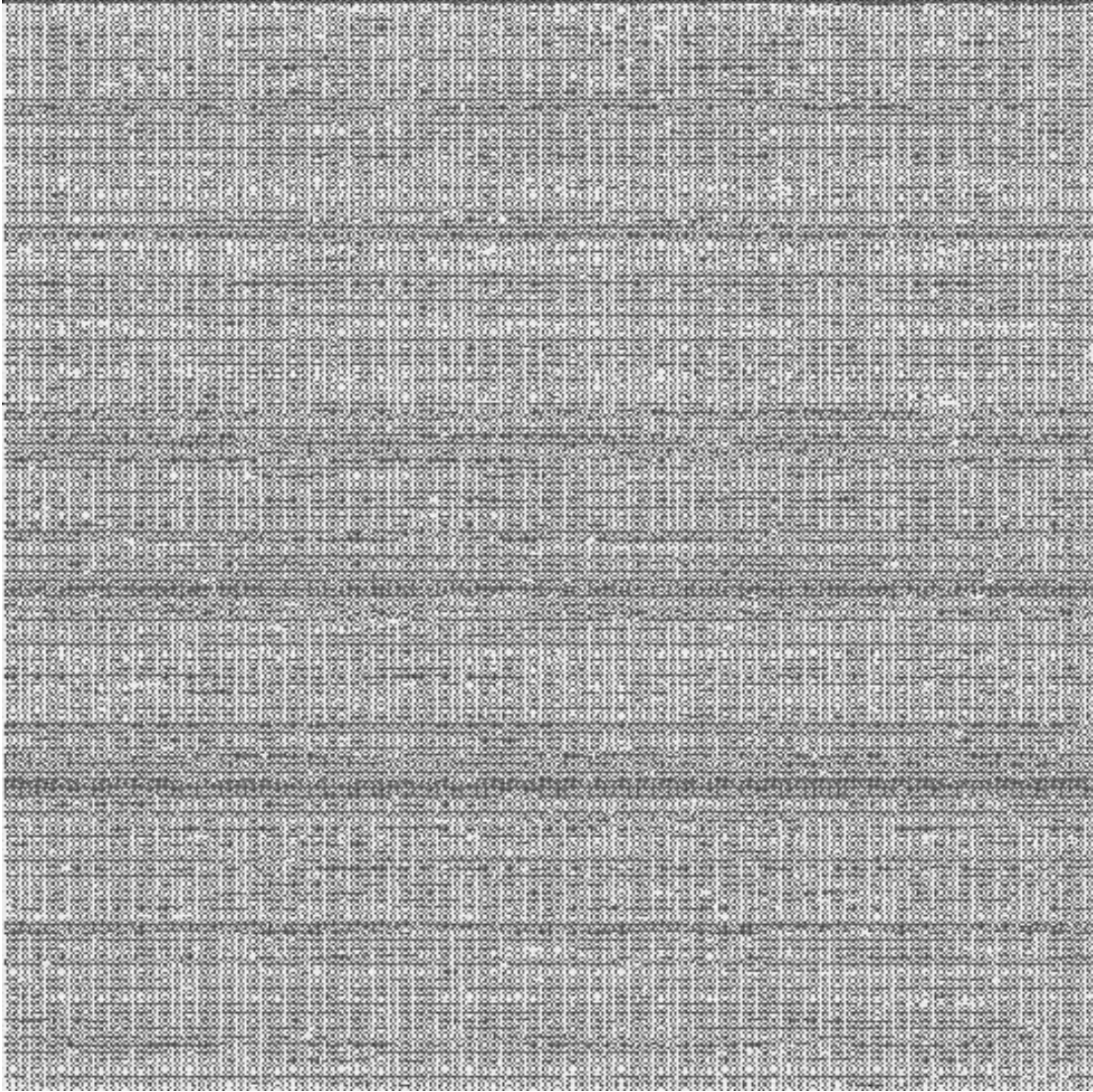


Figure 6.10 Simulated Fabric Image for Sample #10

The results from comparing these two images are also consistent with the results from 2-D image comparison.

6.4 Variance-Area Curves

According to the calculation method described in section 4.2, the values of $CB(A)$ and $CV(A)$ of 7 different unit areas are evaluated for 10 samples in each of 2 models. Results from model I are shown in Table 2 and results from model II are shown in Table 3. If $CB(A)$ of sample #2 and #10 are plotted in a same coordinate (as shown in Fig. 6.11), the difference between the two $CB(A)$ curves can be clearly seen. This is consistent with the result from comparison made in section 6.3. $CV(A)$ curves of these two samples also show that sample #2's 'within' variance is larger than #10's.(Fig. 6.12)

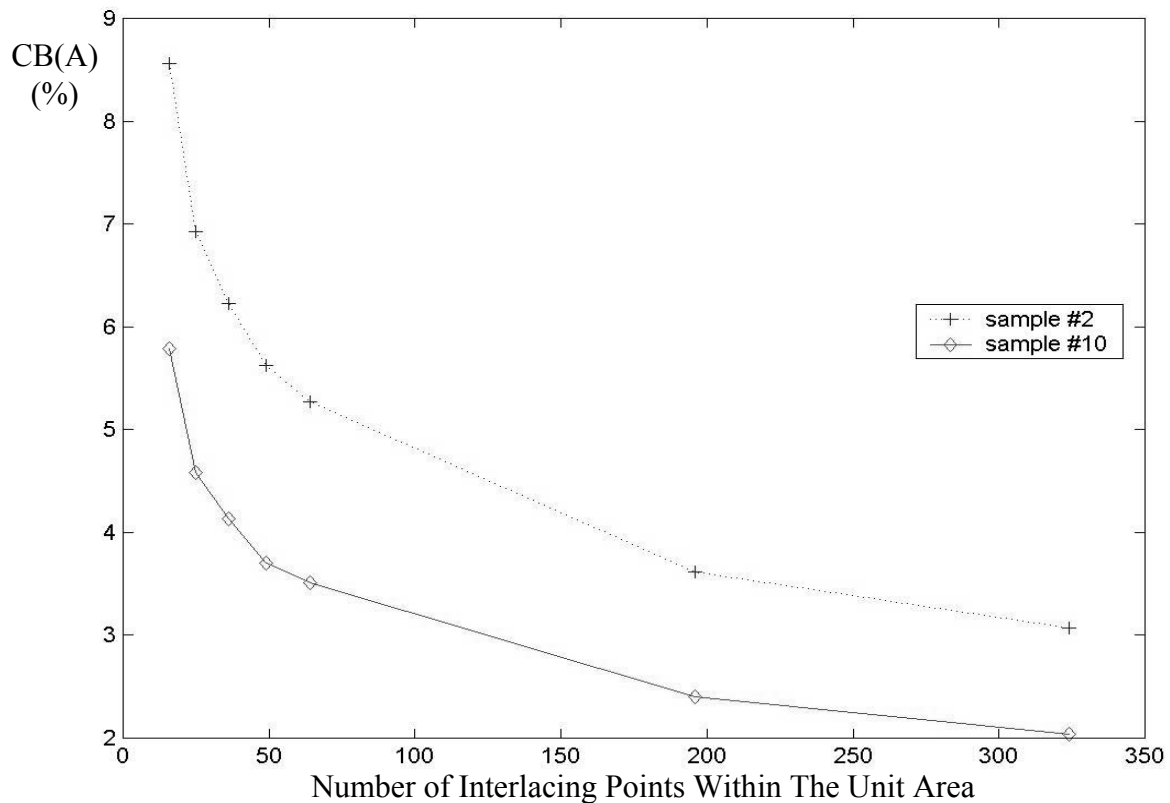


Figure 6.11 The $CB(A)$ Curves for Sample #2 and #10 (Model I)

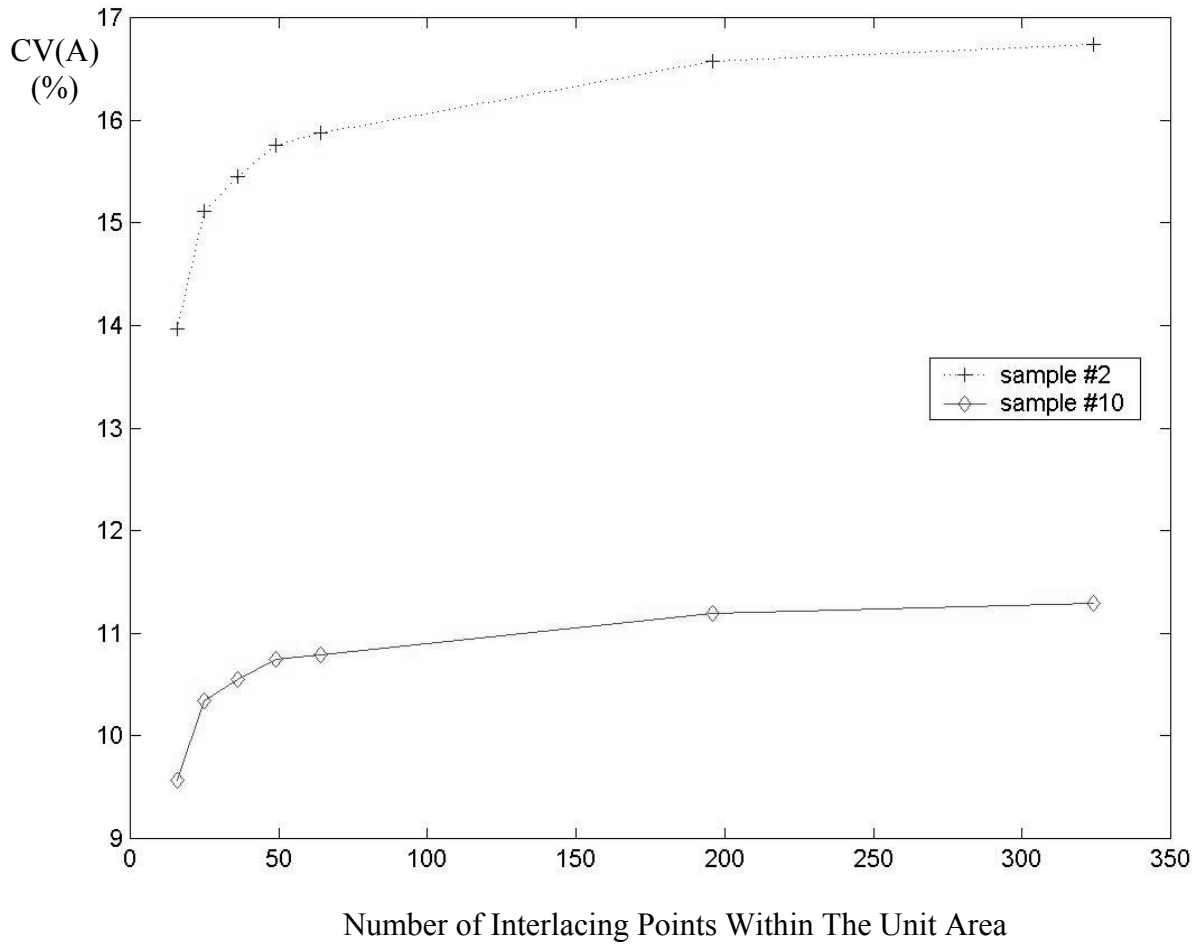


Figure 6.12 The CV(A) Curves for Sample #2 and #10 (Model I)

Unit area (Pt.) Sample #		16	25	36	49	64	196	324
		1	CV(A)	10.607	11.481	11.750	11.999	12.094
	CB(A)	6.616	5.358	4.835	4.372	4.098	2.785	2.368
2	CV(A)	13.965	15.108	15.450	15.755	15.874	16.571	16.743
	CB(A)	8.559	6.924	6.229	5.621	5.274	3.616	3.072
3	CV(A)	11.126	12.079	12.317	12.548	12.603	13.082	13.185
	CB(A)	6.735	5.254	4.713	4.185	3.989	2.621	2.231
4	CV(A)	10.941	11.806	12.056	12.292	12.370	12.896	13.016
	CB(A)	6.749	5.469	4.942	4.449	4.220	2.807	2.377
5	CV(A)	12.612	13.465	13.755	14.025	14.149	14.747	14.914
	CB(A)	7.683	6.410	5.821	5.278	4.955	3.510	3.016
6	CV(A)	12.876	13.798	14.089	14.361	14.451	15.031	15.167
	CB(A)	7.758	6.370	5.750	5.170	4.916	3.410	2.944
7	CV(A)	11.361	12.134	12.369	12.568	12.657	13.119	13.231
	CB(A)	6.996	5.773	5.254	4.803	4.544	3.213	2.811
8	CV(A)	10.906	11.729	11.984	12.200	12.295	12.788	12.914
	CB(A)	6.608	5.373	4.833	4.377	4.104	2.815	2.393
9	CV(A)	13.060	14.337	14.641	14.944	15.023	15.669	15.820
	CB(A)	8.191	6.322	5.672	5.021	4.765	3.089	2.558
10	CV(A)	9.564	10.347	10.547	10.741	10.795	11.195	11.287
	CB(A)	5.790	4.587	4.132	3.699	3.514	2.405	2.034

Table 6.2 The CV(A) And CB(A) Results of Ten Samples for Model I

Unit area (Pt.) Sample #		16	25	36	49	64	196	324
		1	CV(A)	10.631	11.495	11.767	12.018	12.101
	CB(A)	6.589	5.338	4.794	4.328	4.088	2.802	2.379
2	CV(A)	13.924	15.077	15.408	15.727	15.840	16.532	16.701
	CB(A)	8.535	6.865	6.201	5.571	5.255	3.585	3.056
3	CV(A)	11.137	12.082	12.323	12.551	12.609	13.091	13.195
	CB(A)	6.727	5.243	4.704	4.172	3.978	2.611	2.219
4	CV(A)	10.953	11.816	12.052	12.289	12.353	12.852	12.973
	CB(A)	6.629	5.310	4.810	4.286	4.095	2.756	2.310
5	CV(A)	12.670	13.497	13.809	14.082	14.196	14.809	14.966
	CB(A)	7.672	6.438	5.818	5.279	4.980	3.535	3.063
6	CV(A)	12.799	13.733	14.025	14.280	14.376	14.959	15.092
	CB(A)	7.733	6.317	5.702	5.164	4.885	3.372	2.926
7	CV(A)	11.496	12.221	12.472	12.689	12.754	13.195	13.290
	CB(A)	6.801	5.622	5.036	4.523	4.310	2.972	2.605
8	CV(A)	10.904	11.743	11.984	12.211	12.296	12.799	12.909
	CB(A)	6.632	5.375	4.867	4.381	4.140	2.828	2.478
9	CV(A)	13.151	14.416	14.712	15.012	15.074	15.714	15.855
	CB(A)	8.088	6.199	5.536	4.890	4.659	2.961	2.474
10	CV(A)	9.585	10.362	10.557	10.752	10.814	11.208	11.298
	CB(A)	5.767	4.555	4.109	3.668	3.463	2.322	1.973

Table 6.3 The CV(A) And CB(A) Results of Ten Samples for Model II

An other property of $CV(A)$ and $CB(A)$ curves found in these results is that for a same data set, the $CV(A)$ curves from the two different models are always similar in shape and value. The same can be said for the $CB(A)$ curves. We call this invariance property of variance-area curve. $CV(A)$ and $CB(A)$ curves are plotted in a double-Y-axis coordinate for every sample. $CV(A)$, within variation, refers to the left Y-axis and $CB(A)$, between variation, refers to the right Y-axis. One example is shown in Fig. 6.13 and Fig. 6.14. These two plots are for sample #1. Other plots will be in appendices.

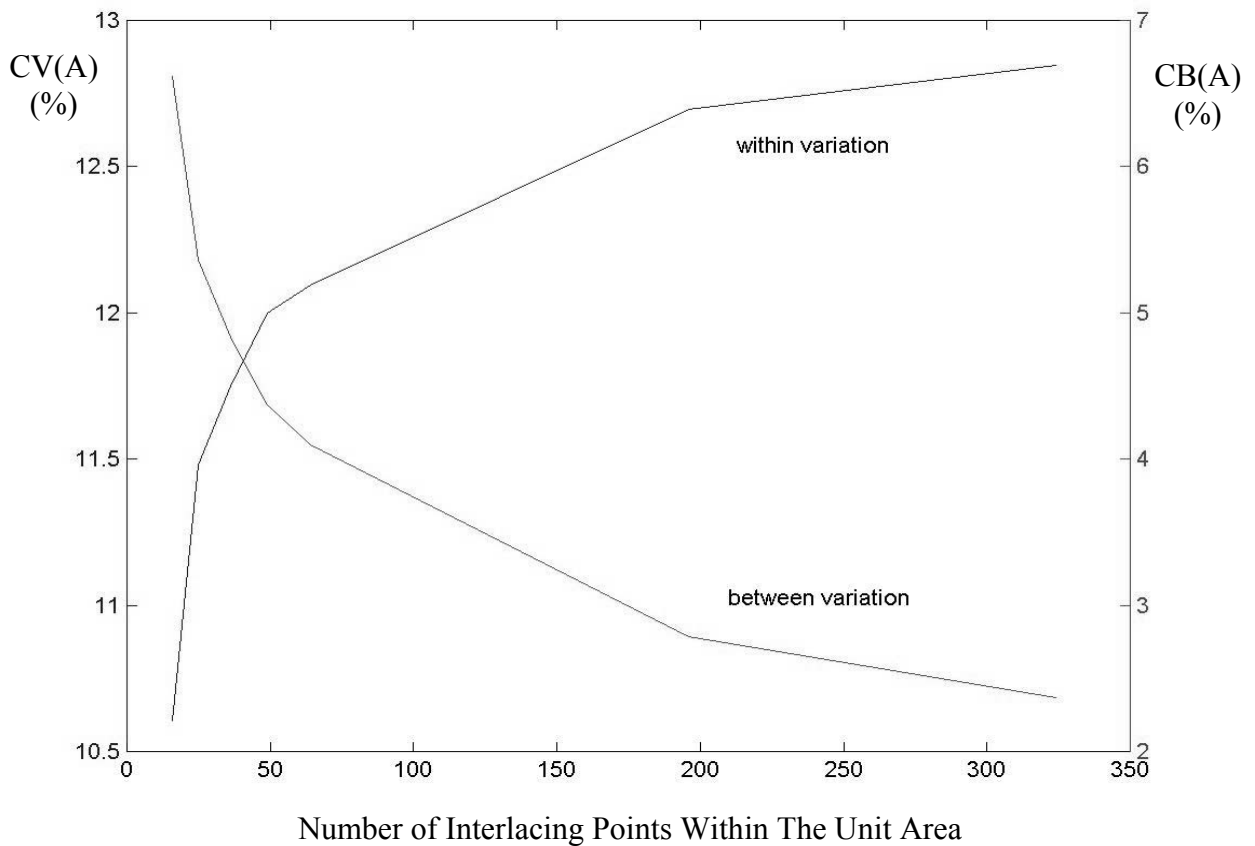


Figure 6.13 The $CV(A)$ And $CB(A)$ Curves of Sample #1 from Model I

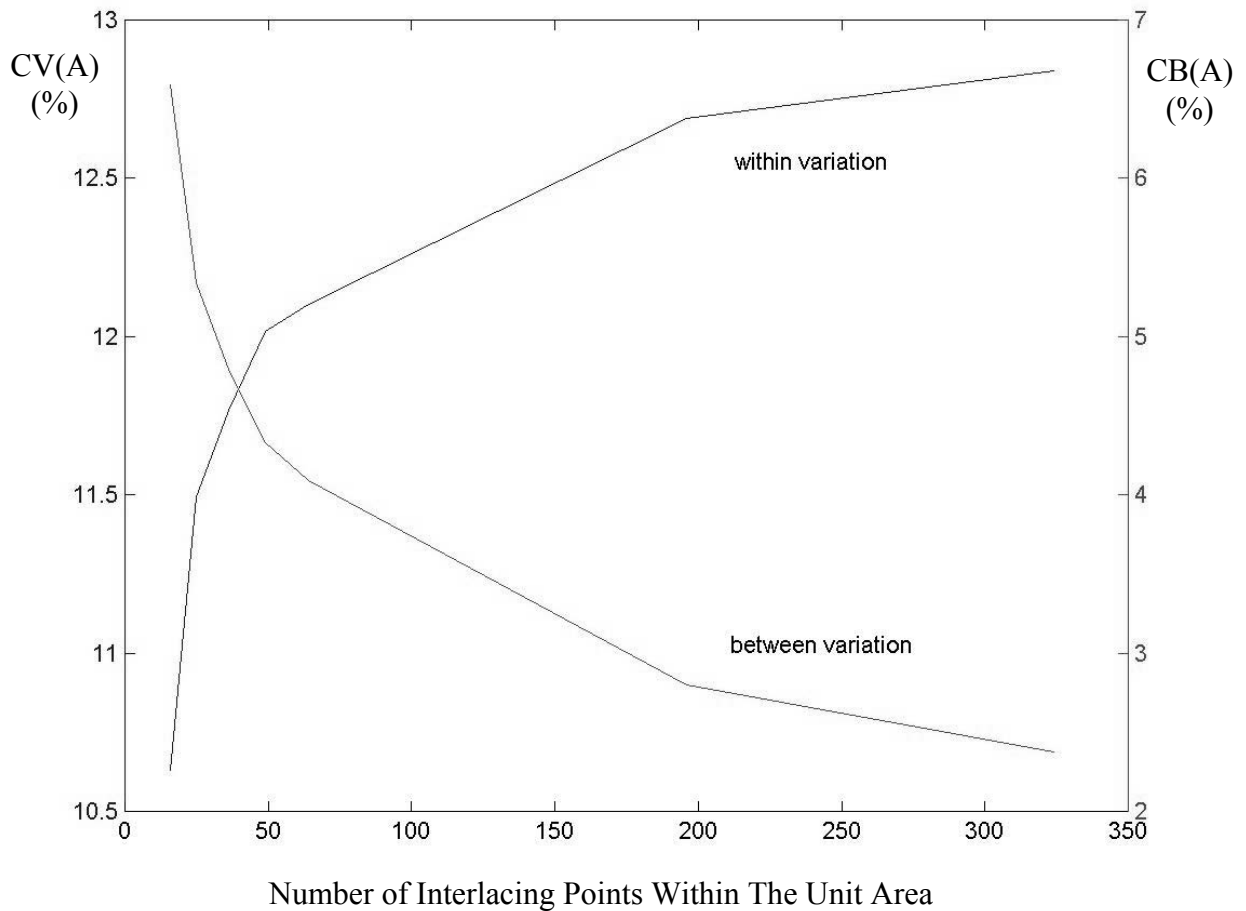


Figure 6.14 CV(A) And CB(A) Curves of Sample #1 from Model II

Plotted curves from model I and model II are close to each other in shape and value.

6.5 A Specialty Yarn Sample and The 3-D image Representation for The Overall Quality and Local Quality

A specialty yarn sample was also tried to be measured. This yarn sample has a very high variation in diameter. Some statistics of this yarn are shown below:

Mean Diameter: 0.92mm

Minimum Diameter: 0.22mm

Maximum Diameter: 2.55mm

Overall CV% in Diameter: 36.17%

An attempt was made to obtain a 3-D image of this specialty yarn sample. In order to show the 3-D micro images, two resolutions are chosen; one (Fig. 6.16) consisting of 100X100 interlacing points where each point providing the original value from the diameter measurement, and the other one (Fig. 6.15) consisting of 200X200 interlacing points where each point is an average of 10X10 original points. The quadrant, denoted by Q in Fig. 6.15, is shown in original scale in Fig. 6.16.

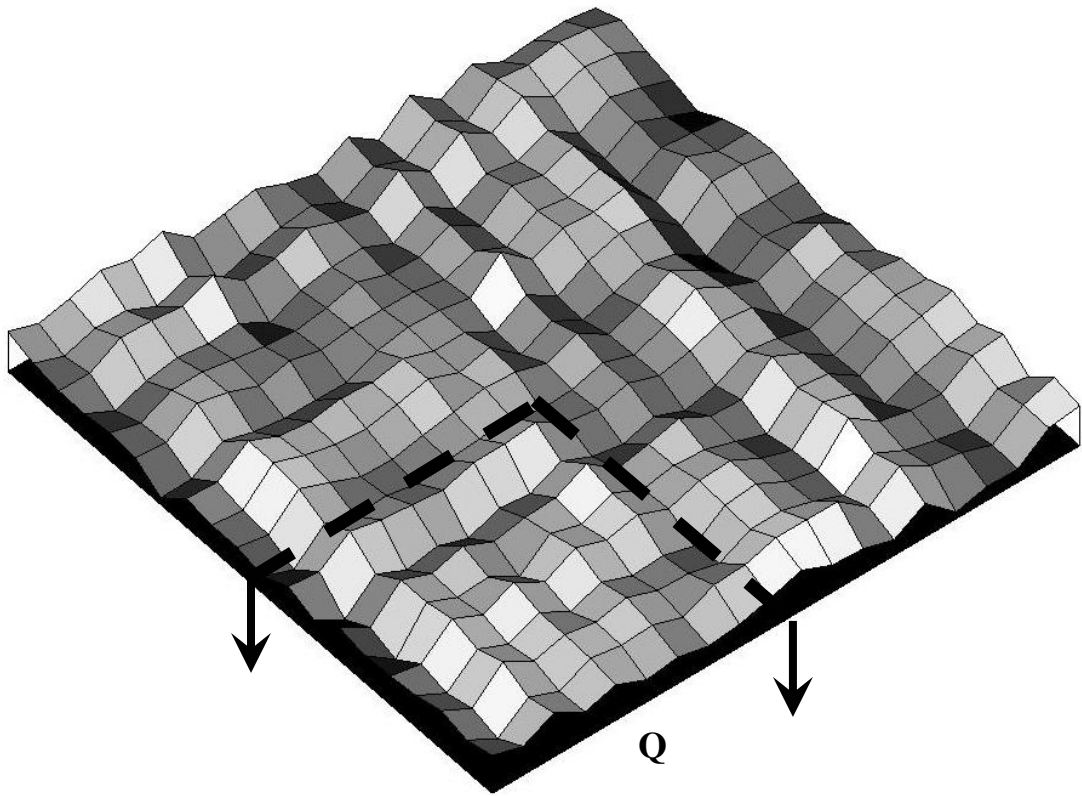


Figure 6.15 Smoothed Local 3-D Image of an Extended Area
- Containing 200X200 Original Interlacing Points
and Q as a Quadrant Shown in Fig. 6.16

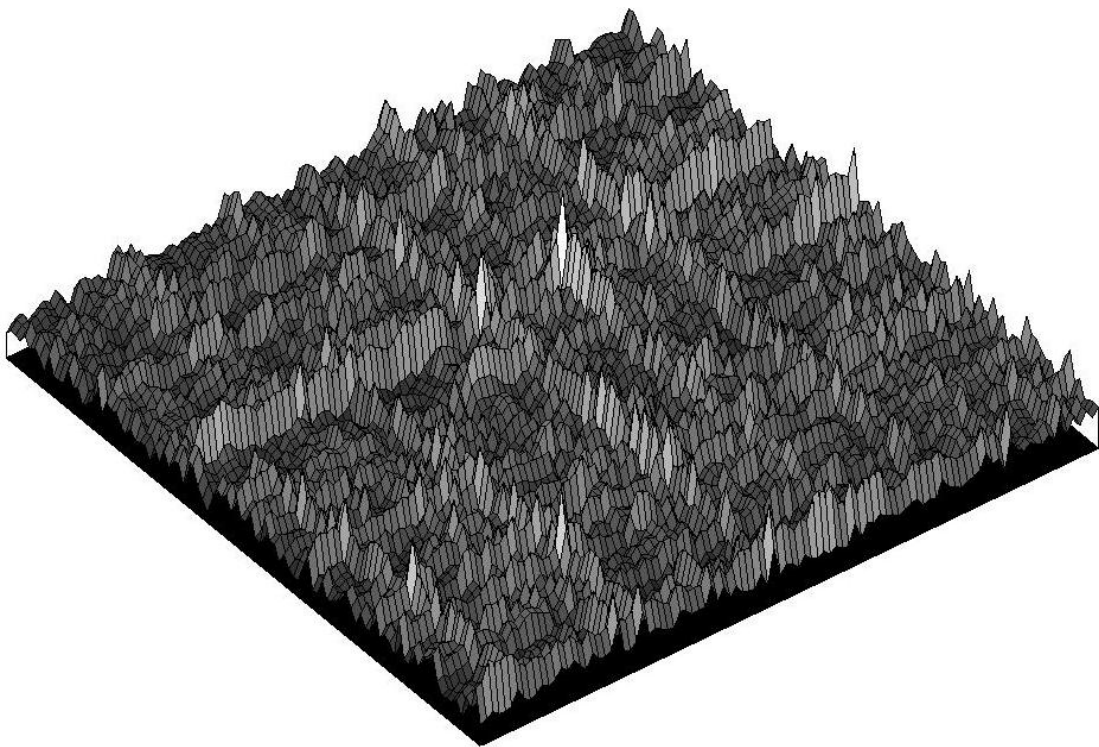


Figure 6.16 Unsmoothed Local 3-D Micro Image
- Containing 100X100 Interlacing
Points; Denoted by Quadrant Q in
Fig. 6.15

6.6 Major Conclusions

The original objectives of the present research were: 1) to construct models for representing fabric appearance qualities; 2) to study the relationship between fabric appearance qualities and the newly developed variance-area curves; 3) to investigate existence of an invariance property of the variance-area curves.

By applying the results of the image representation methods and the variance-area curves for ten measured yarn diameter data sets, the following conclusions could be obtained:

- The newly developed 2-D gray scale image representation is a better method to show the overall appearance quality variation of a fabric, whereas the 3-D image representation is a better method to express the local visual qualities within a fabric. The thick place and thin place on a fabric can be seen clearly in the 3-D images.
- The 2-D gray scale images and CYROS[®] simulated fabric images are shown to be related to the differences that can be found in the CV(A) and CB(A) curves. A larger CB(A) value implies a greater appearance variation, especially in the form of scattered fabric non-uniformity such as cloudiness and barre.
- It has been shown that the shapes and values of variance-area curves are almost identical regardless of the way the weft yarns are arranged in a

woven fabric (random or location-specific), as long as the original yarn data sets remain the same.

- Similarly to the cases for the variance-length curves $B(L)$ and $V(L)$, the $CB(A)$ curves shown to decrease as the size of the unit area increases, while the $CV(A)$ curves show the opposite trends. These two curves will approach asymptotic limits as the unit area increases to its maxim.

6.7 Major Accomplishments

The work performed in this research includes instrumentation relating to yarn diameter measurement and data acquisition and development of new methods for quantifying and visualizing the visual qualities of the resulting woven and knitted fabrics based on the two-dimensional fabric mass variation. The major accomplishments are as follows:

1. Developed patch control software to correct errors generated by CCD line scan camera in the yarn diameter measurement and data acquisition system.
2. Developed an algorithm to transform the CTT yarn diameter data directly to a set of input data for the CYROS[®] system so that a CYROS[®] 3-D fabric image can be obtained from the CTT yarn data.
3. Developed two models for mapping yarn diameter data onto a specific position within a woven fabric:

Model I: Cases when the weft yarns are mapped onto a specific location of a woven fabric.

Model II: Cases when the weft yarns are mapped onto a woven fabric randomly.

4. Developed 2-D and 3-D fabric imaging systems to represent the fabric non-uniformities based on the measured yarn diameter data.
5. Developed Variance-Area Curves, $CB(A)$ and $CV(A)$, the between and within variance curves, in order to quantitatively and graphically represent the non-uniformity of the resulting woven fabric.
6. Demonstrated the application methods for the data acquisition system, 2-D and 3-D systems for visualizing the fabric non-uniformity and the new variance-area curves, based on 10 different spun yarns.
7. Overall, the work done to date provides a set of new systems for evaluating fabric mass uniformity and other fabric qualities in two and three dimensions directly from a set of on-line or off-line yarn data.

Chapter 7. References

1. J. Kim *On-Line Measurement And Characterization of Yarn And Fabric Qualities Using A Wavelet-Stochastic Hybrid Method* Ph.D Dissertation North Carolina State University
2. W.L. Balls Studies of Quality in Cotton Macmillan Co. 1928
3. A. C. Goodings *Roller Drafting in The Worsted Industry* Journal of The Textile Institute 22 T1 1931
4. J. G. Martindale *Irregularities in Rovings And Yarns* Journal of The Textile Institute 33 P9 1942
5. J. G. Martindale *A New Measuring The Irregularity of Yarns with Some Observations on The Origin of Irregularities in Worsted Slivers And Yarns* Journal of The Textile Institute 36 T35 1945
6. G. A. R. Foster *The Investigation of Periodicities in The Products of Cotton Spinning The Drafting Wave* Journal of The Textile Institute 36 T229 1945
7. V.M. Vanden Abeele *Contribution to The Study of Irregularity of Yarns, Rovings and Slivers* Journal of The Textile Institute 42 P162 1951
8. P. Grosberg *Correlation Between Mean Fiber Length and Yarn Irregularity* Journal of The Textile Institute 47 T179 1956
9. G. A. R. Foster *Fiber Motion in Roller Drafting* Journal of The Textile Institute 42 T335 1951

10. D. R. Cox and J. Ingham *Some Cause of Irregularity in Worsted Drawing and Spinning* Journal of The Textile Institute 41 P376 1950
11. J. S. Rao *A Mathematical Model for The Ideal Sliver And Its Applications to The Theory of Roller Drafting* Journal of The Textile Institute 52 T571 1961
12. B. Cavaney and G. A. R. Foster *The Irregularity of Materials Dragged on Cotton Spinning Machinery and Its Dependence on Dragi, Doubling and Roller Setting. Part I, The Speed Frames* Journal of The Textile Institute 46 T529 1955
13. M. W. Suh *Probabilistic Assessment of Irregularity in Random Fiber Arrays – Effect of Fiber Length Distribution on “Variance-Length Curve”* Textile Research Journal 46 No.4 291 1976
14. H. Breny *The Calculation of The Variance-Length Curve from The Length Distribution of Fibers* Journal of The Textile Institute 44 P1 1953
15. R. Z. Burnashiv, A. F. Ei-Sharkawy and A. M. Sharrouf *Twist Structure in Open End Friction Spun Yarns* Investigacion e informacion textil y de tensioactivos 30 No.4: 197 Dec. 1987
16. A. Barella *A New Photoelectric Device for The Measurement of Yarn Diameter And Yarn Evenness* Journal of The Textile Institute 89 No.4 711 1998
17. J. Kim, W. J. Jasper, M. W. Suh and J. L. Woo *Effect of Measurement Principle and Measuring Field on Uniformity Measures of Spun Yarns* Textile Research Journal 70(7) 584 2000
18. A. Barella *The Influence of Twist on The Regularity of The Apparent Diameter of Worsted Yarns* Journal of The Textile Institute 43 P734 1952

19. H. Unwin and J. W. Reast *The Effect of Yarn Irregularities on Fine Gauge* Journal of The Textile Institute 41 P547 1950
20. R. A. McFarlane *Yarn Irregularities And Their Effect on Viscose Rayon Fabrics* Journal of The Textile Institute 41 P566 1950
21. E. M. Walker and C. E. Sleath *Defects in Knitted Structures Due to Yarn Irregularities* Journal of The Textile Institute 41 P559 1950
22. D. C. Snowden and J. Sidi *The Efficient Mixing of Irregular Weft Yarns* Journal of The Textile Institute 41 P507 1950
23. T. Bleakley *The Importance of Regularity in Linen Yarns* Journal of The Textile Institute 41 P526 1950
24. S. D. Mahajan *Weft Bars in Cloth – Three Cases* Textile Digest 32 145 1971
25. A. R. Garde, S. Bandyopadhyay and T. A. Subramanian *The Influence of Yarn Unevenness And Cover Factor on Fabric Appearance* Proceedings of 13th Technological Conference Vol.1 120 1972
26. American Society for Testing and Materials, Committee D-13, “Grading cotton yarns for appearance.” D-2255-75. ASTM Standards, Part 32, Philadelphia (1976)
27. G. L. Louis *Grading Open-End Spun Cotton Yarns* America’s Textiles Reporter/Bulletin Ed. 88 Apr. 1978
28. S. G. Barker *A Gravimetric Method for Investigation of The Variation and Levelness of Yarn* Journal of The Textile Institute 17 T259 1926

29. C. Mack *Some Factors Affecting The Change in Capacity of A Parallel-Plate Condenser Due to The Insertion of A Yarn* Journal of The Textile Institute 46 T500 1955
30. W. R. Pelton and K.Slater *Fringe Effects in Capacitance-Type Evenness Testers* Journal of The Textile Institute 63 295 1972
31. G. N. Body *An Electronic Instrument for Measuring Weight Variations in Slivers, Rovings And Yarns* Journal of The Textile Institute 40 T407 1949
32. P. H. Walker *The Electronic Measurement of Sliver, Roving, and Yarn Irregularity, With Special Reference to The Use of The Fielden Bridge Circuit* Journal of The Textile Institute 41 P446 1950
33. K. Slater *Yarn Evenness* Textile Progress 14 1985
34. V. K. Kothari *Yarn Evenness and Appearance Progress in Textiles: Science & Technology* Vol.1 Testing and Quality Management 1st Ed. IAFL Publications 1999
35. M. Gerig and B. Wulfhorst *Yarn-Engineering Based on The Simulation of Knitted Fabrics – Innovative Chances for The Engineering of Blended Yarns* Proceedings of The Beltwide Cotton Production Conference P805 Jan. 1998
36. P. de Malatinszky and P.Grosberg *The Medium And Long Term Variations of A Yarn – II* Journal of The Textile Institute 46 T310 1955
37. M. W. H. Townsend and D. R. Cox *The Analysis of Yarn Irregularity* Journal of The Textile Institute 42 P107 1951

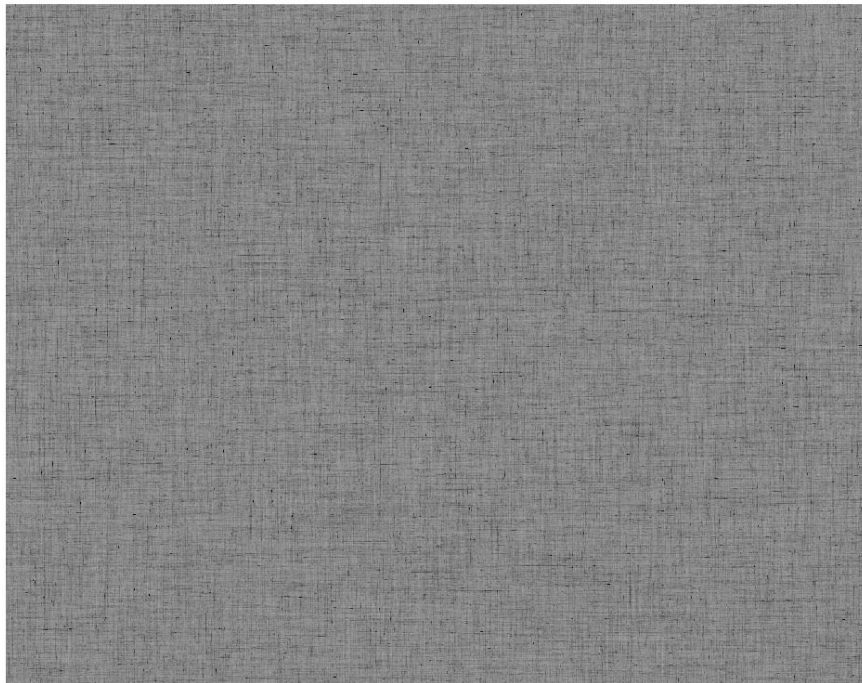
38. W. Wegener *The Irregularity of Woven and Knitted Fabrics* Journal of The Textile
Institute 77 69 1986

Appendices

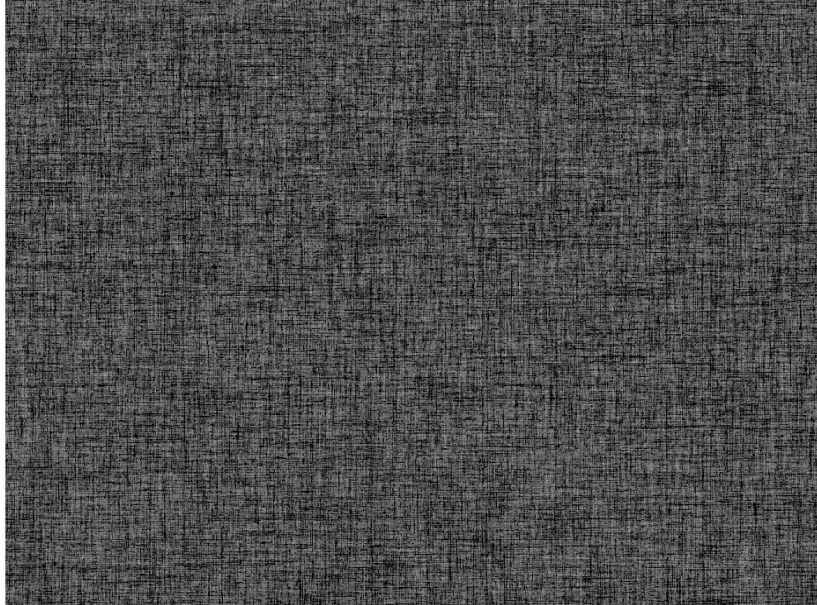
Appendix I 2-D Gray Scale Images for 10 Samples from 2 Models

The number in the parentheses of each title indicates the model.

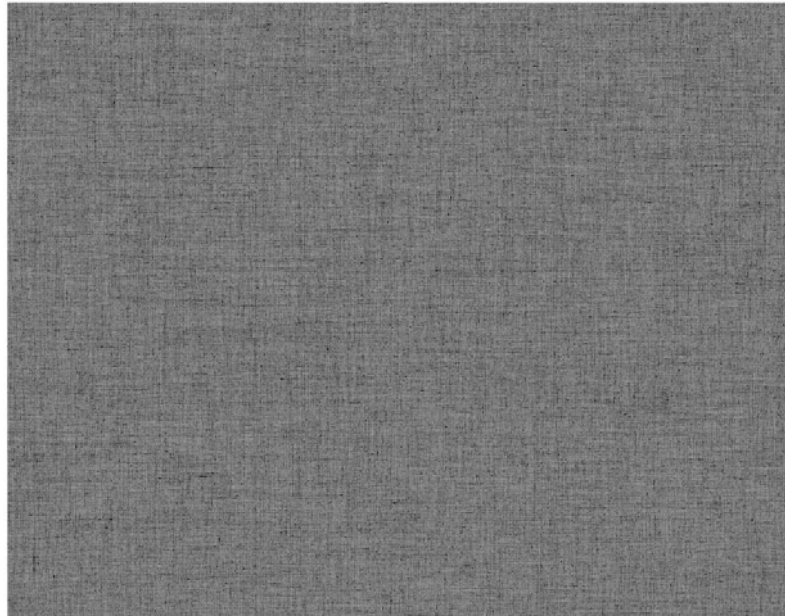
2-D Image For Yarn Sample #1 (I)



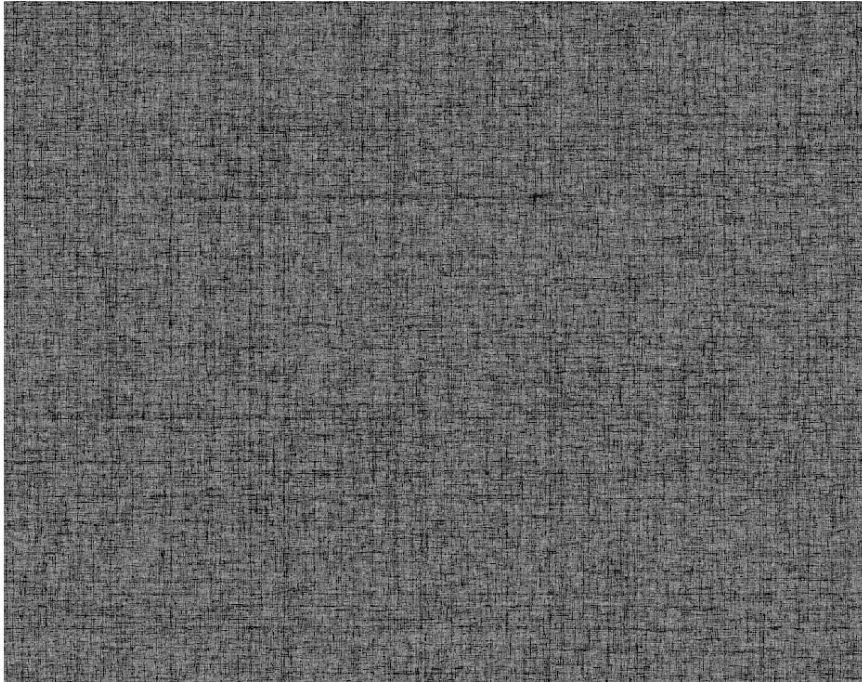
2-D Image For Yarn Sample #2 (I)



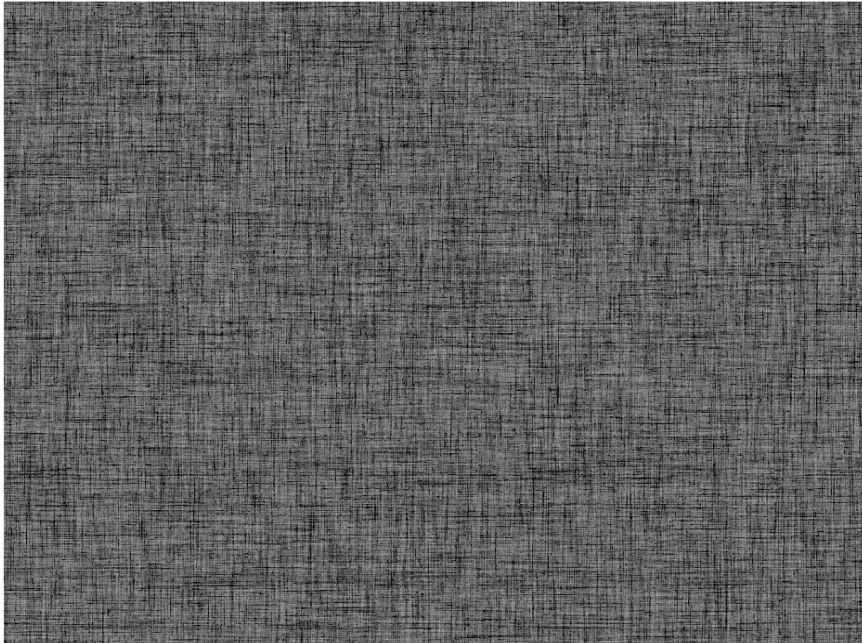
2-D Image For Yarn Sample #3 (I)



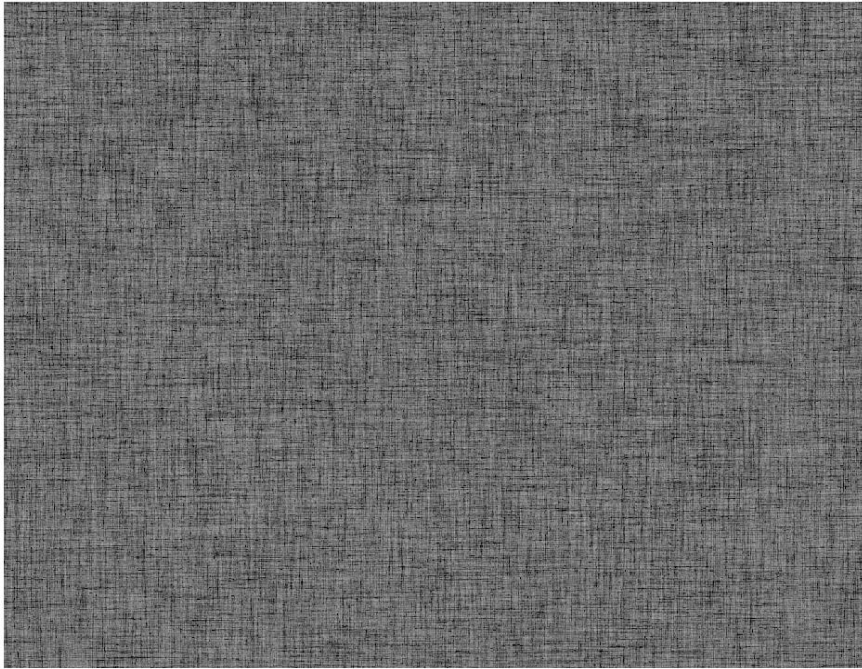
2-D Image For Yarn Sample #4 (I)



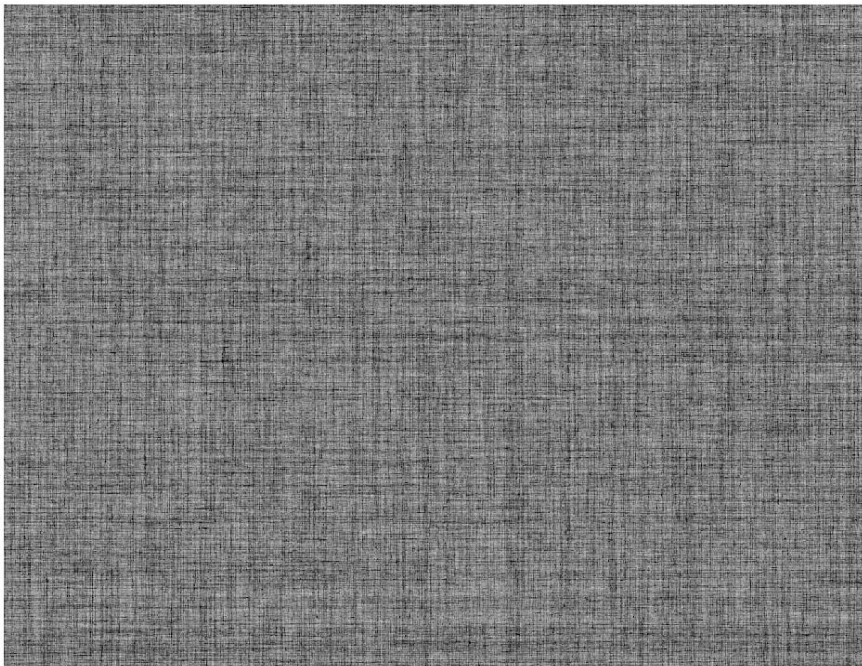
2-D Image For Yarn Sample #5 (I)



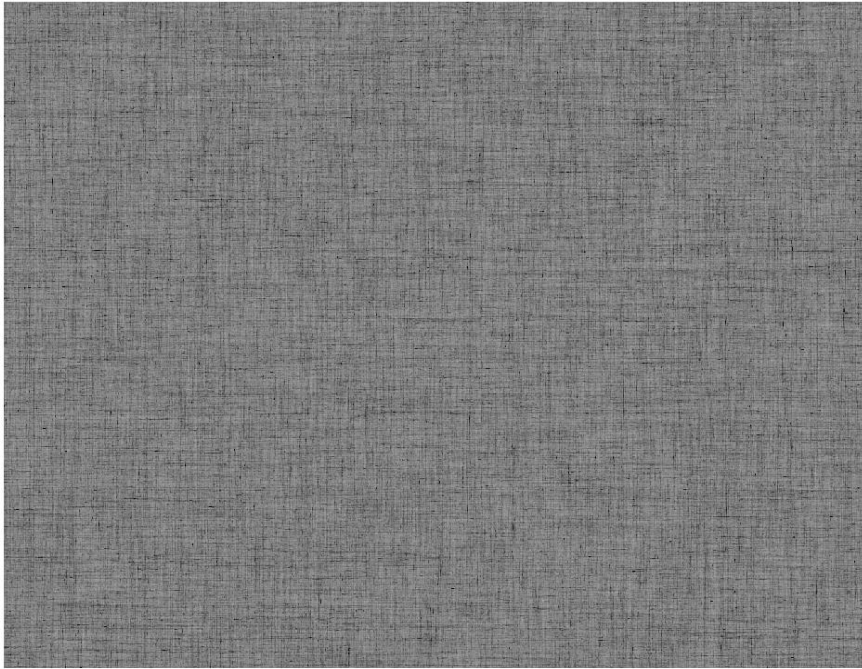
2-D Image For Yarn Sample #6 (I)



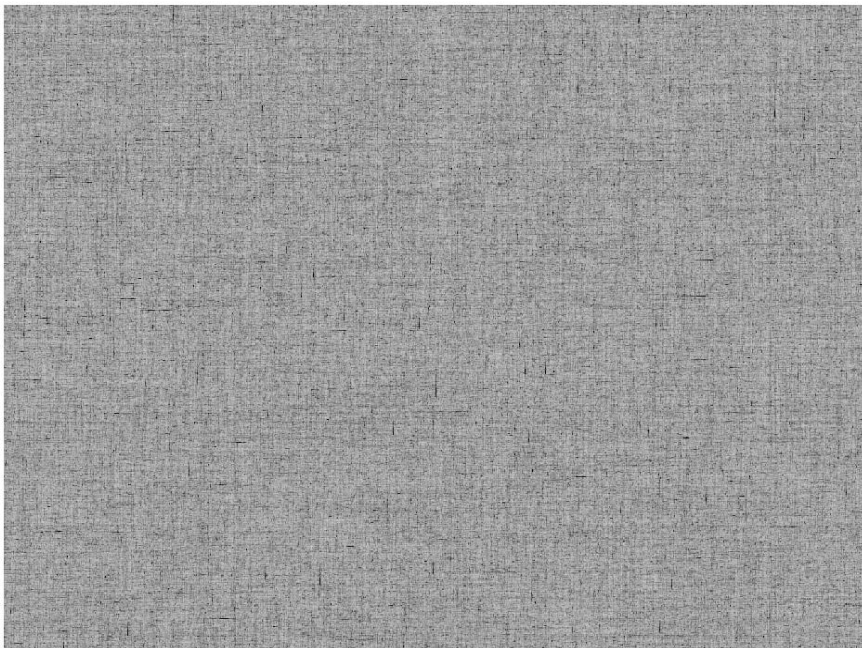
2-D Image For Yarn Sample #7 (I)



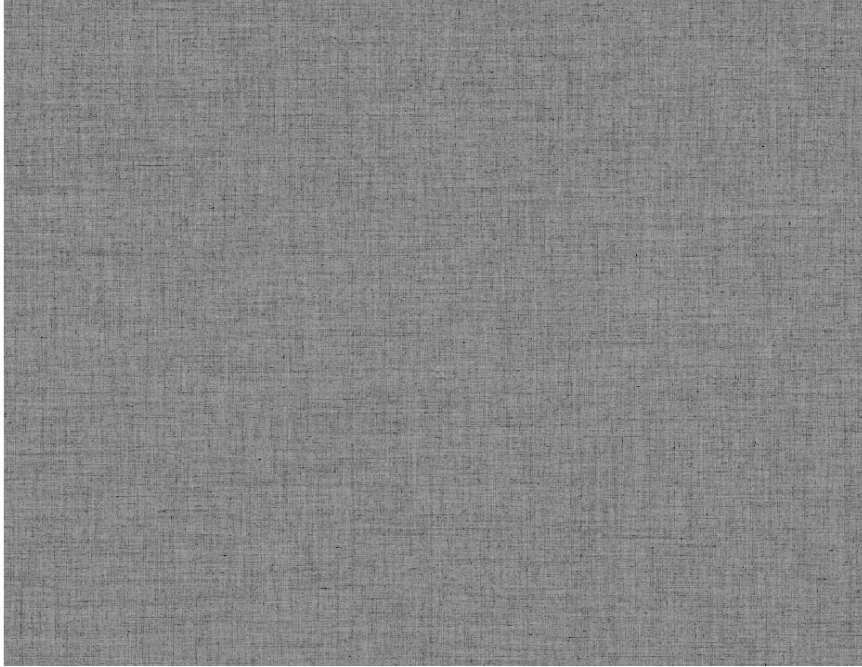
2-D Image For Yarn Sample #8 (I)



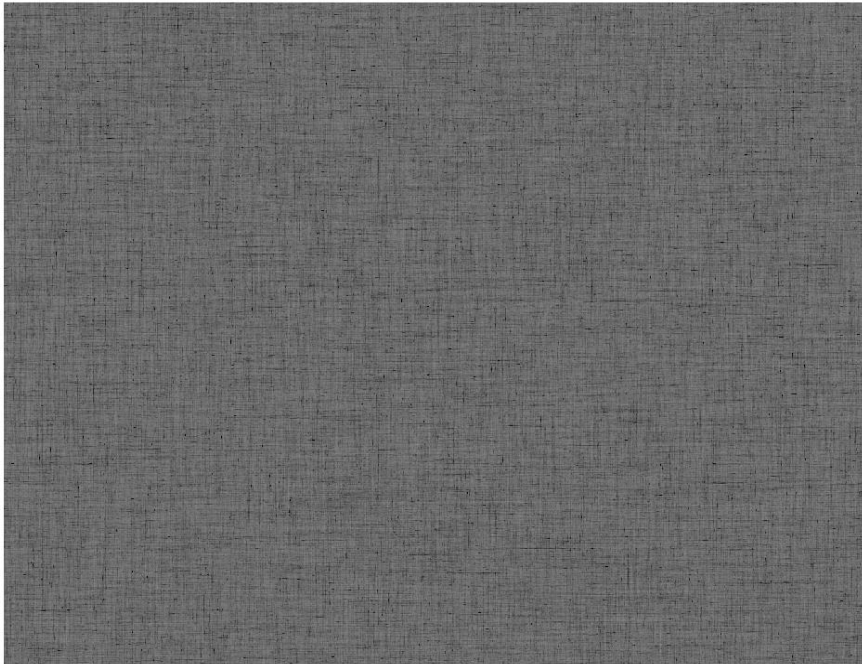
2-D Image For Yarn Sample #9 (I)



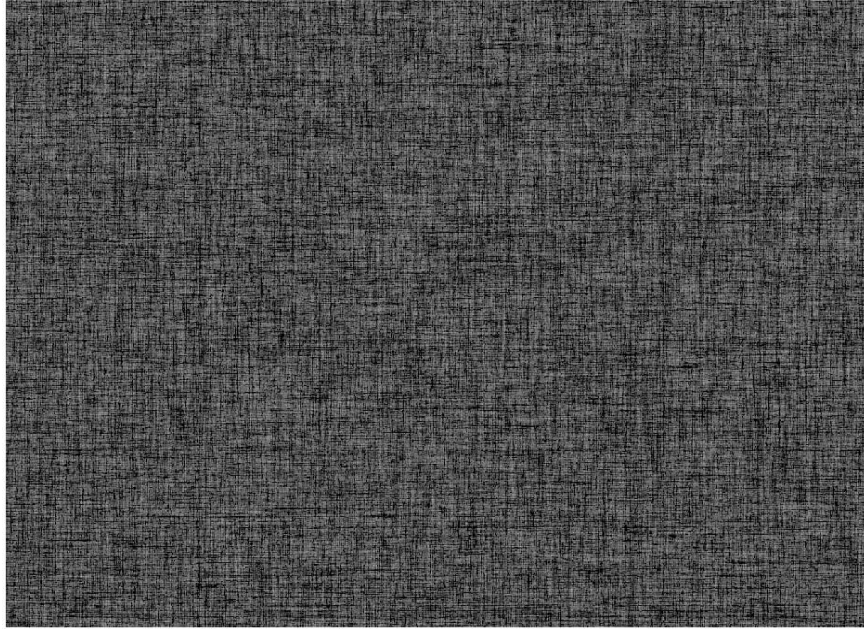
2-D Image For Yarn Sample #10 (I)



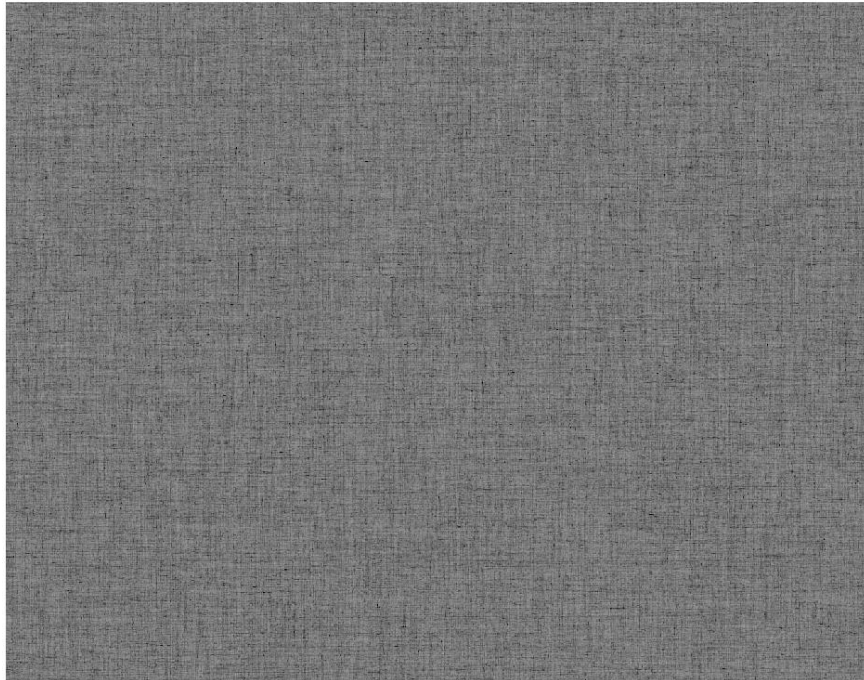
2-D Image For Yarn Sample #1 (II)



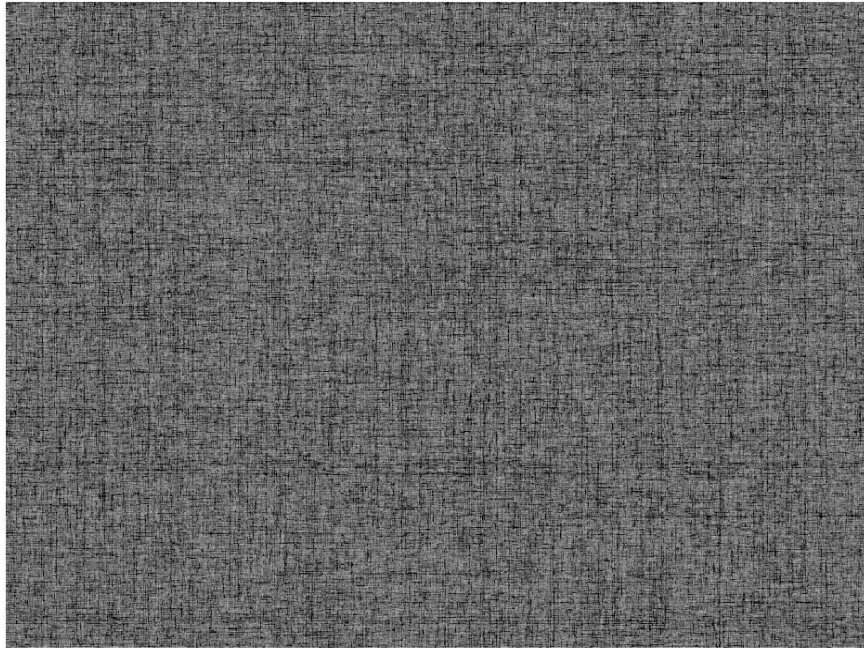
2-D Image For Yarn Sample #2 (II)



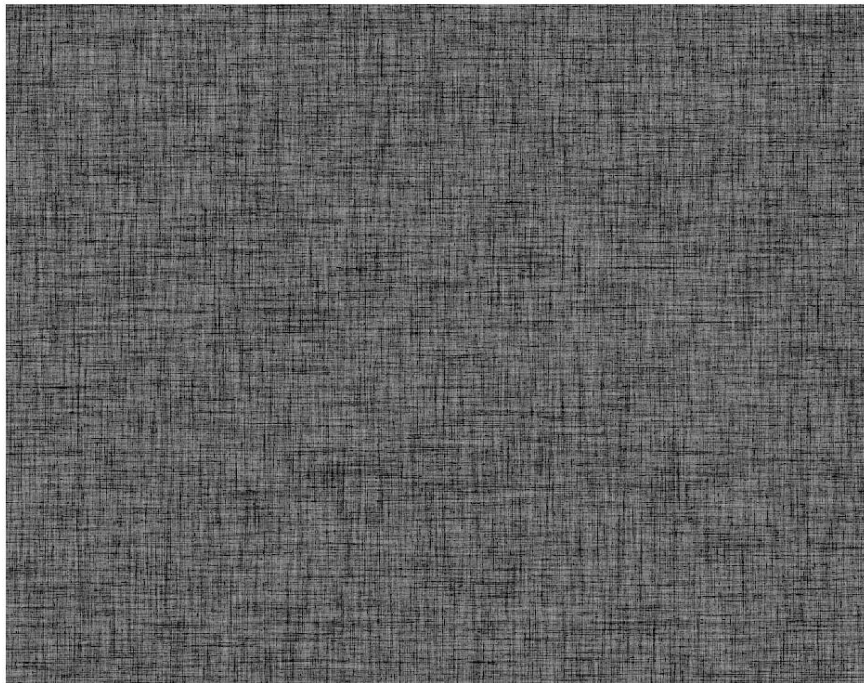
2-D Image For Yarn Sample #3 (II)



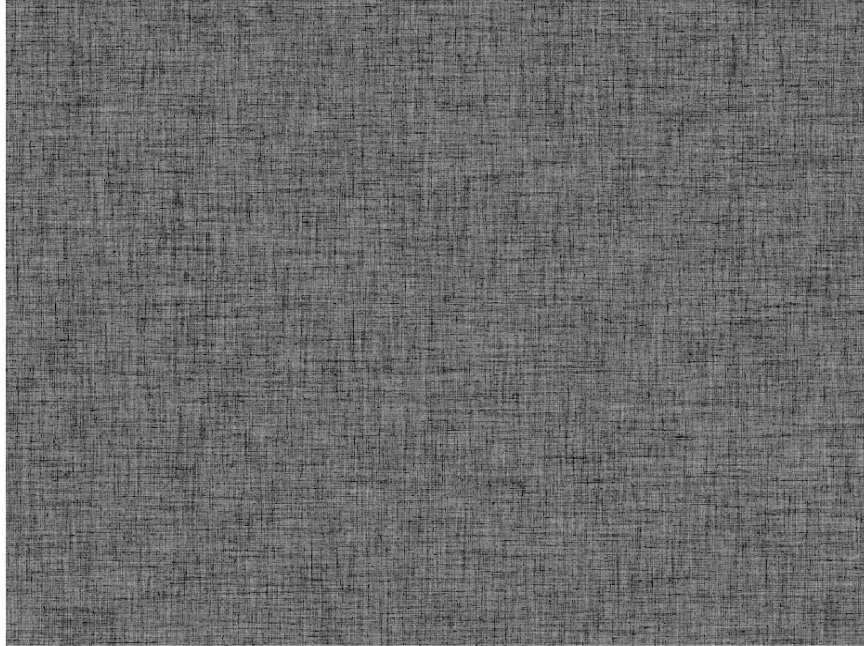
2-D Image For Yarn Sample #4 (II)



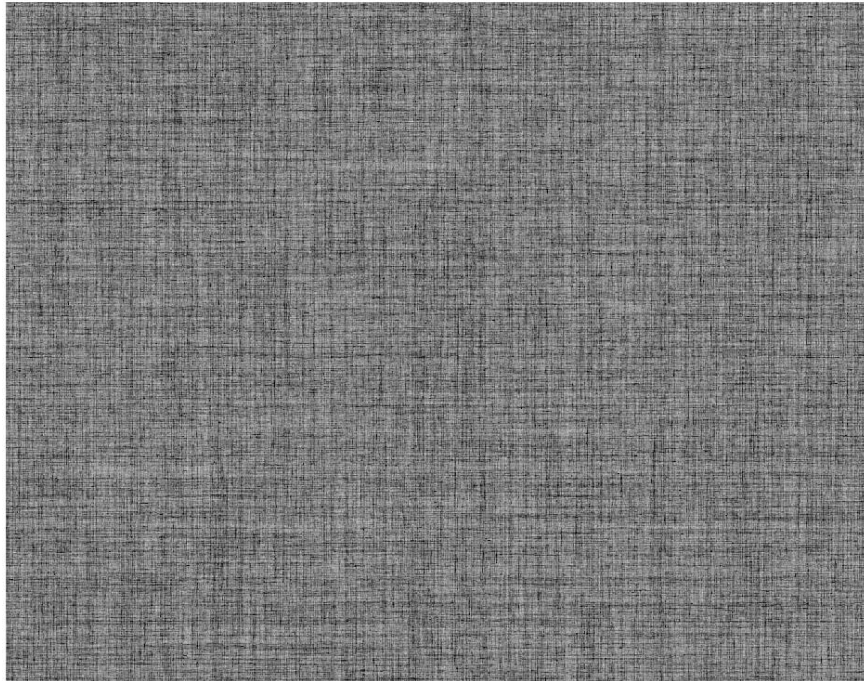
2-D Image For Yarn Sample #5 (II)



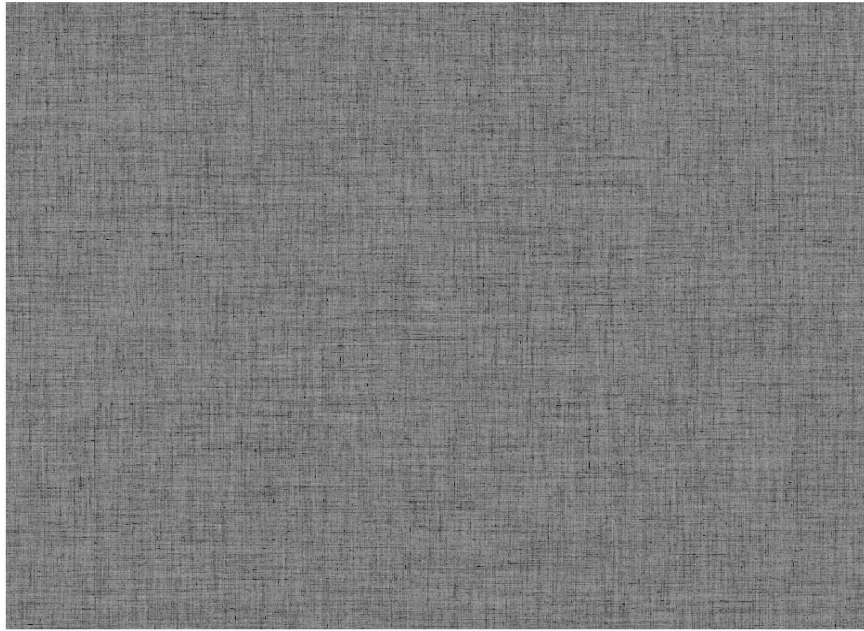
2-D Image For Yarn Sample #6 (II)



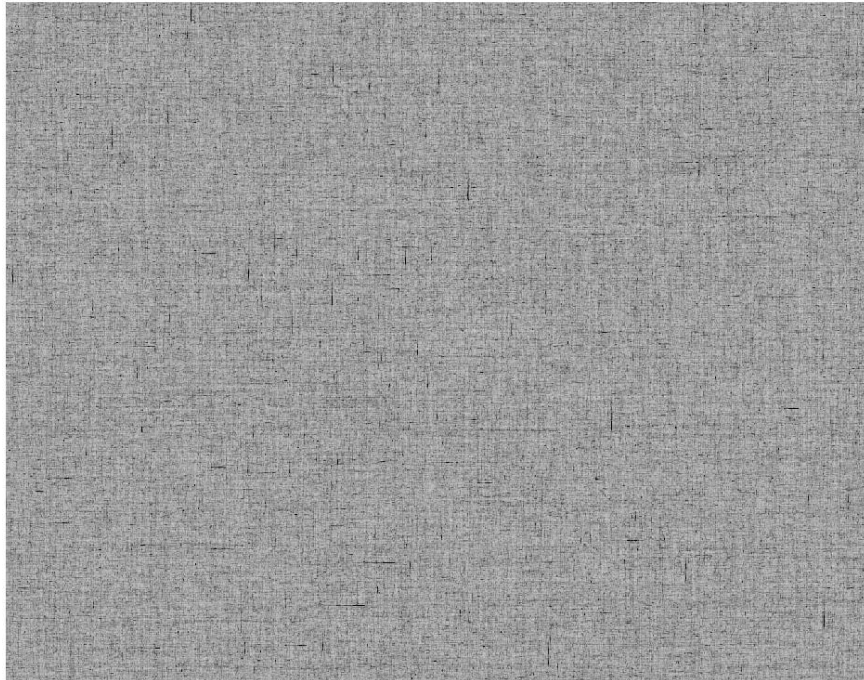
2-D Image For Yarn Sample #7 (II)



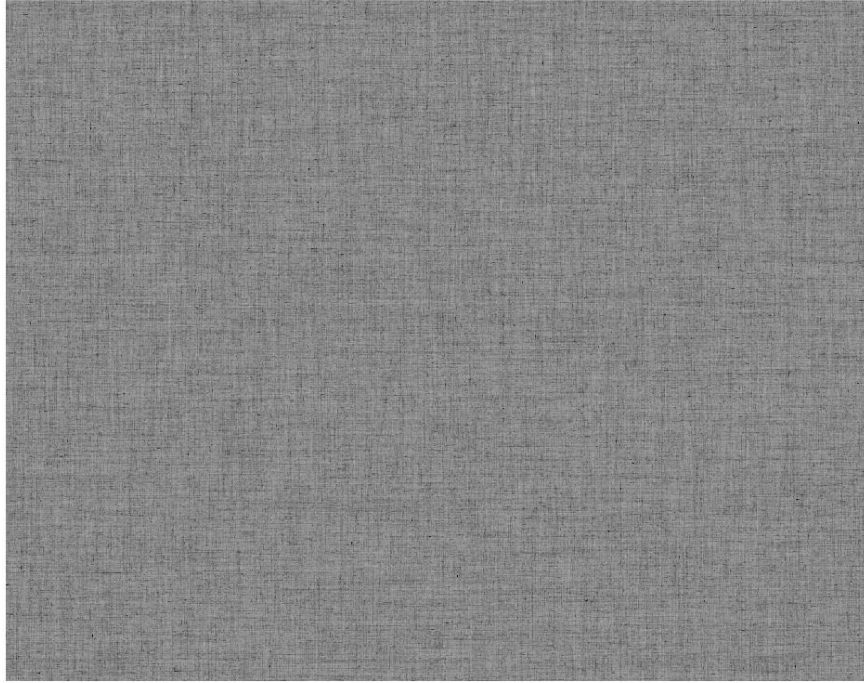
2-D Image For Yarn Sample #8 (II)



2-D Image For Yarn Sample #9 (II)



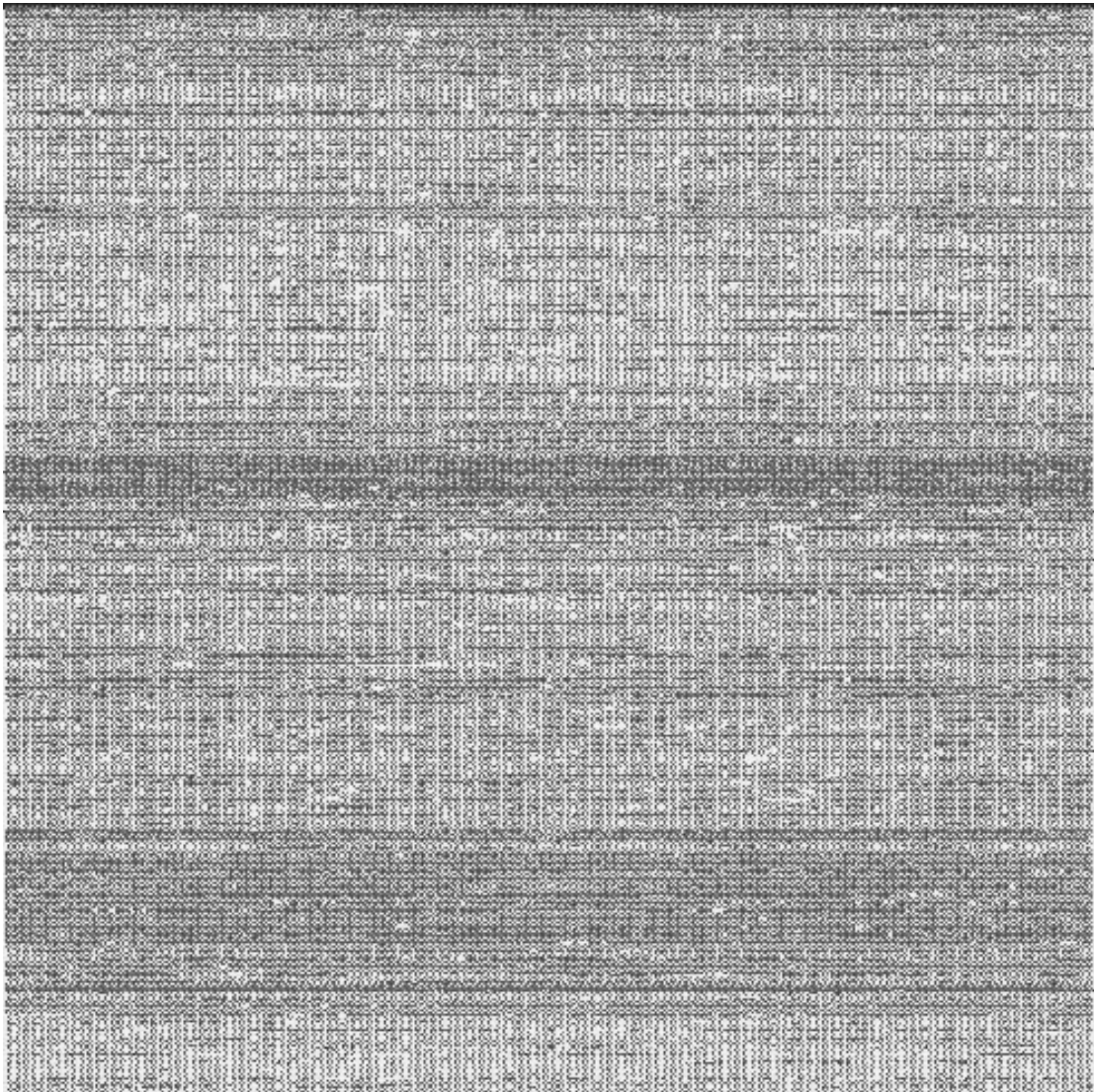
2-D Image For Yarn Sample #10 (II)



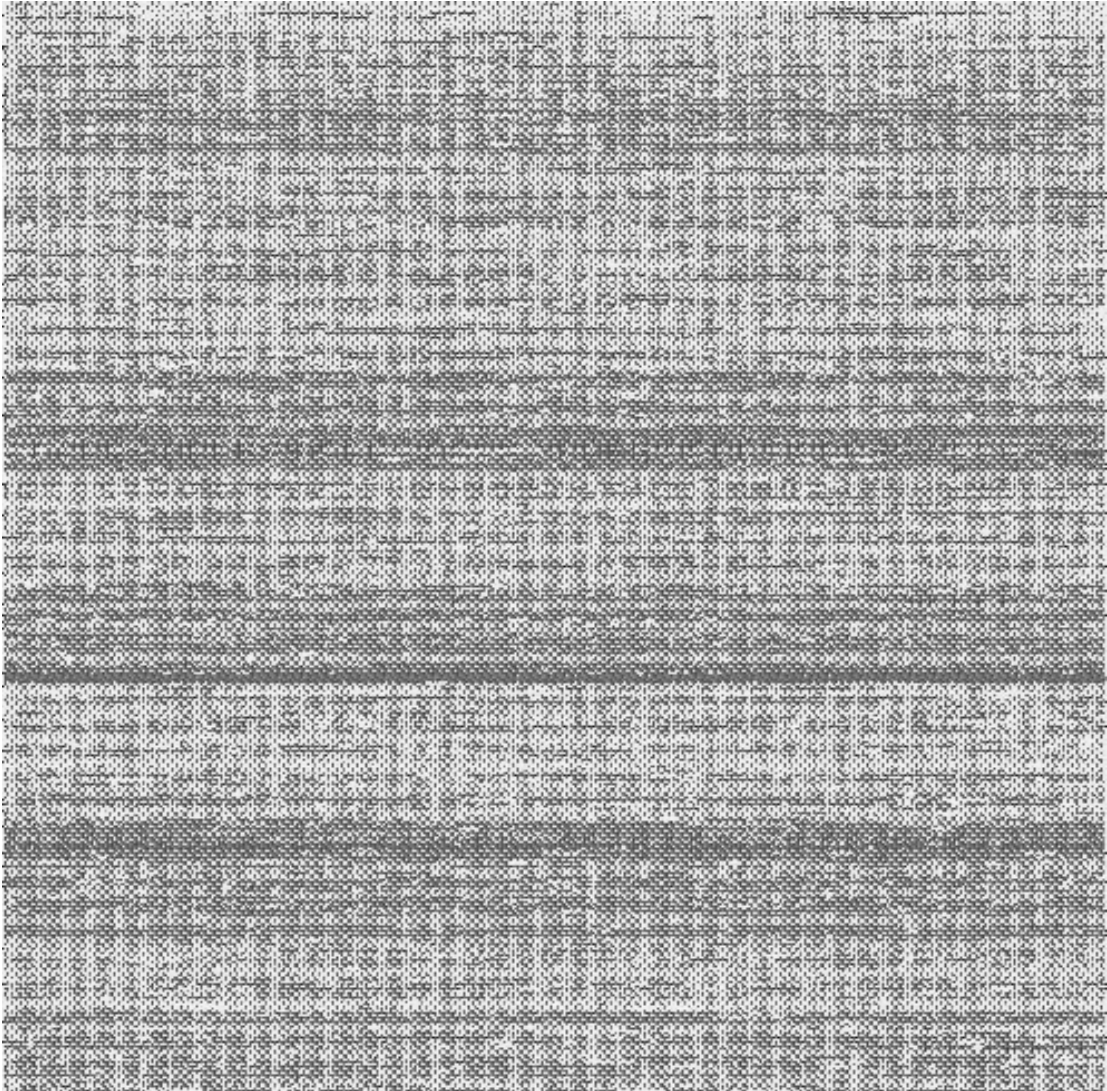
Appendix II Simulated Images from CYROS[®]

System

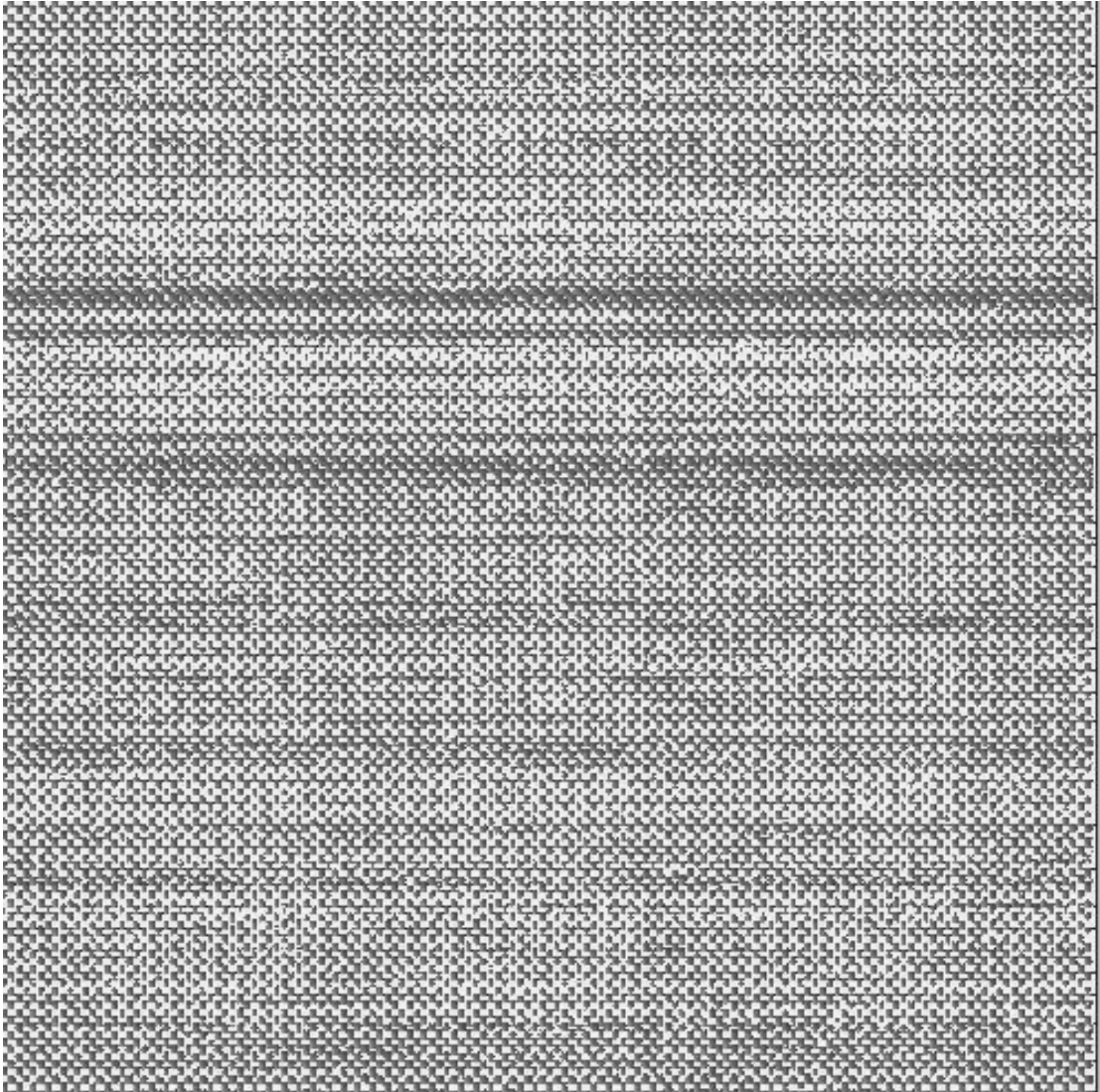
Sample #1



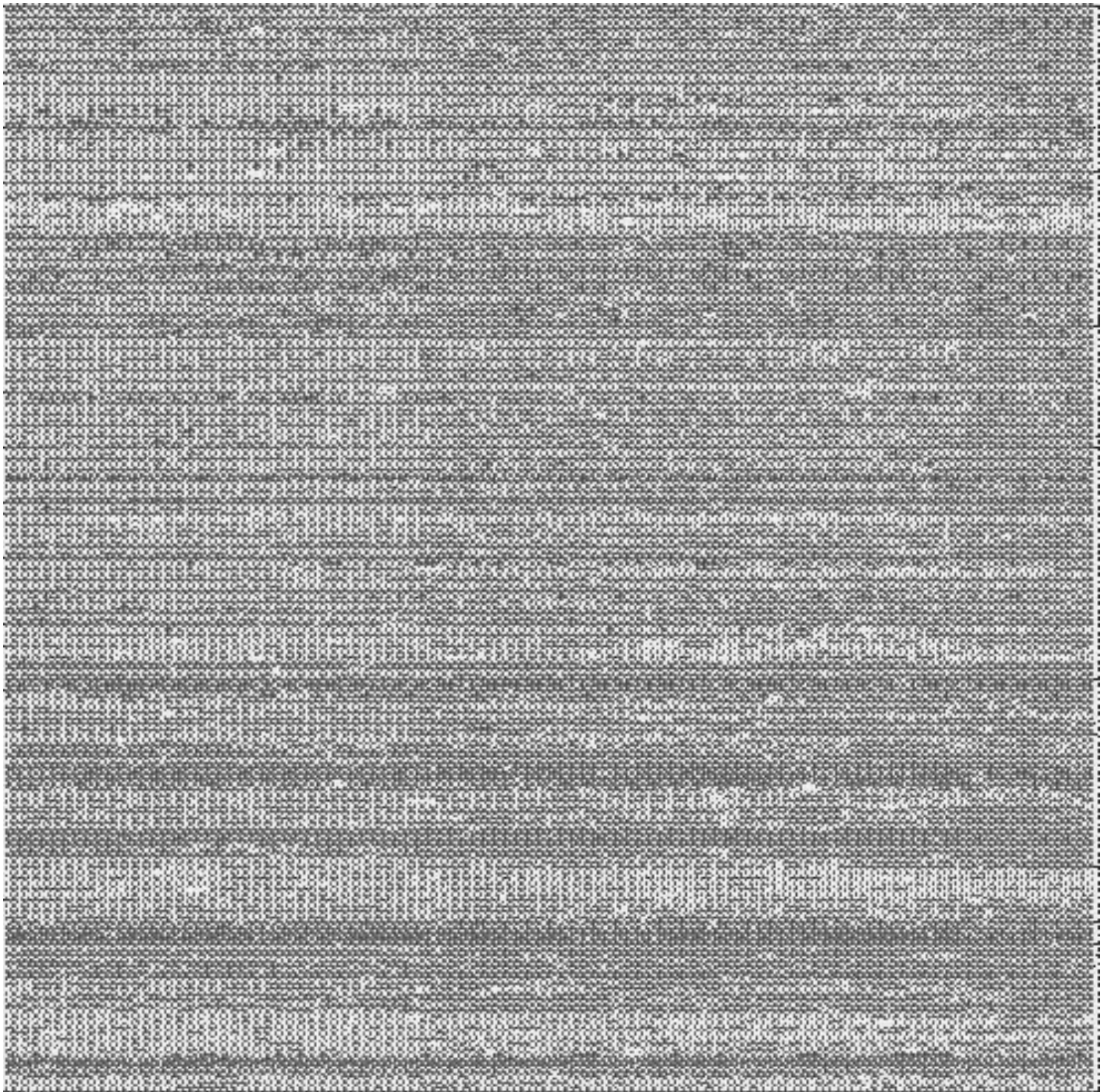
Sample #2



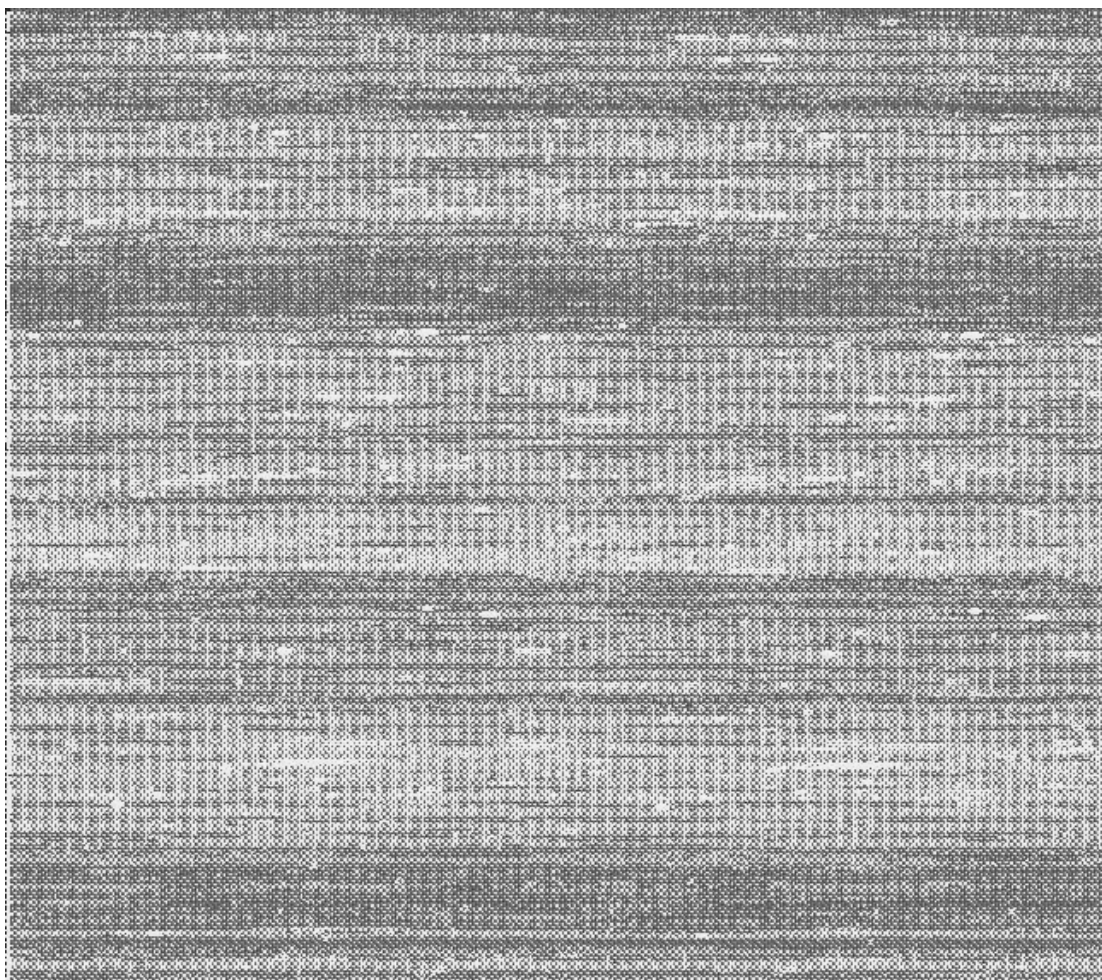
Sample #3



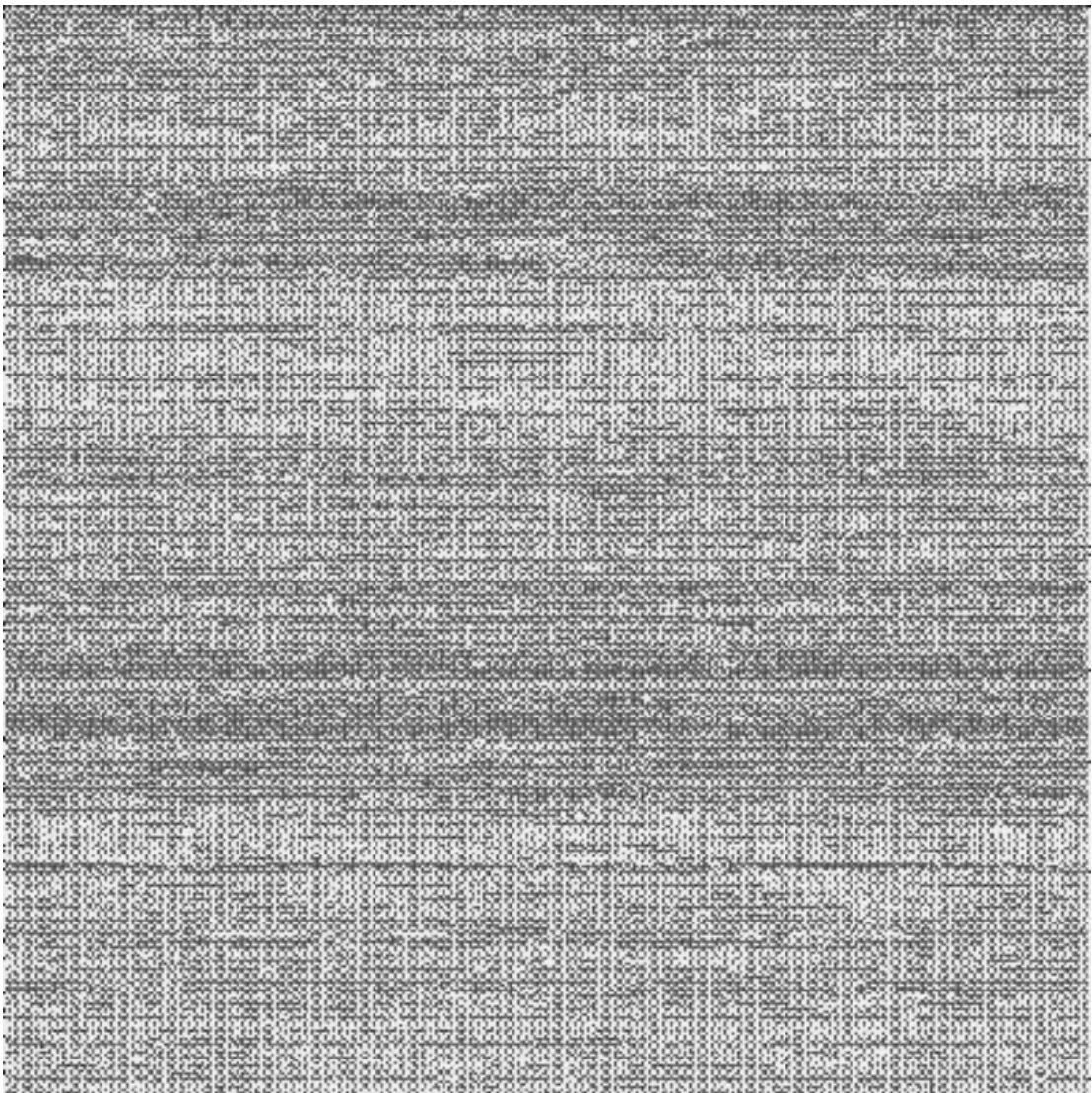
Sample #4



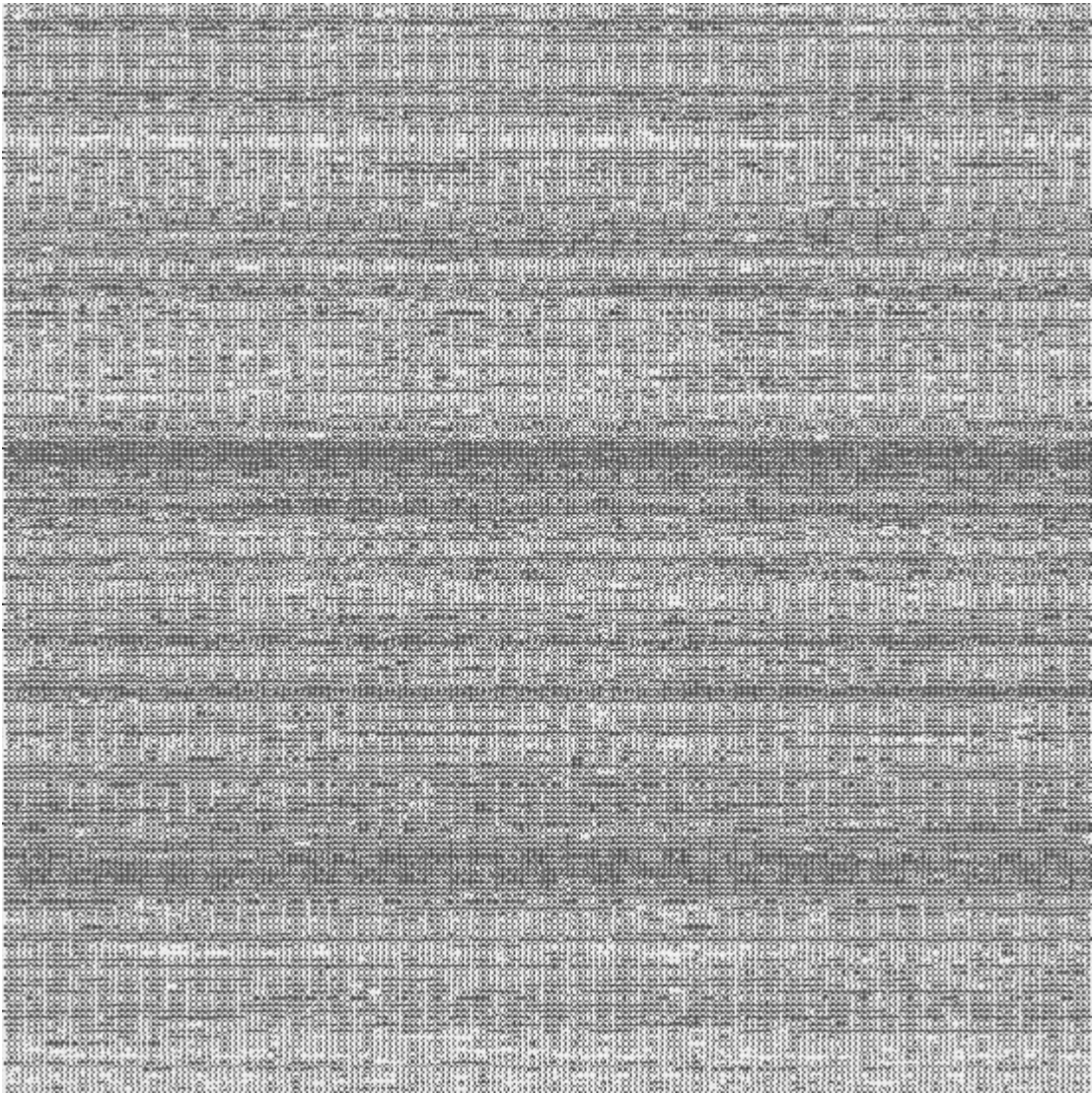
Sample #5



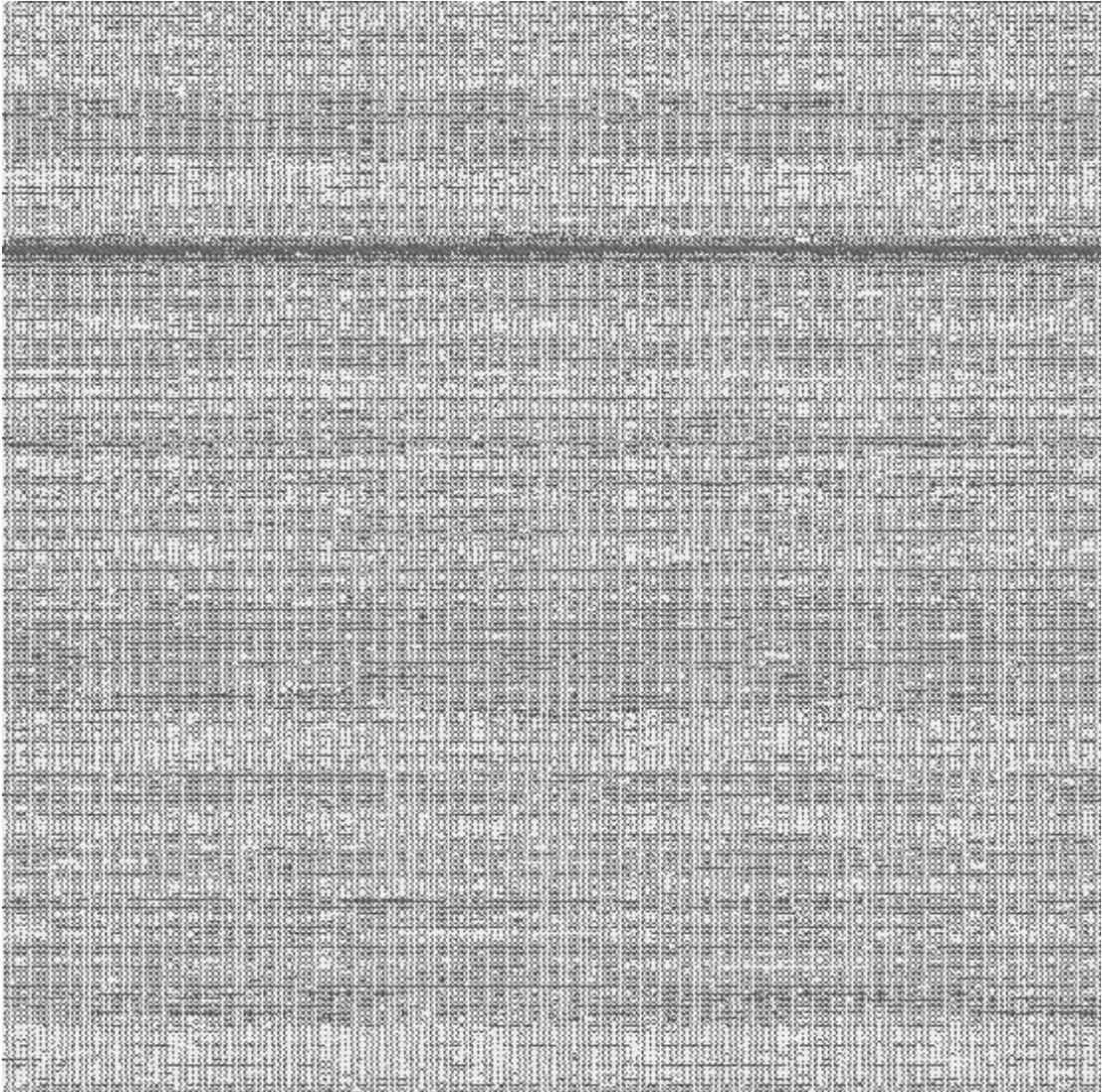
Sample #6



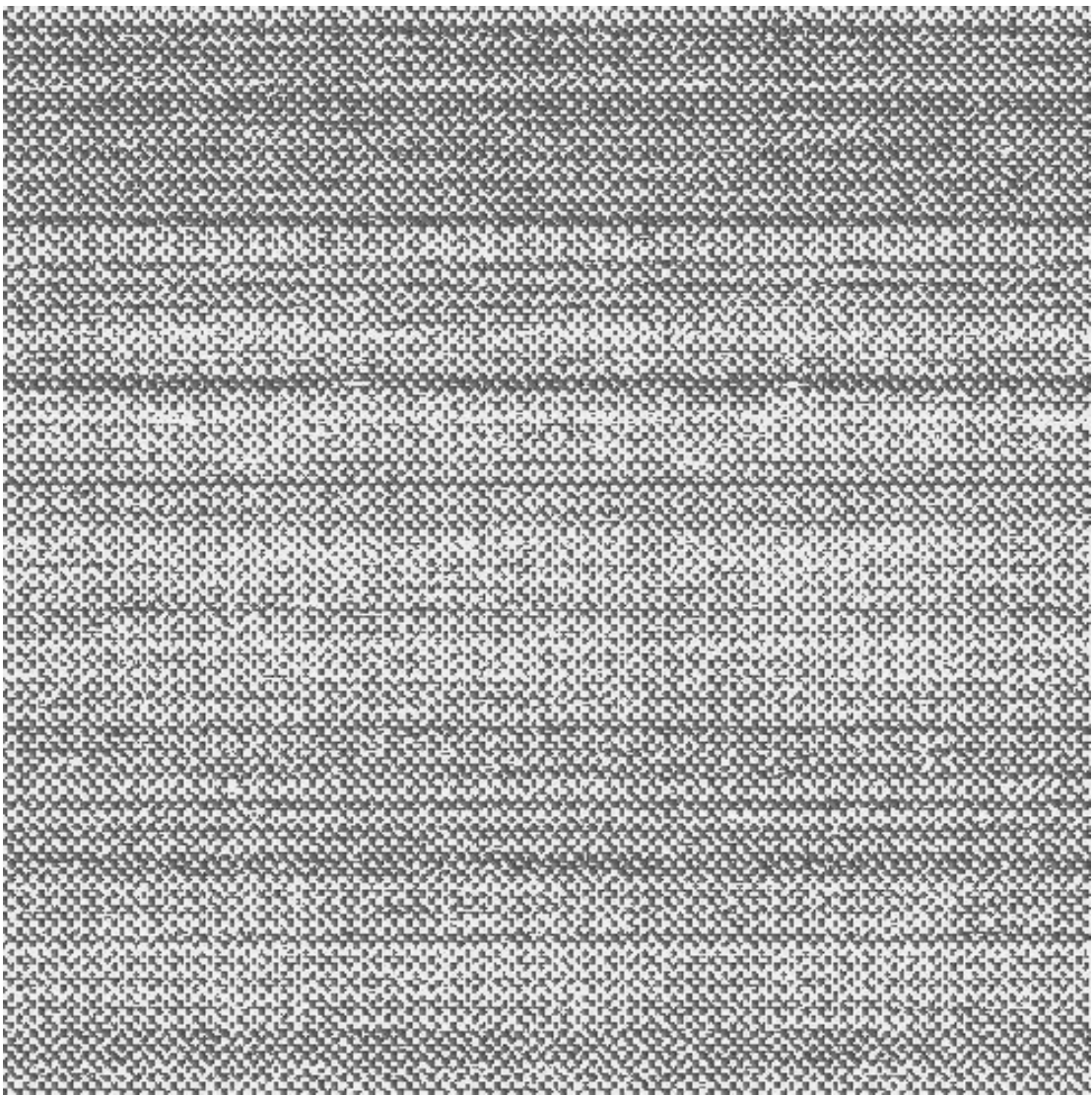
Sample #7



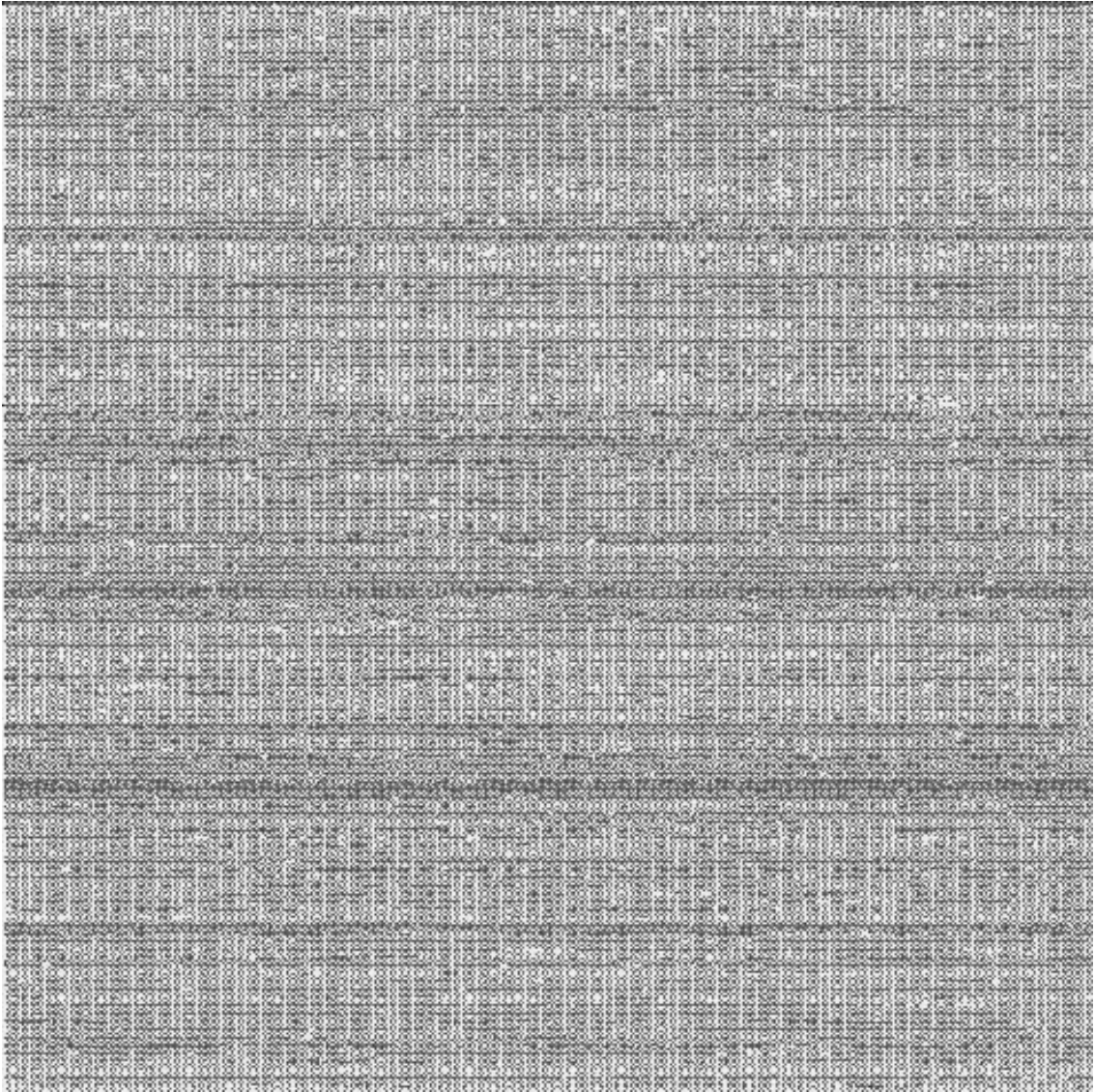
Sample #8



Sample #9

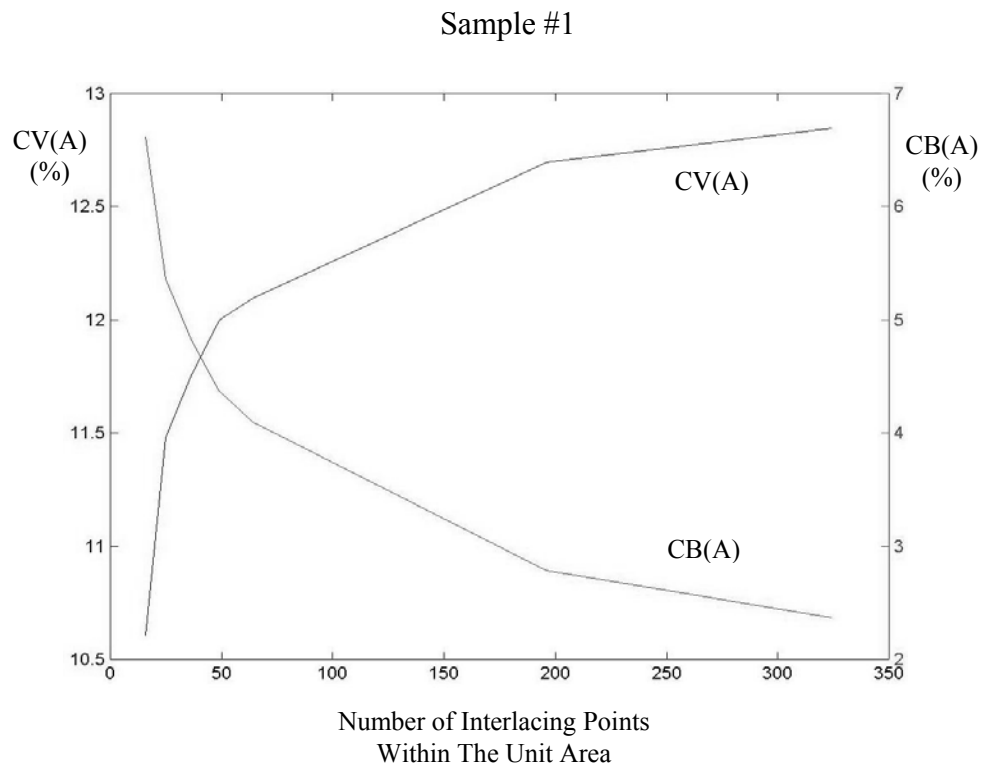


Sample #10

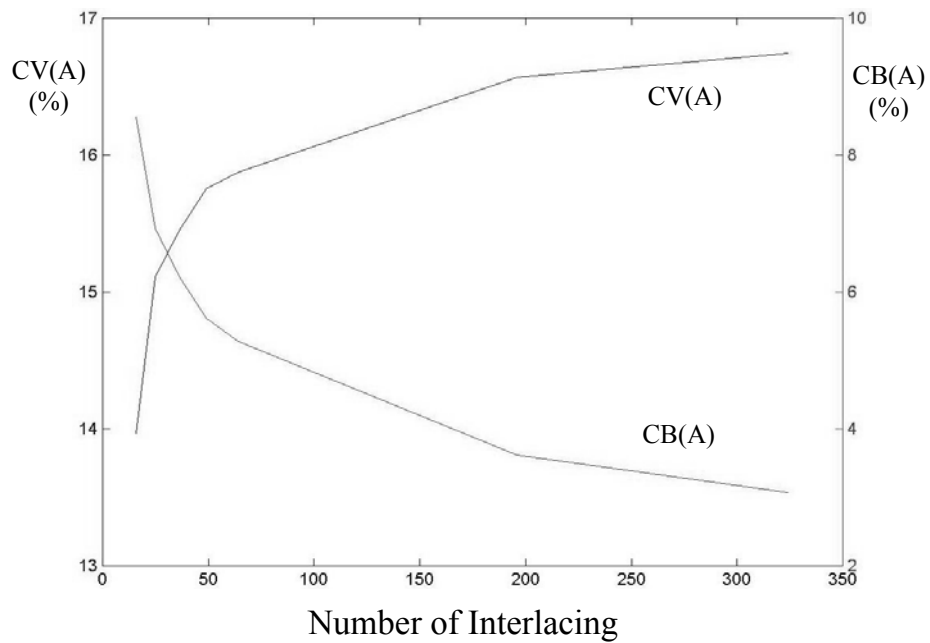


Appendix III Variance-Area Curves of 10 Samples

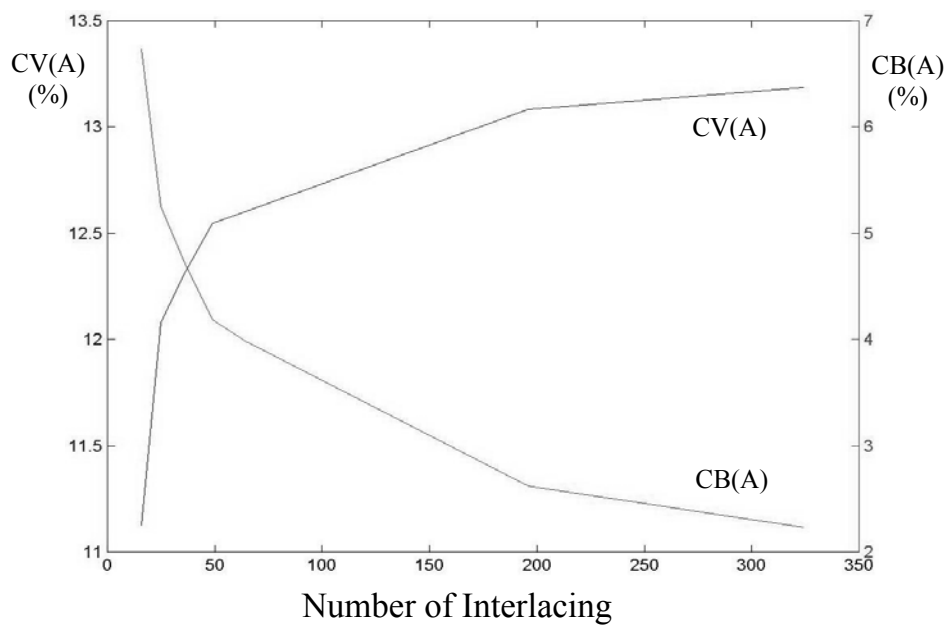
CV(A), within variation, and CB(A), between variation, curves of ten samples from model I. CV(A) curves refer to left Y-axis and CB(A) curves refer to right Y-axis.



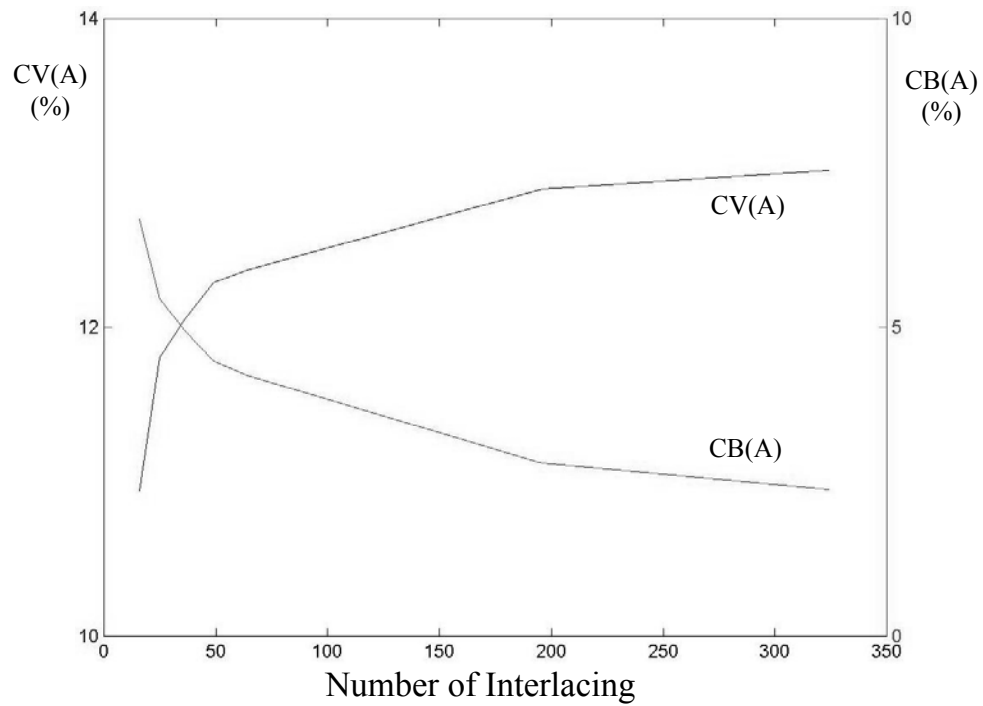
Sample #2



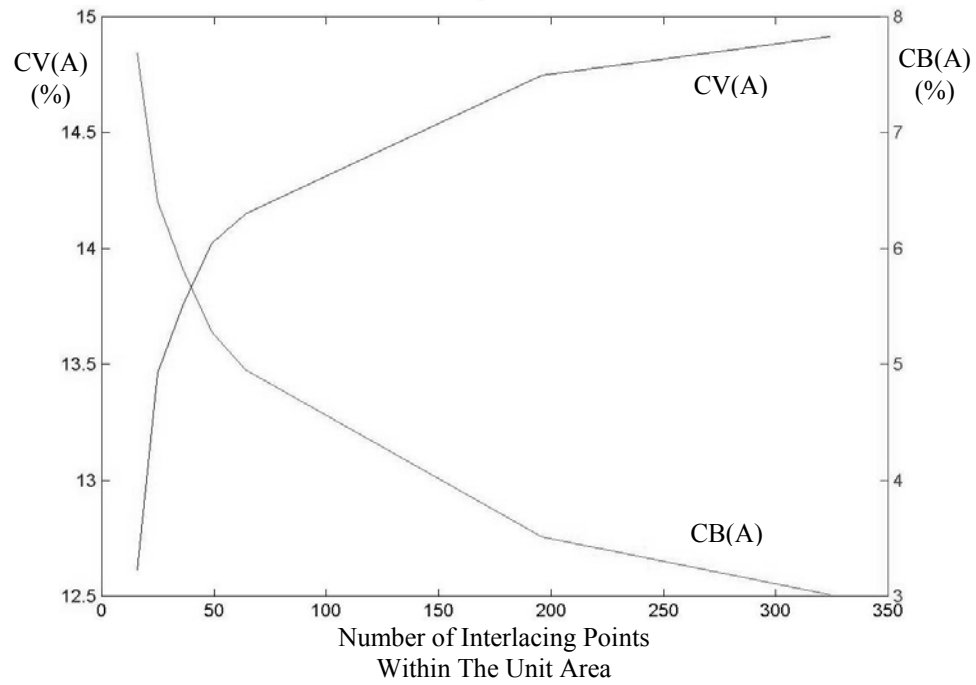
Sample #3

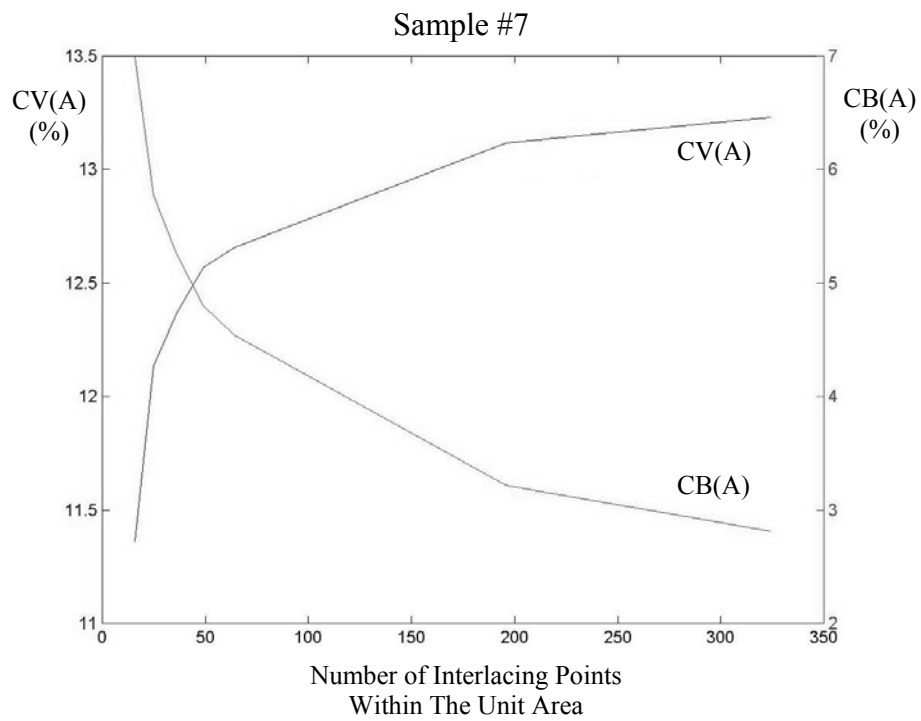
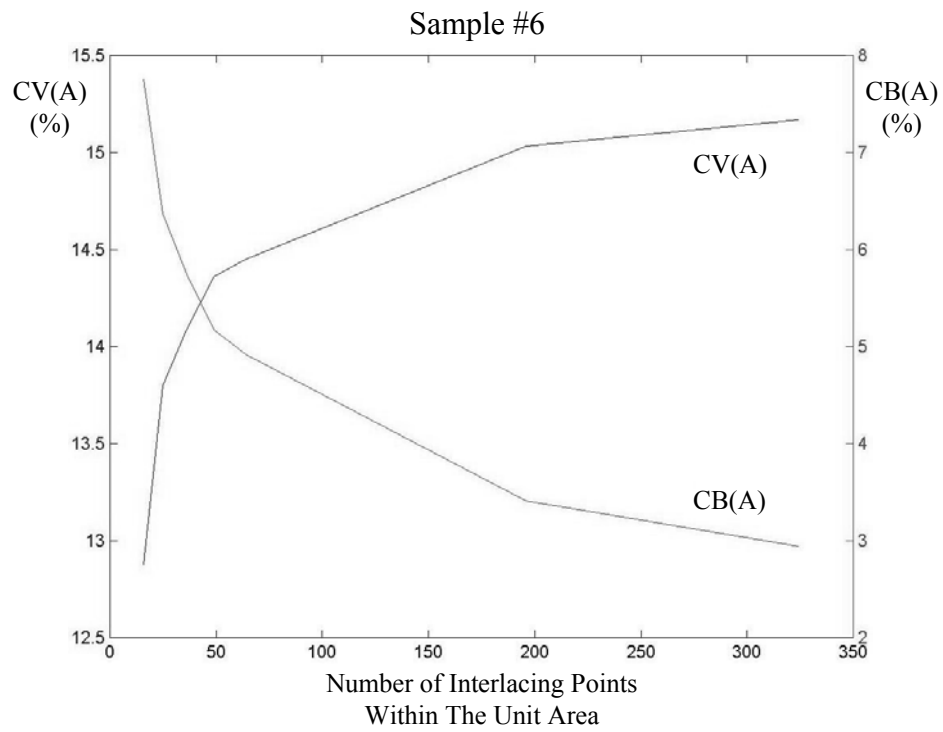


Sample #4

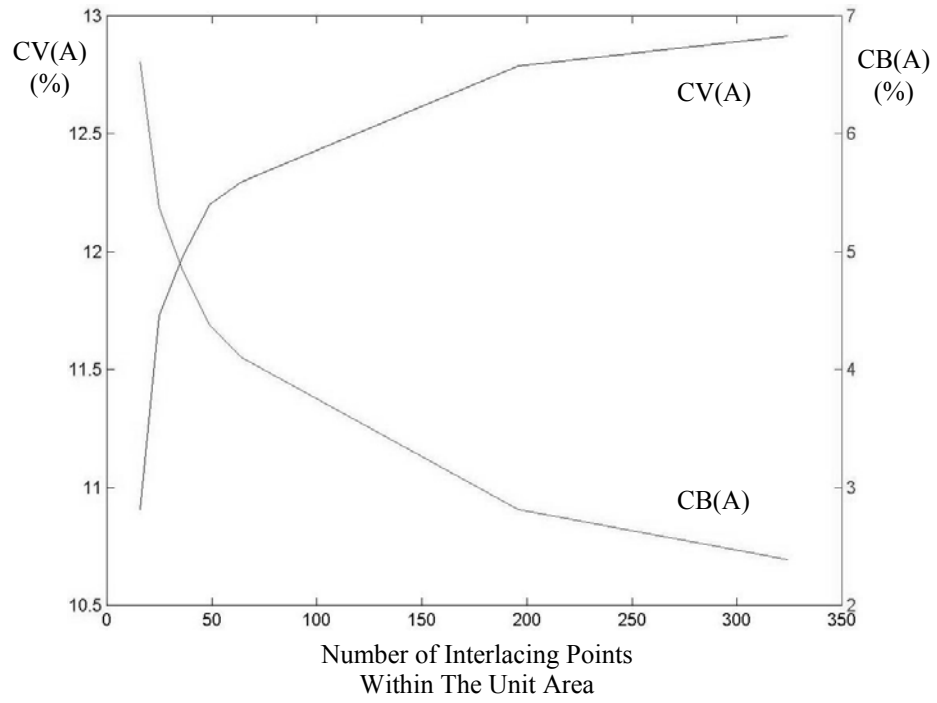


Sample #5

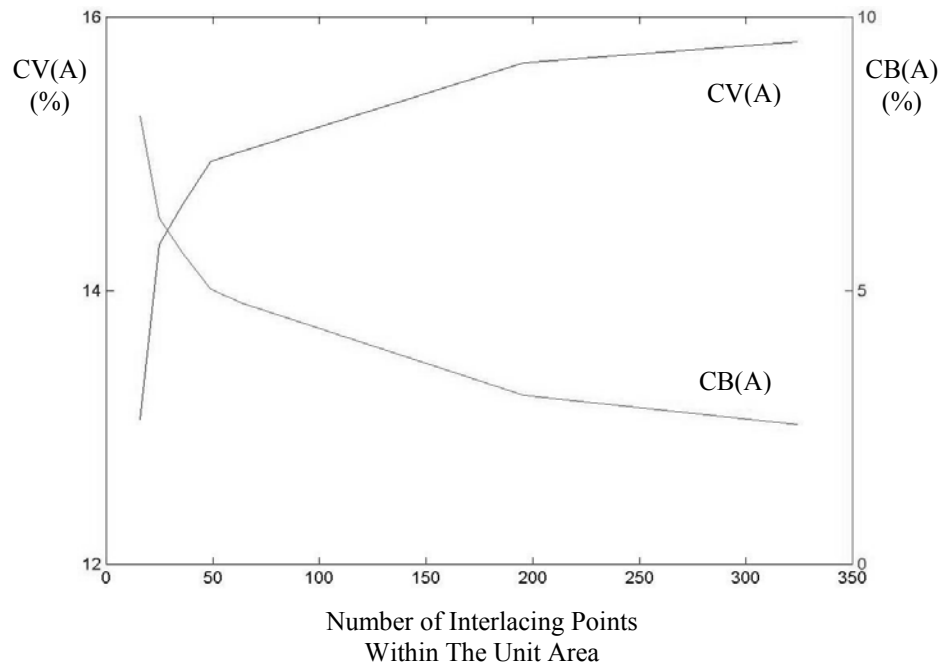




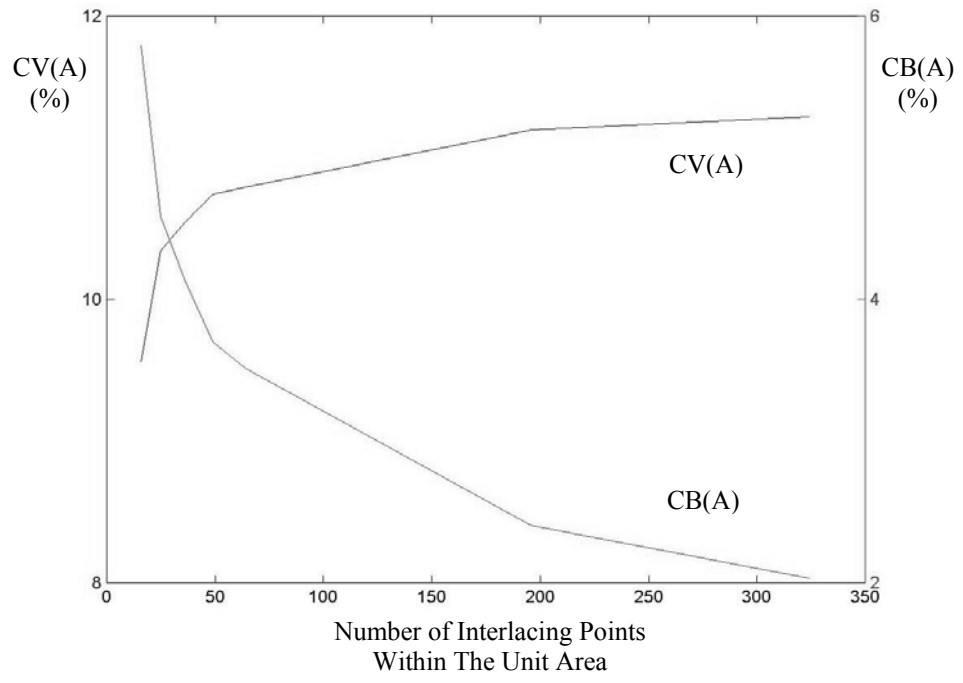
Sample #8



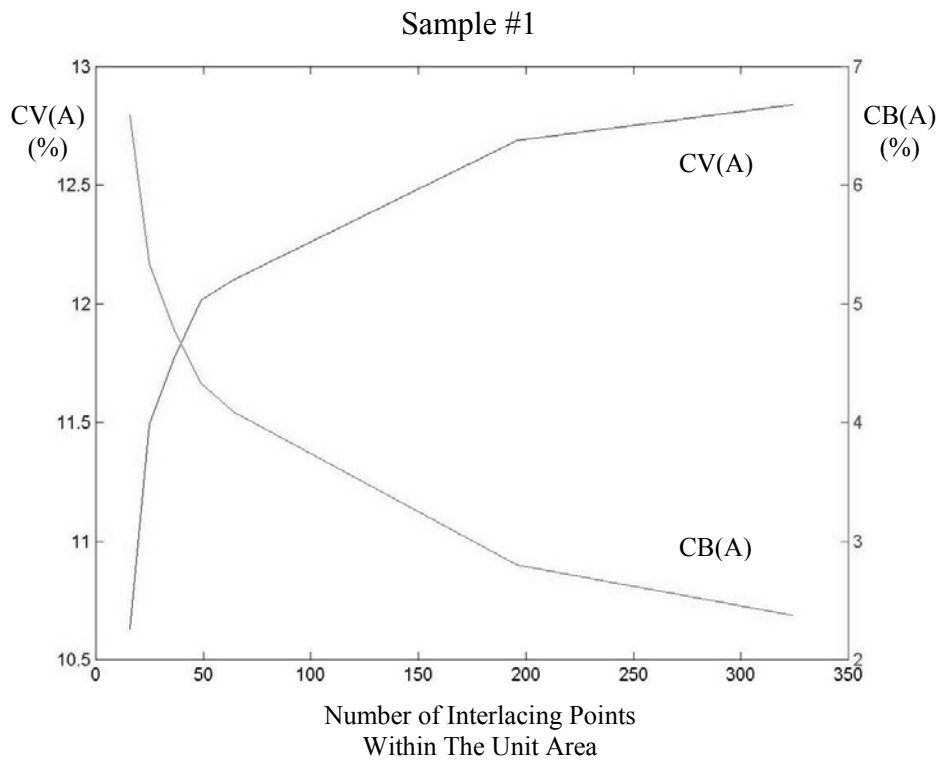
Sample #9

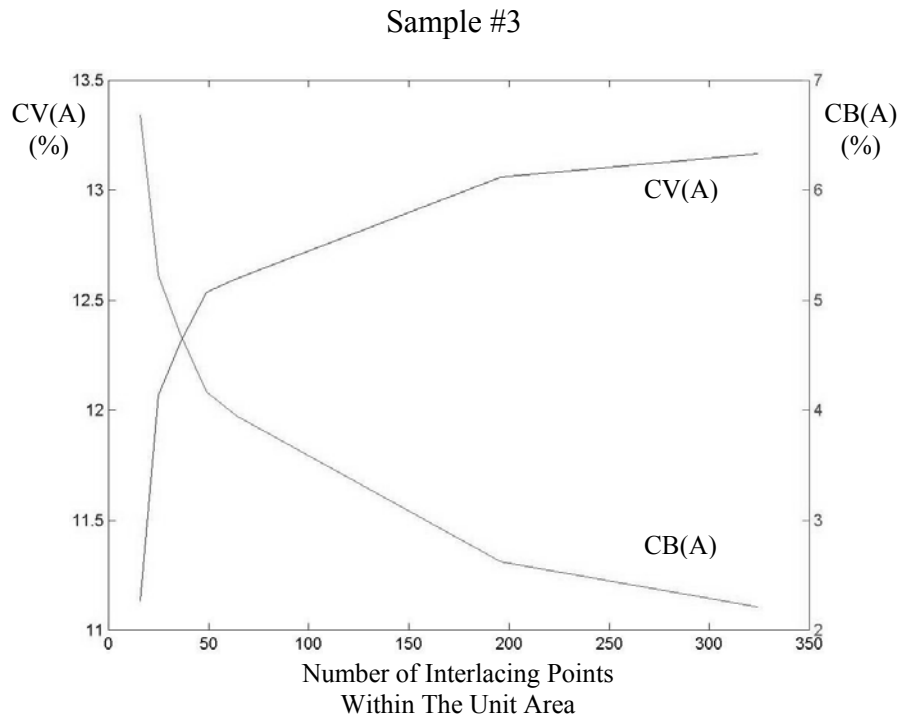
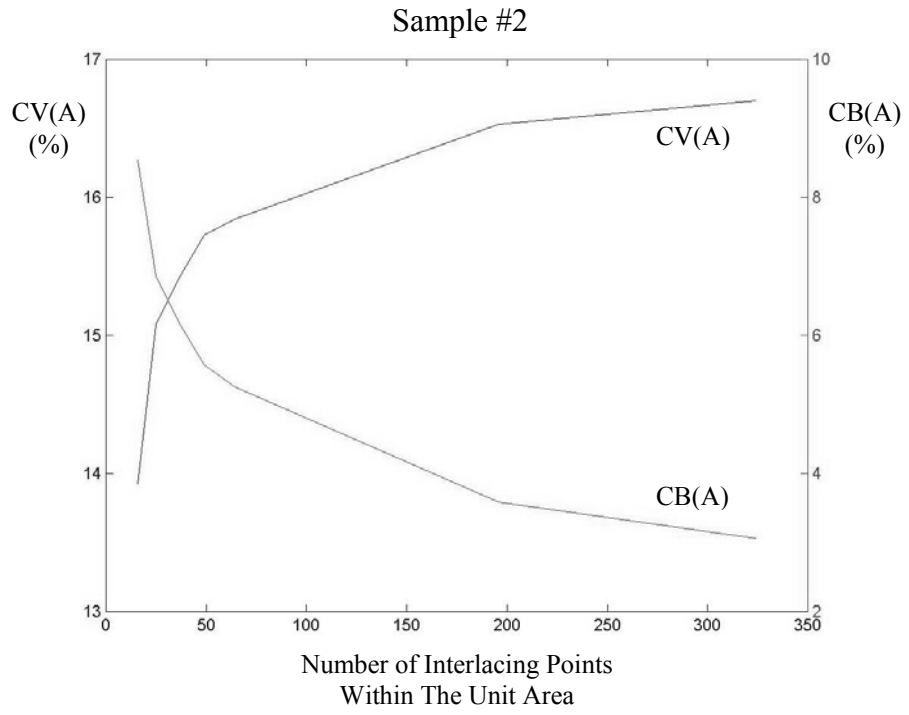


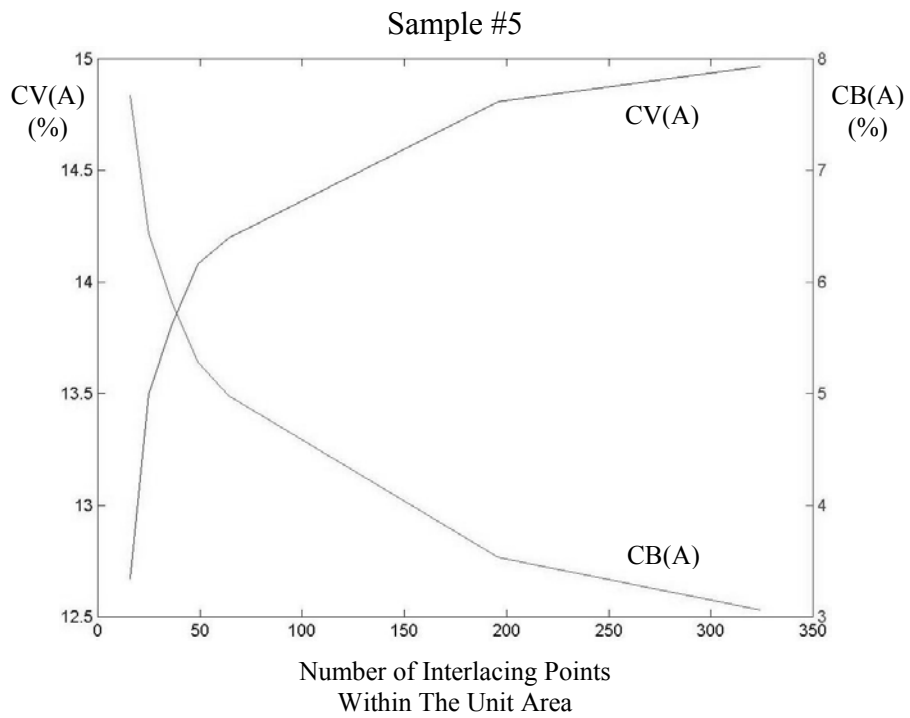
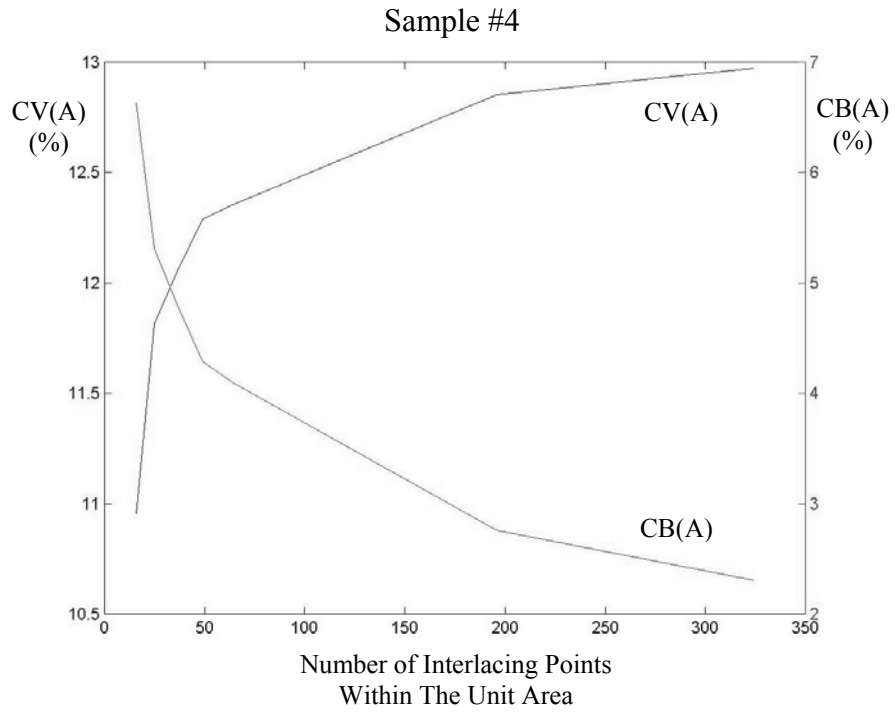
Sample #10



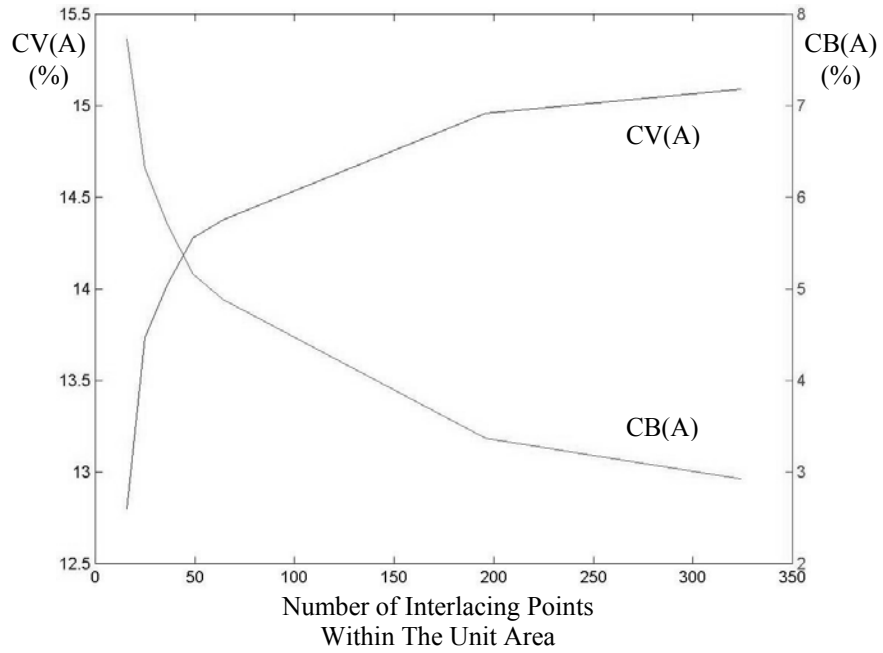
CV(A), within variation, and CB(A), between variation, curves of ten samples from model II. CV(A) curves refer to left Y-axis and CB(A) curves refer to right Y-axis.



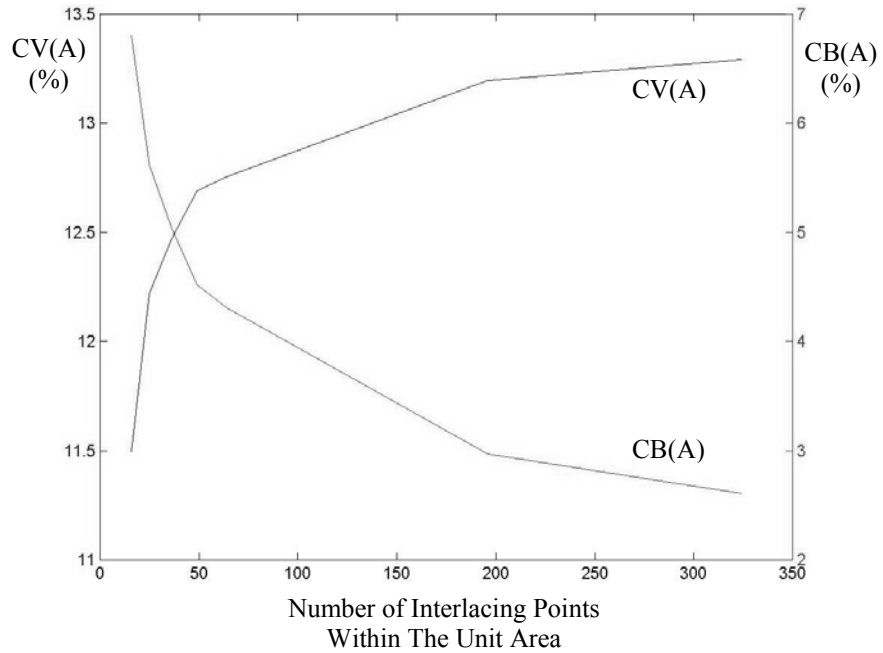


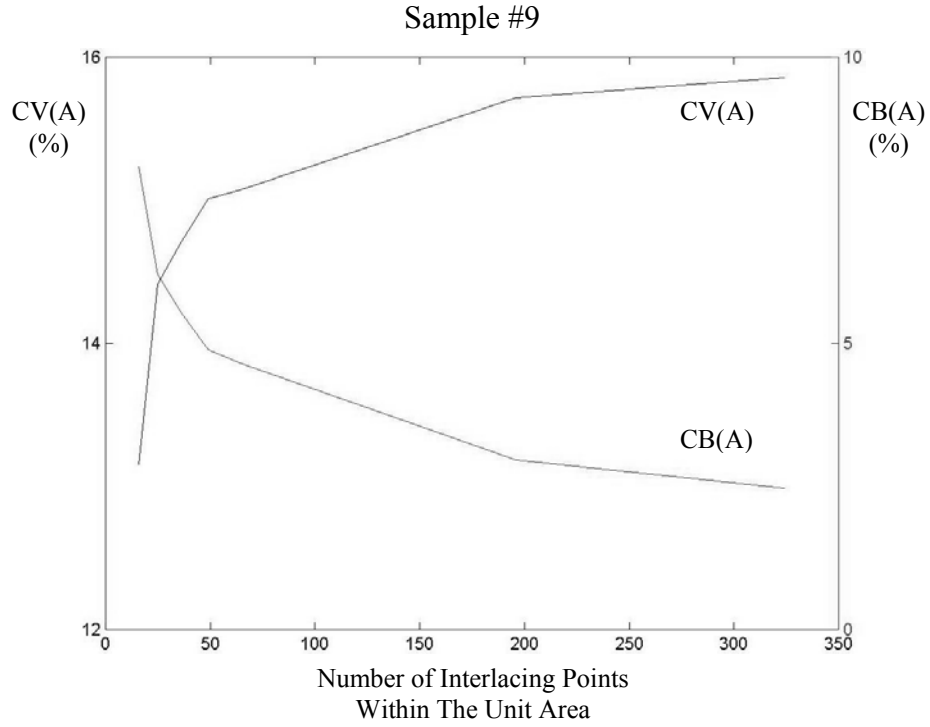
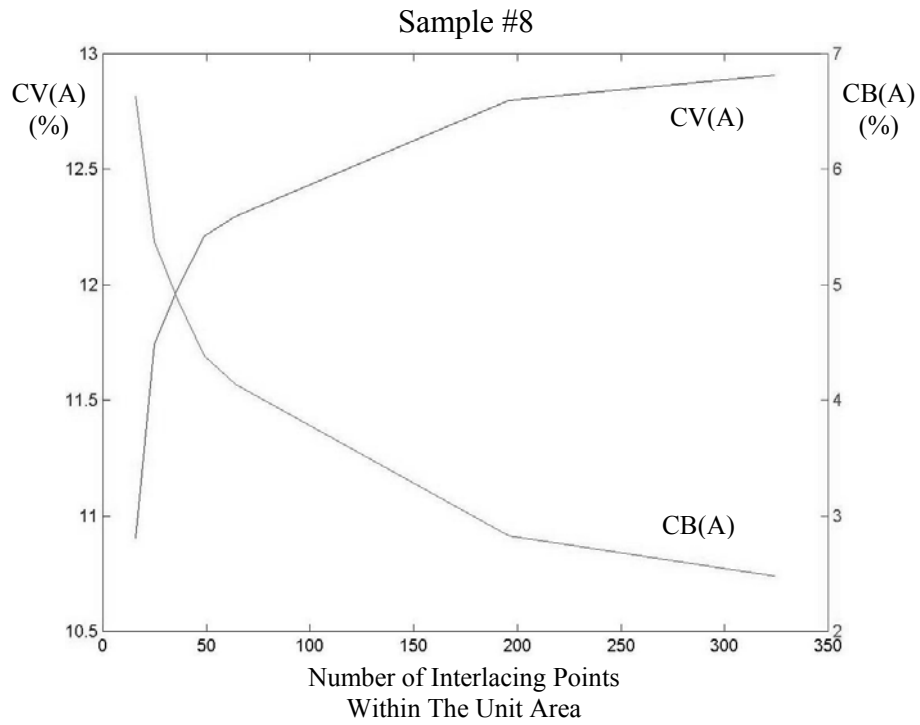


Sample #6

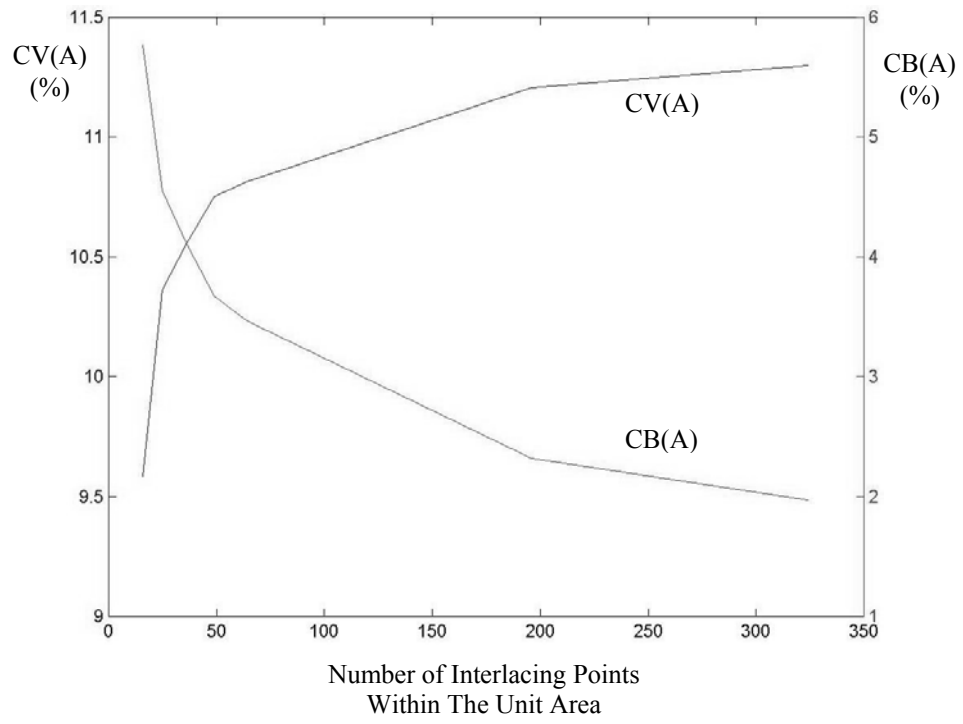


Sample #7





Sample #10



Appendix IV Matlab Program Samples

Coeff.m

```
function Y=coeff(X)

[m,n]=size(X);
for i=1:n
    h1=1+(i-1)*m;
    h2=i*m;
    r(h1:h2,1)=X(:,i);
end
Y(1)=100*std(r)/mean(r);
Y(2)=mean(r);
```

Draw1.m

```
clear
clc
load fabdata.mat
min_2d=min(min(FabShuttleless))
max_2d=max(max(FabShuttleless))
mean_2d=mean(mean(FabShuttleless))

m1_3d=m1;
m2_3d=m2;
n1_3d=n1;
n2_3d=n2;
minimum=min(min(FabShuttleless(m1_3d:m2_3d,n1_3d:n2_3d)))
;
z=FabShuttleless(m1_3d:m2_3d,n1_3d:n2_3d)-
FabShuttleless(m1_3d:m2_3d,n1_3d:n2_3d)+minimum;
figure
imagesc((10-FabShuttleless))
title('2-D Image For Yarn Sample #11 (II)')
axis off
colormap(gray)

figure
A=FabShuttleless(m1_3d:m2_3d,n1_3d:n2_3d);
surf(A);
hold on
```

```

surf(z);
colormap(gray)
aa=[A(1,1),A(mm,1),A(1,nn),A(mm,nn)];
bb=[z(1,1),z(mm,1),z(1,nn),z(mm,nn)];
xx=[1,mm,1,mm];
yy=[1,1,nn,nn];
for i=1:4
    YY=[xx(i),xx(i)];
    XX=[yy(i),yy(i)];
    ZZ=[aa(i),bb(i)];
    plot3(XX,YY,ZZ,'k')
end
axis off

```

fab_map_rand.m

```

clear
clc
data_weft=load('testdata11.txt');
data_warp=load('testdata11.txt');
pick_total=1412;
warp_total=1412;
for i=1:pick_total
    n=1+floor(rand*499600);
    for p=1:warp_total/4
        FabShuttleless(i,4*p-3)=data_weft(n+p-1,1);
        FabShuttleless(i,4*p-2)=data_weft(n+p-1,1);
        FabShuttleless(i,4*p-1)=data_weft(n+p-1,1);
        FabShuttleless(i,4*p)=data_weft(n+p-1,1);
    end
end
for i=1:warp_total
    n=1+floor(rand*499600);
    for p=1:pick_total/4
        FabShuttleless(4*p-3,i)=FabShuttleless(4*p-3,i)+data_warp(n+p-1,1);
        FabShuttleless(4*p-2,i)=FabShuttleless(4*p-2,i)+data_warp(n+p-1,1);
        FabShuttleless(4*p-1,i)=FabShuttleless(4*p-1,i)+data_warp(n+p-1,1);
    end
end

```

```
FabShuttleless(4*p,i)=FabShuttleless(4*p,i)+data_warp(n+p-1,1);
```

```
end  
end  
save fabdata.mat FabShuttleless
```

fab_mapping.m

```
clear  
clc  
data_weft=load('testdata11.txt');  
data_warp=load('testdata11.txt');  
pick_total=1412;  
warp_total=1412;  
for i=1:pick_total  
    for p=1:warp_total/4  
        FabShuttleless(i,4*p-3)=data_weft((warp_total/4*(i-1)+p),1);  
        FabShuttleless(i,4*p-2)=data_weft((warp_total/4*(i-1)+p),1);  
        FabShuttleless(i,4*p-1)=data_weft((warp_total/4*(i-1)+p),1);  
  
        FabShuttleless(i,4*p)=data_weft((warp_total/4*(i-1)+p),1);  
    end  
  
end  
for i=1:warp_total  
    n=1+floor(rand*499600);  
    for p=1:pick_total/4  
        FabShuttleless(4*p-3,i)=FabShuttleless(4*p-3,i)+data_warp(n+p-1,1);  
        FabShuttleless(4*p-2,i)=FabShuttleless(4*p-2,i)+data_warp(n+p-1,1);  
        FabShuttleless(4*p-1,i)=FabShuttleless(4*p-1,i)+data_warp(n+p-1,1);  
  
        FabShuttleless(4*p,i)=FabShuttleless(4*p,i)+data_warp(n+p-1,1);  
    end  
end
```

```
end
save fabdata.mat FabShuttleless
```

test.m

```
function vv=test(A)
area=20;
%calculate 8 area based values
for i=1:8
    area=area*2;
    xaxis(i)=area;
    %calculate edge length of unit area
    m(i)=floor(sqrt(area));
    n(i)=m(i);
    resultvector=vector(A,m(i),n(i));
    [h,l]=size(resultvector);
    cvmean(i)=mean(resultvector(h,1:l-1));
    cv(i)=resultvector(h,l);
    clear resultvector
end
cvmean
cv
figure
plotyy(xaxis,cvmean,xaxis,cv)
gtext('within variation')
gtext('between variation')
```

vector.m

```
function result=vector(A,m,n)

[h,l]=size(A);
%calculate loop counter for two directions
num1=floor(h/m);
num2=floor(l/n);
k=0;
for i=1:num1
    for j=1:num2
        h1=1+(i-1)*m;
        h2=i*m;
        l1=1+(j-1)*n;
        l2=j*n;
        k=k+1;
```

```
        y=coeff(A(h1:h2,11:12));
        result(k)=y(1);
        averagevector(k)=y(2);
    end
end

result(k+1)=100*std(averagevector)/mean(averagevector);
```